Application of Population Pharmacokinetic Modeling to Assess Kidney Function and Renal Excretion of Substances in Humans

Inaugural Dissertation

zur

Erlangung des Doktorgrades

philosophiae doctor (PhD) in Health Sciences

der Medizinischen Fakultät

der Universität zu Köln

vorgelegt von

Zhendong Chen

aus Sichuan, China

Köln

2025

Betreuerin / Betreuer:	Prof. Dr. Uwe Fuhr
Gutachterin / Gutachter:	Prof. Dr. Thomas Streichert
	Prof. Dr. Paul Brinkkötter
Datum der Mündlichen Prüfung:	16.06.2025

Content

List of tables

List of figures

List of abbreviations

AKI	Acute kidney injury
AUC_{24}	Daily area under the curve
BBB	Blood-brain barrier
BMI	Body mass index
^{51}Cr-EDTA	Chromium-51 ethylenediaminetetraacetic acid
CGR	Creatinine generation rate
CKD	Chronic kidney disease
CKD-EPI	Chronic Kidney Disease Epidemiology Collaboration
CL	Clearance
CNS	Central nervous system
CrCL	Creatinine clearance
CSF	Cerebrospinal fluid
C_{trough}	Trough concentrations
CV	Coefficient of variation
DR	Diet restriction
eGFR	Estimated glomerular filtration rate
EVDs	External ventricular drains
F1	Bioavailability
FAS	Full Age Spectrum
f_{risk}	Acute kidney injury risk factor
GFR	Glomerular filtration rate
HQC	Higher quality control
IIV	Inter-individual variability
IMF	IS normalized matrix factor
IoCL	Iohexol clearance
IS	Internal standard
Ka	Absorption rate
KDIGO	Kidney Disease: Improving Global Outcomes
LC-MS/MS	Liquid chromatography with tandem mass spectrometry
LLOQ	Lowest limit of quantification
LQC	Lower quality control
MATE	Multidrug and toxin extrusion protein

MDRD	Modification of Diet in Renal Disease
MIC	Minimum inhibitory concentration
MQC	Middle quality control
MRPs	Multidrug resistance-associated proteins
MRSA	*Staphylococcus aureus*
nCTS	Net creatinine tubular secretion
OAT	Organic anion transporter
OCT	Organic cation transporter
OFV	Objective function value
PBPK	Physiologically-based pharmacokinetic
PK	Pharmacokinetics
PK/PD	Pharmacokinetic/pharmacodynamic
popPK	Population pharmacokinetic
PsN	Perl-speaks-NONMEM
QC	Quality control
Q_{CSF}	Clearance between central and cerebrospinal fluid compartments
Q_p	Inter-compartmental clearance between central and peripheral compartments
rCrCL%	Relative change in creatinine clearance following surgery
RE	Relative error
RRF	Relative response factor
RSE	Relative standard error
Scr	Serum creatinine
SD	Standard deviation
TBW	Total body weight
^{99m}Tc-DTPA	Technetium-99m diethylene triamine pentaacetic acid
TDM	Therapeutic drug monitoring
V_c	Central compartment volume
V_{CSF}	Cerebrospinal fluid compartment volume
V_d	Volume of distribution
V_p	Peripheral compartment volume

1 Introduction

1.1 Glomerular filtration rate

Glomerular filtration is the process in the kidneys that filters excess fluids and waste products from the blood, constituting the first step in urine production. The glomerular filtration rate (GFR) represents the total volume of plasma filtered by the kidneys per unit of time, serving as a critical indicator of renal function.[1] Normal GFR levels vary significantly, influenced by a range of factors including sex, age, body size, and physical activity, as well as hydration status, blood pressure, circadian rhythms, and dietary protein intake.[2-4] However, kidney function may be gradually impaired over months or years due to various diseases or conditions, leading to what is known as chronic kidney disease (CKD). A guideline for CKD classification (Table 1) and diagnosis, initially based solely on GFR, was introduced in 2002 and later refined by the Kidney Disease: Improving Global Outcomes (KDIGO) group to include albuminuria categories.[5] This guideline is now widely adopted and remains the standard reference for CKD classification and management. Consequently, GFR remains the most important marker of kidney function.

Table 1 GFR categories for chronic kidney disease classification.

Classification	GFR (mL/min/1.73 m^2)	Description
G1	≥90	Normal or high
G2	60-89	Mildly decreased
G3a	45-59	Mildly to moderately decreased
G3b	30-44	Moderately to severely decreased
G4	15-29	Severely decreased
G5	<15	Kidney failure

1.1.1 Direct measurement of glomerular filtration rate

Direct measurement of GFR provides the most accurate assessment of kidney function and is considered the gold standard. This involves the use of exogenous filtration markers such as inulin, iohexol, and iothalamate, which are freely filtered by the glomerulus and are neither secreted, reabsorbed, nor metabolized by the kidneys.[6] While these methods are often employed in research settings and specific clinical situations requiring precise renal function assessment, they are not commonly used in routine clinical practice due to their complexity.

Table 2 summarizes several direct GFR measurement methods. Among these, urinary clearance of inulin, first introduced in 1935, remains the gold standard for GFR measurement due to its high accuracy.[7] However, this method requires a continuous intravenous infusion of inulin to maintain a steady-state concentration in the blood, along with collection of both blood and

urine samples over timed intervals to calculate the rate of filtration.[7] Therefore, inulin clearance is labor-intensive and costly, making it impractical for routine clinical use and more suitable for research purposes.

Table 2 Comparison of different direct GFR measurement methods.

Marker Used	Accuracy compared to inulin	Pros	Cons
Inulin	Gold standard	Highly accurate; reflects true GFR	Requires IV infusion and urine collection
Iohexol	$r > 0.92$[8,9]	Simplified protocol with single bolus injection; no radiation	Requires multiple blood samples
Iothalamate (^{125}I or non-radiolabeled)	$r = 0.989$[10]	Non-radioactive option available; accurate	Radiation exposure (for ^{125}I version)
^{51}Cr-EDTA	$r > 0.992$[11]	High accuracy; no urine collection required	Radiation exposure; complex sampling
^{99m}Tc-DTPA	$r = 0.984$[10]	Provides functional imaging of kidneys; non-invasive	Radiation exposure; requires gamma camera

GFR, glomerular filtration; IV, intravenous; *r*, correlation coefficient; ^{51}Cr-EDTA, chromium-51 ethylenediaminetetraacetic acid; ^{99m}Tc-DTPA, Technetium-99m diethylene triamine pentaacetic acid.

Iohexol and iothalamate are radiopaque contrast agents also used for GFR measurement that offer practical alternatives to inulin due to their simpler protocols. Unlike inulin, respective use of these agents involves only a single bolus injection followed by plasma sampling, without the need for continuous infusion or urine collection. Both iohexol and iothalamate are filtered exclusively by the glomerulus and remain unmetabolized, providing reliable GFR estimates that strongly correlate with inulin clearance.[10,12] These methods are particularly well-suited for routine clinical practice and research applications involving patients with CKD or those needing frequent monitoring of renal function, due to their simplicity and minimal invasiveness. Moreover, the lack of radiation exposure makes these agents suitable for repeated use, even in vulnerable populations such as children or pregnant women.

Chromium-51 ethylenediaminetetraacetic acid (^{51}Cr-EDTA) and technetium-99m diethylene triamine pentaacetic acid (^{99m}Tc-DTPA) are radiopharmaceuticals widely used for GFR measurement, especially in settings that demand both high accuracy and functional imaging capabilities.[13] ^{51}Cr-EDTA clearance, which involves plasma sampling after a single injection, providing GFR estimates with accuracy similar to inulin.[12] ^{99m}Tc-DTPA, on the other hand, can be used for both plasma clearance and gamma camera imaging, which allows visualization of renal perfusion and differential function.[14] While both ^{51}Cr-EDTA and ^{99m}Tc-DTPA provide

accurate GFR measurements, their use is limited by radiation exposure, making them less suitable for frequent assessments compared to non-radioactive alternatives.

1.1.2 Estimated glomerular filtration rate in clinical settings

Estimated glomerular filtration rate (eGFR) is a calculated measure that provides an approximation of the GFR based on serum markers and patient-specific variables. It is widely used in clinical practice as a practical and accessible method to assess kidney function, especially when direct measurement of GFR is impractical. Unlike direct GFR measurement techniques, which require specialized equipment and invasive procedures, eGFR can be estimated using equations that incorporate routinely collected biomarkers, such as serum creatinine (Scr) or cystatin C (Table 3).

The earliest widely used equation for estimating GFR is the Cockcroft-Gault formula, developed in 1976. This formula estimates creatinine clearance (CrCL) as a surrogate for GFR and takes into account Scr, age, total body weight (TBW), and sex, making it particularly useful for adjusting medication dosages in patients with chronically impaired renal function.[15] Although the Cockcroft-Gault formula has limitations—such as overestimating GFR in individuals with obesity or significant muscle mass—it remains a practical tool in clinical pharmacology, particularly for dosing renally cleared medications.

The Modification of Diet in Renal Disease (MDRD) equation, introduced in 1999, improved upon the Cockcroft-Gault formula by incorporating additional patient variables and using a more standardized approach to Scr measurement.[16] The MDRD equation was widely adopted for its greater accuracy in estimating GFR, particularly in patients with moderate to severe CKD. However, it tends to be less accurate at higher GFR levels.[17]

To address the limitations of the MDRD equation, the Chronic Kidney Disease Epidemiology Collaboration (CKD-EPI) equation was developed in 2009. The CKD-EPI equation is preferred for its improved accuracy across a wider range of GFR values, especially at higher levels of kidney function. It incorporates factors such as age, sex, race, and body size, making eGFR a more individualized measure suitable for a broader spectrum of patients.[18] Studies have also shown that the CKD-EPI equation results in fewer instances of misclassification of CKD stages compared to the MDRD equation.[19] This enhanced precision helps clinicians make more informed decisions regarding patient care and disease management.

Table 3 Commonly employed equations for eGFR based on serum creatinine concentration.

Reference	Year	Equation
Cockcroft-Gault formula[15]	1976	$\mathrm{CrCL} = \frac{(140 - Age) \times Weight}{Scr \times 72} \times 0.85(if\ female)$
Modification of Diet in Renal Disease (MDRD)[16]	1999	$\mathrm{GFR} = 175 \times Scr^{-1.154} \times Age^{-0.203} \times 0.742(if\ female) \times 1.212(if\ black)$
Chronic Kidney Disease Epidemiology Collaboration (CKD-EPI)[18]	2009	$\mathrm{Male, Scr} > 0.9\ \mathrm{mg/dL}: \mathrm{GFR} = 141 \times (\frac{Scr}{0.9})^{-1.209} \times 0.993^{Age} \times 1.159(if\ black)$
		$\mathrm{Male, Scr} \leq 0.9\ \mathrm{mg/dL}: \mathrm{GFR} = 141 \times (\frac{Scr}{0.9})^{-0.411} \times 0.993^{Age} \times 1.159(if\ black)$
		$\mathrm{Female, Scr} > 0.7\ \mathrm{mg/dL}: \mathrm{GFR} = 144 \times (\frac{Scr}{0.7})^{-1.209} \times 0.993^{Age} \times 1.159(if\ black)$
		$\mathrm{Female, Scr} \leq 0.7\ \mathrm{mg/dL}: \mathrm{GFR} = 144 \times (\frac{Scr}{0.7})^{-0.411} \times 0.993^{Age} \times 1.159(if\ black)$
Schwartz formular (revised)[20]	2009	$\mathrm{Children\ aged\ from\ 1\ to\ 18\ years}: \mathrm{GFR} = 0.413 \times \frac{Height}{Scr}$
Berlin Initiative Study[21]	2012	$\mathrm{BSI1}: \mathrm{GFR} = 3736 \times Scr^{-0.87} \times Age^{-0.95} \times 0.82(if\ female)$
		$\mathrm{BSI2}: \mathrm{GFR} = 7470 \times Scr^{-0.72} \times ScysC^{-0.61} \times Age^{-0.81} \times 0.83(if\ female)$
Full age spectrum (FAS)[22]	2016	$\mathrm{Male, age\ from\ 2\ to\ 40}: \mathrm{GFR} = 107.3/(\frac{Scr}{0.9})$
		$\mathrm{Male, age} > 40: \mathrm{GFR} = 107.3/(\frac{Scr}{0.9}) \times 0.988^{(age-40)}$
		$\mathrm{Female, age\ from\ 2\ to\ 40}: \mathrm{GFR} = 107.3/(\frac{Scr}{0.7})$
		$\mathrm{Female, age} > 40: \mathrm{GFR} = 107.3/(\frac{Scr}{0.7}) \times 0.988^{(age-40)}$

CrCL, creatinine clearance; Scr, serum creatinine concentration; ScysC, cystatin C concentration.
Unit: CrCL in mL/min; weight in kg; GFR in mL/min/1.73m^2; Scr in mg/dL; age in years; weight in kg; height in cm.

The Berlin Initiative Study (BIS) equations, BIS1 and BIS2, were developed in 2012 to improve the accuracy of eGFR assessments in individuals aged 70 and older.[21] Previous eGFR equations often overestimate GFR in the elderly due to age-related declines in muscle mass affecting Scr concentrations.[21] The BIS1 equation addresses this by incorporating Scr, age, and sex, while the BIS2 equation further enhances accuracy by including both Scr and cystatin C, a biomarker less influenced by muscle mass. Studies have demonstrated that BIS equations provide more reliable GFR estimates in older adults compared to CKD-EPI,[23] particularly in detecting moderate to severe CKD (GFR less than 60 mL/min/1.73 m^2).[24] However, these equations are population-specific, as they were derived from a cohort of elderly individuals and may not generalize well to younger adults or diverse ethnic groups.[21] Additionally, while BIS2 improves accuracy by incorporating Cystatin C, it requires an additional biomarker that may not always be readily available in clinical settings due to the high cost of Cystatin C testing.[25] Despite these limitations, BIS equations represent a valuable advancement in eGFR estimation for aging populations, assisting clinicians in optimizing medication dosing, assessing kidney function decline, and enhancing CKD management in older patients.

The Full Age Spectrum (FAS) equation was introduced to provide a unified approach for GFR estimation across all age groups. The FAS equation is designed to deliver accurate GFR estimates for children, adults, and the elderly, thereby enhancing the applicability of eGFR across a wide range of patient demographics.[22] By offering a single formula suitable for all ages, the FAS equation simplifies the estimation process and reduces variability that may arise from using different equations for different age groups. Additionally, the Schwartz formula remains specifically used for pediatric patients,[20] and the CKD-EPI equation has been adapted for elderly populations to ensure accuracy in these demographics.

The use of eGFR is critical for early detection of CKD, monitoring disease progression, and making informed decisions about medication dosing, particularly for drugs that are renally excreted. However, the accuracy of eGFR is affected by several limitations. Scr concentration, for instance, is influenced not only by renal function but also by factors such as circadian rhythms, food intake, muscle mass, and other disease processes.[3,4,26,27] These non-renal factors contribute to variability, and changes in renal function may not be immediately reflected in Scr, particularly in acute or unstable conditions. All commonly used equations, such as Cockcroft-Gault, MDRD, and CKD-EPI, are based on the steady-state assumption of creatinine production and elimination, making them less accurate for patients experiencing rapidly changing kidney function, such as those with acute kidney injury (AKI).[28] These limitations

highlight the need for careful interpretation of eGFR values in clinical scenarios involving dynamic changes in renal function.

1.1.3 Dose adjustment for renally excreted drugs based on estimated glomerular filtration or estimated creatinine clearance

Renal excretion of unchanged drugs accounts for 25% to 30% of all drugs and involves three primary mechanisms: glomerular filtration, active tubular secretion, and passive tubular reabsorption.[29] Of these, glomerular filtration is the only passive process, with the amount of drug filtered into the tubular lumen depending on the GFR, renal blood flow, and plasma protein binding, as only unbound drugs are filtered.[30] Drugs with molecular weights below 50 kDa can typically pass through the glomerular capillary walls into the filtrate, while larger molecules, such as most plasma proteins (e.g., albumin, ~66 kDa), are generally restricted.[31]

Impaired kidney function leads to reduced GFR, which can result in decreased clearance of drugs that are renally excreted. This increases the risk of drug accumulation, leading to potential toxicity. Therefore, appropriate dose adjustments based on eGFR or eCrCL are crucial to maintain therapeutic effectiveness while minimizing toxicity. Dose adjustment for renally excreted drugs can be achieved by either reducing the dose or extending the dosing interval, depending on the pharmacokinetics (PK) of the drug and the level of renal impairment. The choice between using eGFR or eCrCL for dose adjustment often depends on the specific drug and clinical guidelines.

Table 4 lists examples of drugs that require dose adjustment in patients with renal impairment. Gentamicin is an aminoglycoside antibiotic used to treat various bacterial infections and typically requires therapeutic drug monitoring (TDM) due to its narrow therapeutic level (plasma concentrations of 5–10 μg/mL) and the increased risk of nephrotoxicity when plasma concentrations exceed 12 μg/mL.[32] Metformin is the first-line treatment for type 2 diabetes mellitus, but in patients with renal impairment, caution is required to prevent lactic acidosis, which can result from elevated drug concentrations.[33] Digoxin is a cardiac glycoside used to manage heart failure and atrial fibrillation. Due to its narrow therapeutic index (plasma concentrations of 0.8–2.0 ng/mL) and the risk of toxicity,[34] careful dose adjustment and monitoring of plasma concentrations are crucial to avoid serious adverse effects such as arrhythmias.[35] Enoxaparin is a low molecular weight heparin used for anticoagulation in conditions such as deep vein thrombosis and pulmonary embolism. Dose adjustment for enoxaparin is necessary to prevent bleeding complications, as reduced renal clearance can lead

Table 4 Examples of dose adjustment for patients with renal impairment.

Drug	Indication	Renal elimination fraction	Method for dose adjustment	Dosing recommendations for eCrCL/eGFR categories	
Gentamicin[36]	Antibiotic	95%[37]	eCrCL	eCrCL (mL/min)	Dosing interval
				>70	8 hourly (standard dose: 1 mg/kg)
				3–70	12 hourly
				10–29	24 hourly
				5–9	48 hourly
Metformin[38]	Type 2 diabetes	90–100%[39]	eCrCL or eGFR	eCrCL or eGFR (mL/min/1.73m^2)	Predicted daily metformin dose range
				90–120	1700–2250 mg
				60–89	1250–1700 mg
				45–59	1000–1250 mg
				30–44	750–1000 mg
				15–29	500–750 mg
Digoxin[40]	Heart failure	70-85%[41]	eCrCL	eCrCL (mL/min)	Maintenance dose after loading dose
				Adult	125–250 mg once daily
				Elderly	62.5–125 mg, once daily
				30–60	62.5–250 mg, once daily
				10–30	62.5–125 mg, once daily
				<10	62.5 once daily or on alternate days
Enoxaparin[42]	Anticoagulant	~70%[43]	eCrCL	eCrCL (mL/min)	Recommended dose for every 12 hours
				>50	1.0 mg/kg
				40–49	0.6 mg/kg
				30–39	0.5 mg/kg
				20–29	0.4 mg/kg
				10–19	0.3 mg/kg

eCrCL, estimated creatinine clearance using Cockcroft-Gault equation; eGFR, estimated glomerular filtration rate.

to increased drug concentrations.[44] Vancomycin, a widely used antibiotic, requires dose adjustment to optimize therapy and minimize toxicity. The Infectious Diseases Society of America recommends an initial dose of 15–20 mg/kg every 8–12 hours for adults with normal renal function, but dosing should be individualized based on renal function, weight, and infection severity.[45] Further discussion on vancomycin therapy is provided in 1.3.

1.1.4 Acute kidney injury

AKI refers to a sudden decline in kidney function over a short period, often occurring within days or even hours. Unlike CKD, which involves a gradual decline, AKI is characterized by rapid changes in renal function that can be triggered by factors such as cardiac surgery,[46] sever trauma,[47] sepsis,[48] cardiovascular events,[49] or drug-induced nephrotoxicity.[50]

Studies have shown that AKI affects up to 30% of patients undergoing cardiac surgery, with an associated increase in morbidity and mortality rates.[51] During cardiac surgery, hemodynamic instability, such as fluctuations in blood pressure, and reduced renal perfusion can lead to AKI. Factors such as cardiopulmonary bypass, systemic inflammation, and the use of vasopressors contribute to decreased renal blood flow and ischemic injury, thereby increasing the risk of AKI.[52] These rapid fluctuations pose significant challenges in assessing and managing kidney health. In clinical practice, AKI is often detected using criteria such as the KDIGO classification (Table 5), which defines AKI and AKI stages based on increases in Scr or decreases in urine output.[53]

Table 5 Definition of AKI and staging of AKI based on KDIGO guideline.

AKI definition		
1	Increase in SCr by ≥0.3 mg/dl (≥26.5μmol/L) within 48 hours; or	
2	Increase in SCr to ≥1.5 times baseline, which is known or presumed to have occurred within the prior 7 days; or	
3	Urine volume <0.5 ml/kg/h for 6 hours.	
Staging of AKI		
Stage	Serum creatinine	Urine output
1	1.5–1.9 times baseline; or ≥0.3 mg/dL (≥26.5 μmol/L) increase	<0.5 mL/kg/h for 6-12 hours
2	2.0-2.9 times baseline	<0.5 mL/kg/h for ≥12 hours
3	3.0 times baseline; or Increase in serum creatinine to ≥4.0 mg/dL (≥353.6 μmol/L); or Initiation of renal replacement therapy; or In patients <18 years, decrease in eGFR to <35 mL/min per 1.73 m^2	<0.3 mL/kg/h for ≥24 hours; or Anuria for ≥12 hours

AKI, acute kidney injury; KDIGO, Kidney Disease: Improving Global Outcomes.

Patients with AKI often experience rapid changes in Scr concentrations, which makes accurate assessment of kidney function challenging. Scr concentrations may not directly reflect real-time alterations in GFR due to the lag in creatinine kinetics. This delayed response is particularly problematic in critically ill patients, where timely decisions regarding fluid management and drug dosing are crucial.

The primary challenge in detecting AKI is the reliance on markers like Scr and eGFR, which assume a steady state of creatinine production and elimination. In cases of AKI, these markers can lead to inaccurate assessments, resulting in inappropriate clinical decisions. For example, underestimating GFR during a transient decline could lead to unnecessary dose reductions, while overestimating GFR during a recovery phase could increase the risk of drug toxicity.

1.1.5 Estimated glomerular filtration and estimated creatinine clearance by pharmacokinetic modeling approach

Physiologically-based pharmacokinetic (PBPK) modeling and compartmental nonlinear mixed-effects modeling provide alternative approaches to estimate GFR under challenging conditions where traditional estimation methods may be less reliable. PBPK modeling can account for dynamic factors such as transporter-mediated interactions and disease-related changes, offering a more comprehensive assessment of GFR in patient populations with complex renal function alterations. For instance, a PBPK model was successfully used to predict changes in Scr in CKD patients, particularly during drug interactions with transporter inhibitors like trimethoprim and cimetidine.[54]

In critically ill patients, eGFR is further complicated by unstable renal function, making steady-state assumptions unreliable. In such cases, measured CrCL has traditionally been used, but it is susceptible to inaccuracies due to challenges in proper urine collection. A compartmental nonlinear mixed-effects model has been developed to overcome these limitations by incorporating serum and urine data with arbitrary timings and explicitly accounting for residual errors.[55] This dynamic model was shown to outperform traditional equations, such as Cockcroft-Gault and the MDRD, in assessing CrCL and describing drug elimination in critically ill patients.[55] The model-based approach, combined with population pharmacokinetics, allows for a more flexible and accurate estimation of renal function during non-steady-state conditions, providing valuable information for appropriate dose adjustments of renally eliminated drugs.

The use of PBPK and mixed-effects modeling not only improves GFR estimation in populations with fluctuating renal function but also enables a better understanding of the impact of disease processes and drug interactions on creatinine dynamics. However, a limitation of both PBPK and mixed-effects modeling in these studies is the assumption that the volume of distribution (V_d) for creatinine is 60% of TBW, which is not well founded on experimental data in humans. This assumption may introduce errors in estimating other parameters, potentially affecting the accuracy of the models. The magnitude of creatinine V_d is important because it determines how fast changes in CrCL are reflected by changes in plasma concentrations. Despite these limitations, the modelling approach shows promise for improving precision in clinical care, particularly for patients with rapidly changing kidney function, such as those with CKD or critical illnesses. This field of modeling helps connect laboratory research with clinical practice, leading to better patient outcomes through personalized drug dosing and improved monitoring of kidney function.

1.2 Tubular secretion

Beyond glomerular filtration, tubular secretion also plays a crucial role in drug elimination by actively transporting substances from the peritubular capillaries into the renal tubular lumen. Unlike glomerular filtration, which is a passive process driven by blood pressure, tubular secretion is an energy-dependent process that selectively removes specific compounds from the bloodstream.

In renal tubular cells, drug and metabolite transport often occurs through transporter chains spanning the basolateral and apical membranes.[56] These chains typically involve two distinct transporters working in tandem to facilitate the movement of substances from the bloodstream into the tubular lumen.[56] On the basolateral side, uptake transporters such as organic anion transporters (OAT1/OAT3) or organic cation transporter (OCT2) mediate the entry of substrates into tubular cells.[56] Subsequently, on the apical side, efflux transporters like multidrug and toxin extrusion proteins (MATE1/MATE2-K) or multidrug resistance-associated proteins (MRP2) actively expel these compounds into the urine, completing their renal excretion.[56] This coordinated action ensures efficient clearance of endogenous waste products and xenobiotics, including uric acid,[57] creatinine,[58] and drugs such as penicillin.[59] Additionally, the interplay between these transporters significantly influences drug-drug interactions and the risk of nephrotoxicity.[56]

1.2.1 Tubular secretion in drug elimination

Tubular secretion is essential for the elimination of many drugs, such as furosemide,[60] digoxin,[61] and certain antibiotics. These drugs are secreted via this pathway, which significantly impacts their pharmacological and toxicological responses. In some cases, tubular secretion contributes more to overall renal clearance than glomerular filtration. For instance, the renal clearance of cimetidine has been observed to be three times higher than CrCL, indicating a major role of tubular secretion in its elimination.[62] Similarly, tubular secretion is critical in tenofovir elimination, as renal clearance being 2- to 3- fold higher than CrCL.[63]

Tubular secretion has important clinical implications, particularly in renal clearance and drug-drug interactions. Certain drugs can affect renal transporters, altering the plasma concentrations of substrate drugs, potentially leading to reduced efficacy or increased toxicity. For instance, probenecid, a known OAT1 and OAT3 inhibitor, can reduce the renal clearance of methotrexate by inhibiting its uptake into renal tubular cells,[64] thereby elevating methotrexate plasma concentrations and increasing the risk of adverse effects, including nephrotoxicity and hepatotoxicity.[65] On the other hand, probenecid has also been used therapeutically to prolong the half-life of penicillin by inhibiting its tubular secretion, thereby increasing penicillin concentrations.[66]

1.2.2 Assessment of tubular secretion

Renal function is typically assessed using GFR and urinary albumin excretion, while tubular secretion often remains unquantified. However, tubular secretion does not always perfectly correlate with GFR and has been found to be highly variable among CKD patients.[67] Additionally, independent of GFR and albuminuria, reduced tubular secretion has been associated with a higher risk of adverse effects in patients with hypertension and cardiovascular disease.[68] Therefore, assessing tubular secretion may offer new insights into kidney function and aid in optimizing treatment strategies.

One commonly used method for assessing tubular secretion is to measure the clearance of endogenous compounds known to be secreted by the renal tubules. An ideal endogenous marker for secretion should be excreted into the urine intact, without undergoing metabolic degradation within the body, and should be quantifiable with ease, accuracy, and cost-efficiency.[69]

Table 6 Studied markers for assessment of tubular secretion.

Compound	PPB ratio (%)	Ratio of CL_r to eGFR/eCrCL	Responsible transporters
Endogenous			
Hippurate[70-72]	~40	10.3	OAT1 and OAT3
Pyridoxic acid[70,71,73]	87	10.1	OAT1 and OAT3
Dimethyluric acid[70,71]	~70	10.0	OAT1
Trimethyluric acid[70,71]	80	3.9, 5.8	OAT1
Isovalerylglycine[70,71]	4	5.0	OAT1 and OAT3
Kynurenic acid[70,71,74]	96	2.04	OAT1 and OAT3
N^1-methylnicotinamide[75,76]	0	1.5-3	OCT2 and MATE
Creatinine[77-79]	~4	1.1-1.4	OCT2 and MATE
Exogenous			
Adefovir[80,81]	<10%	2.3	OAT1
Ciprofloxacin[82-84]	0.2-0.3	1.1-3.1	OAT3
Metformin[39,85,86]	0	4.3	OCT2 and MATE

PPB, plasma protein binding; CL_r, renal clearance; eGFR, estimated glomerular filtration; eCrCL, estimated creatinine clearance; OAT, organic anion transporter; OCT, organic cation transporter; MATE, multidrug and toxin extrusion.

Table 6 lists previously studied markers for assessment of tubular secretion. Among these, endogenous compounds such as pyridoxic acid, dimethyluric acid, trimethyluric acid, and kynurenic acid exhibited high secretory clearance, attributed to their elevated plasma protein binding ratios, which effectively limit glomerular filtration.[58] In contrast, other endogenous compounds exhibited renal clearance rates substantially exceeding the GFR, providing evidence of active renal tubular secretion. Another method is to use specific drugs as probes, such as adefovir, ciprofloxacin, or metformin, which are eliminated largely through tubular secretion.[81,84,86] More examples of drugs used to assess transporter activity can be found in the FDA guidelines.[87] By monitoring the renal clearance of these probe drugs in the presence and absence of transporter inhibitors, such as probenecid or cimetidine, it is possible to evaluate the extent of tubular secretion.[88,89]

1.3 Vancomycin

Vancomycin is a glycopeptide antibiotic (structure displayed in Figure 1) widely used to treat severe infections caused by Gram-positive bacteria such as *Staphylococcus aureus* (MRSA).[90] Due to its potent antibacterial activity, vancomycin has been used as a drug last resort in critical care settings where other options have failed.[91] Given its wide use, vancomycin has become an essential tool in combating healthcare-associated infections, despite the challenges associated with its pharmacokinetics and toxicity.[92]

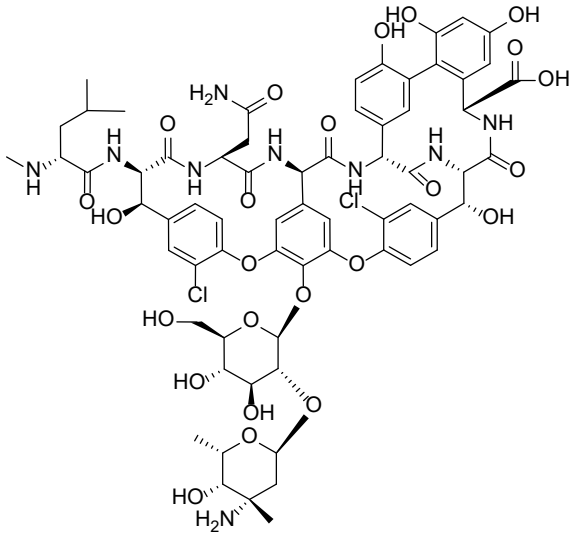

Figure 1 Chemical structure of vancomycin.

1.3.1 Clinical applications and adverse effects

Vancomycin is used to treat a variety of infections caused by Gram-positive bacteria, including endocarditis, pneumonia, osteomyelitis, and bloodstream infections.[93] The oral form of vancomycin is specifically utilized for *Clostridium difficile* infections in the gastrointestinal tract, as its poor systemic absorption allows it to achieve high local concentrations in the gut.[94] Vancomycin is also used as part of empirical therapy for febrile neutropenia and as prophylaxis in surgical settings for patients with prosthetic implants or known MRSA colonization.[95,96]

In addition to its therapeutic effects, vancomycin requires careful monitoring due to its narrow therapeutic index and the associated risks of nephrotoxicity and ototoxicity. A retrospective cohort study involving 5,000 patients demonstrated that vancomycin, when used to treat MRSA infections, had an 80% clinical success rate but was associated with a 15% incidence of nephrotoxicity, underscoring the need for careful dosing and monitoring.[97] Another randomized controlled trial comparing the treatment of MRSA pneumonia with linezolid and vancomycin reported a higher incidence of nephrotoxicity with vancomycin (18.2% vs. 8.4%).[98] Ototoxicity, though less common, can lead to irreversible hearing loss, particularly with prolonged therapy or in patients receiving concomitant ototoxic drugs. A study found that ototoxicity, including symptoms such as tinnitus and hearing loss, occurred in 12% of patients treated with high doses of vancomycin, particularly when used in combination with other ototoxic agents.[99] The risk was notably higher in patients receiving vancomycin monotherapy.

1.3.2 Pharmacokinetics and dosing challenges

Vancomycin pharmacokinetics and dosing present significant challenges due to the narrow therapeutic index and significant inter-individual variability (IIV) among patients.[92] Vancomycin is usually administered intravenously for systemic infections because its oral absorption is negligible, with bioavailability close to 0.[100] After administration, the drug distributes well into body fluids and tissues but is primarily confined to the extracellular fluid as the V_d is typically reported as 0.4–1.0 L/kg.[101] Vancomycin has a low plasma protein binding ratio of approximately 30% and is primarily eliminated via glomerular filtration, with about 80–90% excreted unchanged in the urine in individuals with normal renal function.[101] The elimination half-life of vancomycin is typically 3–9 hours in patients with normal renal function and can be significantly prolonged up to 7.5 days in patients with impaired renal function.[100,102] Therefore, vancomycin dosing requires a cautious and individualized approach in patients with renal impairment. Dosing adjustments should be based on eCrCL or eGFR, and TDM is critical to ensure trough concentrations (C_{trough}) or the daily area under the curve (AUC_{24}) remain within the target therapeutic range while minimizing the risk of adverse effects.

A previous pharmacokinetic/pharmacodynamic (PK/PD) target tentatively suggested for vancomycin TDM was a plasma C_{trough} of 15–20 mg/L for adult patients; however, data supporting this target are very limited.[103] Recent evidence indicates that a more reliable PK/PD target in plasma is an AUC_{24} to minimum inhibitory concentration (AUC_{24}:MIC) ratio of ≥400, considering both efficacy and safety,[104] as the risk of AKI with AUC-guided monitoring is significantly lower than with C_{trough}-guided monitoring.[105] Furthermore, studies evaluating the relationship between AUC_{24} and AKI suggest that maintaining an AUC_{24} in plasma between 400–600 mg·h/L optimizes efficacy while minimizing toxicity.[104]

Despite its effectiveness, vancomycin therapy faces dosing challenges due to IIV in pharmacokinetics, influenced by factors such as age, body weight, renal function, illness, and associated comorbidities.[106] In critically ill patients, augmented renal clearance can lead to subtherapeutic vancomycin concentrations, necessitating higher doses to achieve target concentrations.[107] The increasing prevalence of obesity further complicates vancomycin dosing due to altered drug distribution and clearance, often requiring weight-based dosing adjustments.[108] In pediatric and neonatal populations, immature renal function and rapid physiological changes require careful consideration in vancomycin dose adjustments to avoid toxicity or suboptimal efficacy.[109,110]

The implementation of TDM improves therapeutic precision but is not without limitations, including logistical challenges in sampling and delays in laboratory reporting.[111] The integration of population pharmacokinetic (popPK) models and Bayesian dosing tools has emerged as a promising approach to address these issues. However, popPK models developed using data from limited or specific patient groups may not accurately predict drug behavior in other populations, reducing their applicability to individual patients with different characteristics. Therefore, addressing these challenges is critical for achieving optimal clinical outcomes while minimizing the risks associated with vancomycin use.

1.3.3 Previous population pharmacokinetic models of vancomycin

Vancomycin exhibits significant inter-individual pharmacokinetic variability, necessitating individualized dosing strategies to achieve optimal therapeutic outcomes.[92] To better achieve this, popPK models have been extensively developed across diverse populations, including adults,[112] pediatric patients,[113] neonates,[114] elder patients, obese patients,[115] critically ill patients,[116] and those with renal impairment.[117]

Across studies, one- and two-compartment models with first-order elimination are commonly used in vancomycin popPK models.[118] Given its predominant renal elimination, vancomycin clearance is strongly correlated with CrCL or eGFR, making these key covariates in most popPK models.[112-117] In pediatric and neonatal populations, additional covariates such as postmenstrual age and Scr are used to account for renal maturation.[113] While traditional models rely on Scr-based renal function estimates, recent studies have explored alternative markers like cystatin C to enhance clearance predictions.[119] These models help quantify IIV and refine dosing regimens to achieve therapeutic targets while minimizing toxicity.

Advancements in popPK modeling have increasingly incorporated Monte Carlo simulations to evaluate the probability of achieving AUC-based therapeutic targets (AUC/MIC $\geq$ 400 for efficacy and $\leq$ 600 to avoid toxicity).[119] Furthermore, popPK models are now being integrated into clinical decision support tools and Bayesian forecasting software, supporting model-informed precision dosing approaches in real-world practice.[120,121] These developments highlight the growing role of vancomycin popPK models in optimizing individualized therapy across diverse patient populations.

1.3.4 Applications in patients with external ventricular drain

Vancomycin is a standard therapy for central nervous system (CNS) infections, such as ventriculitis and meningitis.[122] External ventricular drains (EVDs) are commonly used to

manage elevated intracranial pressure or drain cerebrospinal fluid (CSF) in conditions like hydrocephalus or traumatic brain injury. However, due to their invasive nature, EVDs significantly increase the risk of CNS infections.[123] To prevent or treat these infections, vancomycin is frequently administered in patients with EVDs.

In addition to the challenges of individualizing vancomycin therapy due to variable renal function, its use in treating CNS infections is further complicated by its inconsistent penetration into the CSF, with CSF-to-serum ratio of vancomycin varied from 0.00 to 0.81 in 13 identified studies.[124] This variability is primarily attributed to vancomycin's hydrophilic nature and large molecular size, which hinder its ability to traverse the blood-brain barrier (BBB).[125] Consequently, vancomycin CSF concentrations are highly variable and unpredictable, largely depending on the integrity of the BBB.[125] Vancomycin CSF concentrations are highly variable and unpredictable in most cases because the extent of vancomycin penetration depends much on the integrity of the BBB.[124,126,127] The BBB damage caused by the inflamed meninges has also been proven to enhance the penetration of vancomycin into the CSF. So far, only a few studies investigated the pharmacokinetics of vancomycin in CSF, reporting several validated popPK models, in which CSF albumin or lactate concentrations were related to the distribution of vancomycin into the CSF, thus helping to predict CSF concentration after intravenous administration.[128-130] Available data in individual studies is sparse, validation of developed predictors is limited, and there is still insufficient knowledge on vancomycin CSF penetration and the respective covariates in neurological/neurosurgical patients.

2 Aim and objectives

2.1 Refinement and application of creatinine population pharmacokinetic model

The aim of this study is to develop and refine a popPK model for creatinine to enhance the understanding of its kinetics and its utility in assessing renal function and transporter activity. The specific objectives are:

a) To estimate the PK parameters of creatinine using a popPK approach based on published data;
b) To refine the existing creatinine model and reduce bias in PK parameter estimation using new data from dense plasma and urine sampling in healthy volunteers;
c) To improve the characterization of creatinine kinetics through a joint model with iohexol, enabling more reliable assessments of renal function and/or OCT/MATE transporter activity;
d) To investigate the influence of creatinine V_d on the prediction of GFR following AKI;
e) To evaluate a limited sampling strategy for simultaneous assessment of GFR and OCT/MATE transporter activity.

2.2 Vancomycin pharmacokinetics investigation in patients with external ventricular drains

As a renally excreted drug, vancomycin pharmacokinetics are highly dependent on renal function, making an accurate assessment of kidney function essential for optimizing its dosing. This section aims to investigate vancomycin pharmacokinetics in patients with EVDs using popPK approach. The specific objectives are:

a) To describe the systemic pharmacokinetics of vancomycin including the influence of renal function in patients with EDV;
b) To describe the link between systemic and CSF pharmacokinetics of vancomycin in patients with EDV;
c) To identify predictors of vancomycin penetration into CSF;
d) To assess the feasibility of collecting CSF samples from the distal port of EVDs for TDM using a newly developed popPK model;
e) To evaluate the benefits of different infusion modes and dosages through model-based simulations.

3 Methods

3.1 Retrospective analysis on published creatinine pharmacokinetic data in healthy participants following ingestion of meat

The PK data for creatinine were captured from the publication by Mayersohn *et al.*[131] Both plasma and urine data during 24 hours following a breakfast containing 225 g boiled beef or no beef ingestion in 6 healthy male subjects were obtained to establish the model. A creatinine popPK model was developed, incorporating a zero-order creatinine generation rate (CGR) and first-order clearance (CL). The individual creatinine "dose" for each subject was estimated using a predefined arbitrary population dose, with post-hoc estimates of apparent bioavailability (F1) serving as an individual correction factor for this dose. A schematic diagram of the creatinine model is shown in Figure 2.

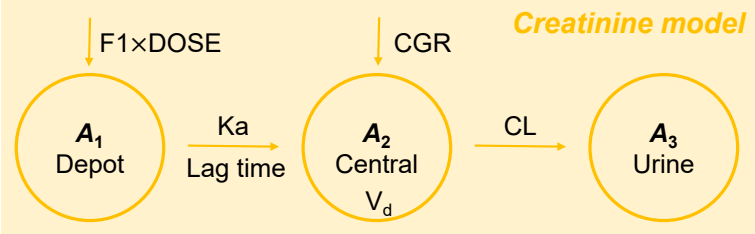

Figure 2 Schematic diagram of the creatinine model.
The structural model for creatinine was parameterized in terms of absorption rate constant (Ka), clearance (CL), volume of distribution (V_d), and creatinine generation rate (CGR). Creatinine from boiled beef entered the depot compartment (A_1) and was absorbed into the central compartment (A_2). Meanwhile, endogenously produced creatinine entered the central compartment directly at a zero-order CGR. Finally, creatinine was eliminated into the urine compartment (A_3) through first-order elimination.

For further details, please refer to the publication below.

Chen Z, Chen C, Taubert M, Mayersohn M, Fuhr U. A population pharmacokinetic model for creatinine with and without ingestion of a cooked meat meal. *Eur J Clin Pharmacol*. 2022. 78:1945-1947. https://doi.org/10.1007/s00228-022-03398-9

3.2 A new clinical study in healthy volunteers following iohexol administration and meat ingestion with simultaneous population pharmacokinetic modelling on iohexol and creatinine data

A crossover clinical study was designed, with participants receiving either iohexol intravenously without breakfast (non-meat period) or 250 g cooked beef as a breakfast 25 minutes after intravenous administration of iohexol (meat period). A dense time-sampling strategy was implemented for both plasma and urine samples following iohexol administration. A new liquid chromatography with tandem mass spectrometry (LC-MS/MS) method was developed, validated, and applied for measurement of creatinine concentrations in plasma and

urine. A joint pharmacometric model for iohexol and creatinine was developed using dense plasma and urine sampling. A schematic diagram of the creatinine model is shown in Figure 3.

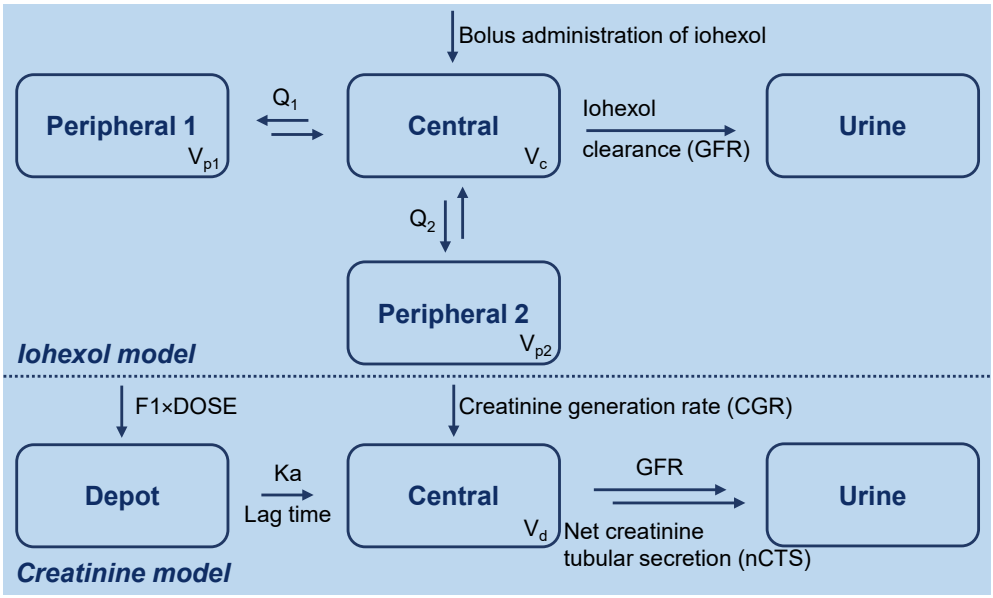

Figure 3 Schematic diagram of the joint model of iohexol and creatinine.
Iohexol was modelled using a three-compartment linear elimination model, and creatinine with a one-compartment model. A first-order process with lag time and a zero-order process described creatinine uptake from meat and endogenous production, respectively. In this joint model, iohexol clearance represented GFR and creatinine clearance represented the sum of glomerular filtration and net creatinine tubular secretion.

The popPK modeling was conducted using a nonlinear mixed-effects approach with NONMEM version 7.4.0 (ICON Development Solutions, USA), Perl-speaks-NONMEM (PsN) version 5.3.0 (Uppsala University, Sweden), using the first-order conditional estimation with interaction method throughout model development. The following assumptions were made for all participants: 1) no changes in typical value of iohexol clearance (IoCL), CrCL, and CGR throughout the study; 2) iohexol and creatinine are solely eliminated via the kidneys; and 3) the circadian rhythms of IoCL and CrCL follow a consistent sine function pattern within a day.[3] Simulations were used to evaluate the effect of different creatinine V_d values on CrCL estimation after AKI and to assess the impact of limited sampling strategies on GFR and nCTS (net creatinine tubular secretion) estimation.

A detailed description of the bioanalysis method is provided in Section 3.2.1. For additional details on this study, please refer to the publication below.

Chen Z, Dong Q, Dokos C, Boland J, Fuhr U, Taubert M. A joint pharmacometric model of iohexol and creatinine administered through a meat meal to assess GFR and renal OCT2/MATE activity. *Clin Pharmacol Ther*. 2025. Epub ahead of print. https://doi.org/10.1002/cpt.3612

3.2.1 Determination of plasma and urine concentrations by liquid chromatography with tandem mass spectrometry

3.2.1.1 Chemicals and reagents

Creatinine ($C_4H_7N_3O$) and creatinine-d_3 ($C_4H_4D_3N_3O$) were bought from Cayman Chemical Company. (Ann Arbor, Michigan). HPLC-grade acetonitrile, methanol, and ammonium acetate were prepared from Merck (Darmstadt, Germany). Utilizing Milli-Q gradient purification system, water was purified and deionized (Millipore, Molsheim, France).

3.2.1.2 Preparation of calibration standards and quality control samples

Two stock solutions, each containing 8 mg/mL of creatinine in acetonitrile:water (1:1, v/v), were prepared independently and subsequently diluted with acetonitrile:water (1:1, v/v) to produce working solutions. Calibration working solutions for plasma/urine, with the following concentrations – 40.0/200, 80.0/400, 160/800, 240/2000, 320/4000, 480/8000, 640/16000, and 800/20000 µg/mL – were prepared by further dilution of the first stock solutions. Quality control (QC) working solutions were prepared by diluting the second stock solution at concentrations of 120/600 (lower quality control, LQC), 300/3000 (middle quality control, LQC), and 600/15000 (higher quality control, HQC) µg/mL for plasma/urine QC standards. Following this, all working solutions of 10 µL were added to a blank human plasma (more than 95%) of 190 µL to obtain the calibration standards and QC samples of creatinine. Creatinine-d_3 was used as the internal standard (IS). The IS solution, at a concentration of 10.0 µg/mL, was prepared by diluting the stock solution with acetonitrile:water (1:1, v/v) at concentration. All stock and working solutions and samples required for analysis were stored at -20°C.

3.2.1.3 Sample pretreatment

Human plasma (50.0 µL) or urine (10.0 µL) samples were dispensed into separate 96-well plates, followed by the addition of creatinine-d_3 (IS) working solution (10.0 µg/mL) in volumes of 50.0 µL for plasma and 10.0 µL for urine. The samples were deproteinized using 200 µL of acetonitrile, vortexed for 30 seconds, and centrifuged at 4000 rpm for 15 minutes at room temperature.

For plasma samples, a 100-µL aliquot of the resulting supernatant was transferred to a new 96-well plate and mixed with 100 µL of acetonitrile. For urine samples, a 20.0-µL aliquot of the supernatant was transferred and mixed with 200 µL of acetonitrile. All prepared samples were analyzed using LC-MS/MS.

3.2.1.4 Quantification of creatinine via liquid chromatography with tandem mass spectrometry

Quantitative analysis was performed using an Agilent 1200 liquid chromatography system, which includes a binary pump and a 1260 autosampler (Agilent Technologies Deutschland GmbH, Waldbronn, Germany), coupled with an API 5000 triple quadrupole mass spectrometer equipped with an electrospray ionization source (AB Sciex Germany GmbH, Darmstadt, Germany). The data were analyzed using Analyst (version 1.6.2) software.

Creatinine was separated on a ZIC-HILIC HPLC Column (5 µm, 2.1×100 mm, Merck, Germany) at a column temperature of 40°C using mobile phases of water containing 0.1% formic acid (A) and acetonitrile containing 0.1% formic acid (B). The gradient elution mode was set as follow: 0–0.3 min, 15%A; 0.3–1.0 min, 15–70%A; 1.0–2.5 min, 70%A; 2.5–2.51 min, 70%–15%A; 2.51–4.00 min, 15%A, with a flow rate of 0.6 mL/min. The settings for IonSpray voltage and temperature were 4500 V and 400°C, respectively. The ion-pair transitions of 114.0→86.0 and 117.0→89.0 were used to monitor creatinine and creatinine-d_3 (IS), respectively.

3.2.1.5 Method validation

3.2.1.5.1 Matrix effect in plasma and assessment of surrogate matrix for urine

To evaluate the matrix effect of creatinine in plasma, creatinine and IS solutions were spiked into post-extracted plasma. Their peak areas, after baseline subtraction, were compared with those of pure solutions at equivalent concentrations.[132] The matrix effect was evaluated using the IS normalized matrix factor (IMF), calculated as follows:

$$Relative\ response\ factor\ (RRF) = \frac{Creatinine\ peak\ area}{IS\ peak\ area}$$

$$IMF = \frac{RRF(extracted\ QC\ samples) - RRF\ (baseline\ plasma\ samples)}{RRF\ (water)}$$

The appropriateness of using deionized water as a surrogate matrix for urine was investigated by assessing the creatinine-to-IS ratio in mixtures (v/v, 1:1) of pure creatinine and IS with six urine sample aliquots. A percentage difference within ±20% between this ratio in the mixed samples and the theoretical value is deemed acceptable as a potential matrix.[133]

3.2.1.5.2 Linearity

Calibration curves covering concentrations ranging from 2.00 to 40.0 µg/mL (plasma) and 10.0 to 1000 µg/mL (urine) were constructed by analyzing spiked calibration samples over three consecutive batches. Each calibration curve was individually evaluated using weighted (1/x) linear regression, where x represented the nominal analyte concentration. The value of r^2 (a measure of the goodness of fit) was considered to be more than 0.9900.

3.2.1.5.3 Accuracy and precision

Accuracy is defined as the degree of closeness between a measured value and the actual concentration of the analyte and was assessed as the relative error (RE) at four different concentrations. Precision refers to the closeness of repeated measurements of the same analyte and is estimated using the coefficient of variation (CV).

Intra-batch precision and accuracy were evaluated by analyzing the lowest limit of quantification (LLOQ), LQC, MQC, and HQC samples (2.00, 6.00, 15.0, and 30.0 µg/mL in plasma samples; 10.0, 30.0, 150, and 750 µg/mL in urine samples), with six determinations per concentration. The analytical run was repeated over three separate batches to assess inter-batch precision and accuracy. Accuracy (%) and precision (CV, %) were calculated using the following formulas:

$$Accuracy\ (RE, \%)\ = (\frac{Mean\ measured\ concentration}{Theoretical\ concentration} - 1)\ \times\ 100$$

$$Precision\ (CV, \%)\ =\ \frac{Standard\ deviation\ (SD)}{Mean}\ \times\ 100$$

The accuracy was classified as good when RE fell within ±20% and ±15% for the theoretical values of LLOQ and remaining concentration levels, respectively. Both intra- and inter-batch precision fell within the predefined limits if CV was <20% and <15% for the LLOQ and remaining concentration levels, respectively.

3.2.1.5.4 Recovery

Recovery refers to the efficiency with which an analytical method extracts and measures an analyte from a biological matrix (such as plasma or urine), compared to the analyte's true concentration. It should be consistent and reproducible across different concentration levels of the analyte. The recovery of creatinine is assessed using LQC, MQC, and HQC samples and matrix samples extract spiked with target analyte and IS at the same concentrations. Every QC

and post-extraction spiked sample is analyzed six times. The recovery is calculated using the following equation:

$$Recovery\ (\%) = \frac{RRF\ (spiked\ QC\ samples) - RRF\ (spiked\ blank\ samples)}{RRF\ (QC\ samples) - RRF\ (blank\ samples)} \times 100$$

3.2.1.5.5 Stability

The stability of creatinine in human plasma and urine was assessed by analyzing six QC samples at two different concentration levels (LQC and HQC), exposed to various time and temperature conditions. The results were compared with those of freshly prepared stock solutions and QC samples. The storage conditions included short-term stability (room temperature for 6 hours), auto-sampler stability (4°C for 27 hours), three freeze-thaw cycles (from -20°C to room temperature), and long-term storage at -20°C. Creatinine was considered stable if the measured concentrations at LQC and HQC levels were within ±15% of the theoretical values.

3.3 Retrospective analysis on creatinine data in patients following cardiac surgery using established creatinine model

3.3.1 Study design and data organization

Creatinine serum concentration-time profiles in patients after cardiac surgeries, along with demographic information, were obtained from two clinical trials, separately. The first clinical study (KCH) was designed to investigate the impact of short-term diet restriction (DR) on the prevention of AKI in at-risk patients undergoing cardiac surgery.[134] The second clinical study (KMN) aimed to investigate the ability of dietary restriction to prevent contrast-induced AKI in patients undergoing percutaneous coronary angiography.[135] For both studies, creatinine serum concentrations before surgery and at 24 and 48 hours after surgery, the time of concentration measurement, surgery start and end times, diet group (1 for the DR group and 2 for the control group), calorie intake before surgery, CKD stages, iohexol dose, AKI risk factors (f_{risk}), and demographic information were extracted from the raw data. Surgery duration, TBW, body mass index (BMI), and lean body mass were subsequently calculated for further evaluation using reported equations. Patients without documented concentration measurement times and/or surgery start and end times were excluded from the study (4 from KCH and 6 from KMN). It was assumed that AKI occurred with an immediate change in CrCL at the start of surgery and persisted throughout the observation period for all patients. The schematic diagram is shown in Figure 4.

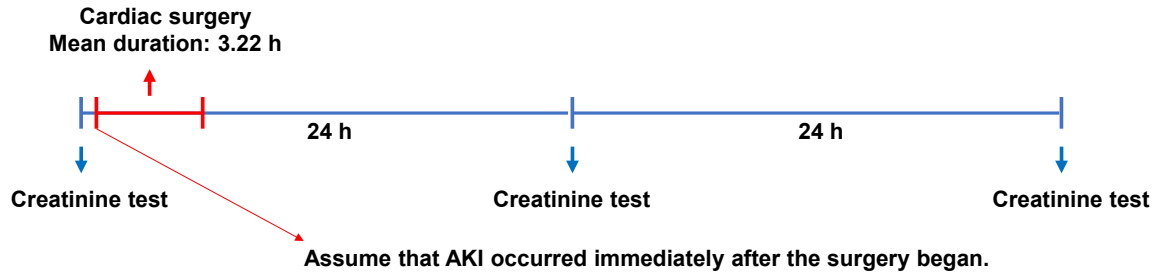

Figure 4 Schematic diagram of the study protocol and occurrence of acute kidney injury.

3.3.2 Creatinine model

Model execution and diagnostic procedures were performed using PsN version 5.3.0 (Uppsala University, Sweden). The first-order conditional estimation with interaction method was used throughout model development. A statistical criterion based on a difference of >3.84 in the objective function value (OFV) between two nested models ($p < 0.05$) that differed by one parameter was employed for model selection.

The structural model was developed based on creatinine plasma and urine data in healthy volunteers (see section 3.2). A one-compartment model with first-order elimination kinetics was applied in this model. The IIV for PK parameters was modeled exponentially as following equation: $\theta_i = \theta \times e^{\eta_i}$, where θ_i represents the value of the individual parameter, θ represents the population point estimate of the parameter, and η_i represents a normally distributed random variable with a mean of 0 and variance of ω^2. A proportional residual error model was used for creatinine concentrations. The relative change in creatinine clearance following surgery (rCrCL%) (indicating AKI degree) for each patient was assessed using an established creatinine model.

$$rCrCL\% = (\frac{changed\ CrCL}{baseline\ CrCL} - 1) \times 100\%$$

For the purpose of the present evaluation, parameters including CrCL, IIV of CrCL, rCrCL%, IIV of rCrCL%, and residual error for creatinine concentration were estimated, while the V_d and CGR along with the IIV of CGR were fixed at estimated values from healthy volunteers.

Covariate analysis was performed on the structural model using forward addition method. In this procedure, variables are incorporated to the model one at a time, starting with the variable that has the strongest correlation with the dependent variable until no more variables meet the criteria for inclusion. A significance level of 0.05 (ΔOFV $\leq$ -3.84) was employed in this procedure. For covariate relationships, continuous covariates were modeled with mean-centered exponential models and categorical covariates were modeled with conditional effects.

Following this, potential relationships between the rCrCL% and the collected information were illustrated through correlation plots. Subgroup analysis was conducted for sex, BMI, and CKD stage in KCH study, and sex, BMI, iohexol dose, and AKI risk factor in KMN study.

3.4 Plasma and cerebrospinal fluid population pharmacokinetics of vancomycin in patients with external ventricular drain

This study was conducted in patients with EVDs who received vancomycin treatment. Blood and CSF samples were collected from the proximal or distal port of the EVDs to measure vancomycin concentrations and clinical parameters.[136] Patients were classified based on whether the primary infection was a CNS infection or not.

The popPK model was developed and diagnosed based on vancomycin plasma and CSF concentrations using NONMEM and PsN. Model development employed the first-order conditional estimation with interaction method, using a decrease of >3.84 in the OFV between two nested models ($p < 0.05$) as the statistical criterion for parameter inclusion. Covariates were assessed through stepwise forward inclusion ($p < 0.05$) using the PsN tool.

Model-based simulations were conducted to evaluate different dosing regimens in virtual patients with primary CNS infection. Three infusion strategies—intermittent infusion, continuous infusion with a loading dose, and continuous infusion without a loading dose—were compared based on the daily area under the plasma concentration-time curve and the CSF trough concentration, both of which are commonly used PK/PD targets for vancomycin therapy.[104,137]

For further details on this study, please refer to the publication below.

Chen Z, Taubert M, Chen C, Dokos C, Fuhr U, Weig T, Zoller M, Heck S, Dimitriadis K, Terpolilli N, Kinast C, Scharf C, Lier C, Dorn C, Liebchen U. Plasma and cerebrospinal fluid population pharmacokinetics of vancomycin in patients with external ventricular drain. *Antimicrob Agents Chemother*. 2023. 67:e0024123. https://doi.org/10.1128/aac.00241-23

4 Results

4.1 Retrospective analysis on published creatinine pharmacokinetic data in healthy participants following ingestion of meat

The popPK model was developed using a dataset comprising 133 serial plasma values and 11 urine values. A one-compartment PK model with linear elimination, first-order absorption, and zero-order creatinine generation provided a good fit for the creatinine PK data. Diagnostic plots demonstrated an overall good fit of the final model to the data, and bootstrap results confirmed its stability. Finally, the PK parameters estimated from the creatinine model included apparent absorption rate (Ka, 1.76 1/h), CL (7.59 L/h), V_d (53.9 L), F1 (157%), CGR (67.9 mg/h), and lag time (0.344 h). The estimated V_d of creatinine was 53.9 L, corresponding to 73.8% of TBW, which is close to but higher than the fraction of total body water.

For comprehensive results of this study, please refer to the publication below.

Chen Z, Chen C, Taubert M, Mayersohn M, Fuhr U. A population pharmacokinetic model for creatinine with and without ingestion of a cooked meat meal. *Eur J Clin Pharmacol*. 2022. 78:1945-1947. https://doi.org/10.1007/s00228-022-03398-9

4.2 A new clinical study in healthy volunteers following iohexol administration and meat ingestion with simultaneous population pharmacokinetic modelling on iohexol and creatinine data

Fourteen participants, mean age 33 years (range: 23–48), were enrolled, including 2 in the pilot and 12 in the main study. The dataset includes 771 iohexol and 826 creatinine plasma concentrations, and 439 measurements for both iohexol and creatinine in urine. A joint model for iohexol and creatinine was developed to accurately describe plasma and urine concentrations, incorporating CrCL as the sum of GFR (equivalent to IoCL) and nCTS, while accounting for TBW effects and circadian variation. Pharmacokinetic parameters for iohexol and creatinine aligned with reported values, but a lower V_d of 41% of TBW and a nCTS fraction of 31% relative to overall CrCL were observed. Additionally, sex was identified as a statistically significant covariate on nCTS. Commonly used equations based on single-point creatinine measurement all overestimated GFR, with the MDRD equation performing best, followed by CKD-EPI 2009 equation. Simulations demonstrate the effect of V_d estimate accuracy on detecting AKI from creatinine plasma concentrations only. Following low-dose iohexol administration of 259 mg, a single plasma sample at 5 hours and a urine sample from

0–5 hours provided accurate estimates of both GFR and nCTS using the joint model and even enabled adequate correction for possibly incomplete urine collection.

A detailed description of the LC-MS/MS method validation results is provided in Section 4.2.1. For comprehensive results of this study, please refer to the publication below.

Chen Z, Dong Q, Dokos C, Boland J, Fuhr U, Taubert M. A joint pharmacometric model of iohexol and creatinine administered through a meat meal to assess GFR and renal OCT2/MATE activity. *Clin Pharmacol Ther*. 2025. Epub ahead of print. https://doi.org/10.1002/cpt.3612

4.2.1 Validation of the quantification method for determining plasma and urine concentrations

4.2.1.1 Matrix effect in plasma and assessment of surrogate matrix for urine

The mean IMF for creatinine was 0.83 in the plasma. The CV of IMF was within 8.1–10.0% (Table 7). The chromatogram of creatinine is shown in Figure 5.

Table 7 Matrix effect of plasma.

Matrix	Theoretical concentration	IMF (mean ± SD)	IMF (CV)
Plasma	LQC (6.00 µg/mL)	0.77 ± 0.07	10.0%
	HQC (30.0 µg/mL)	0.88 ± 0.07	8.1%

IMF, IS normalized matrix factor; SD, standard deviation; CV, coefficient of variation; LQC, lower quality control; HQC, higher quality control.

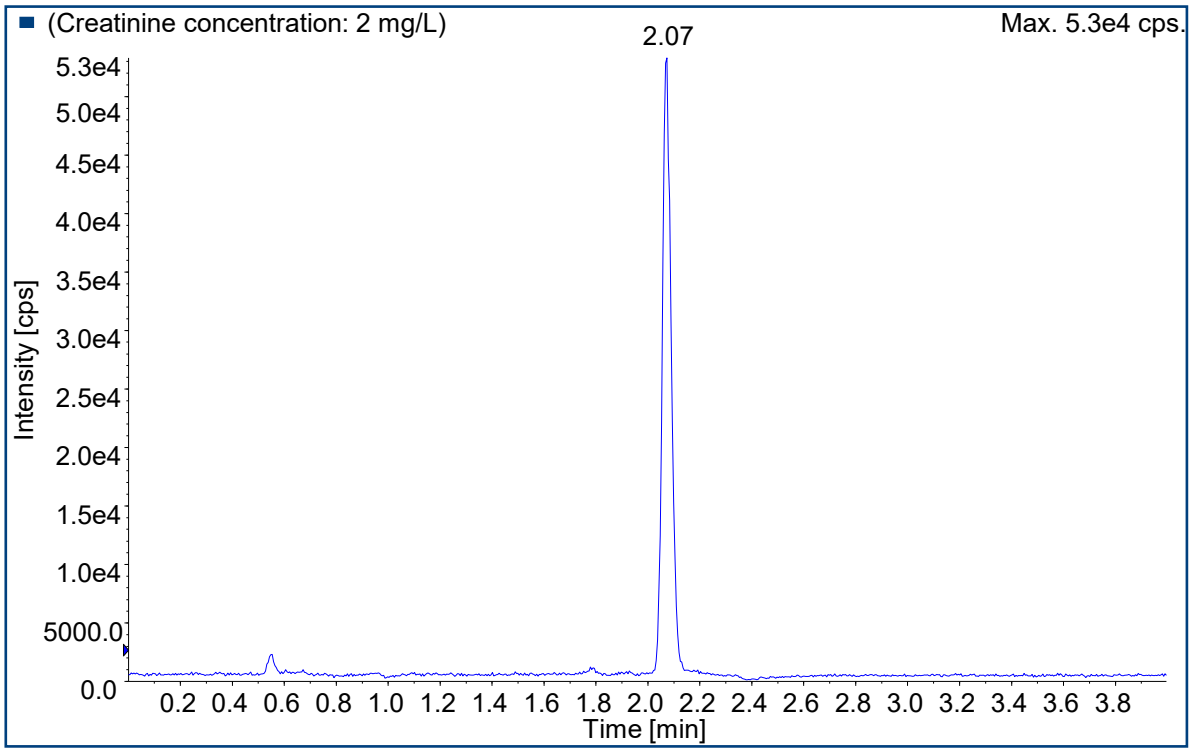

Figure 5 Chromatogram of creatinine at a concentration of 2 mg/L with a retention time of 2.07 min.

The appropriateness of using deionized water as a surrogate matrix for urine was confirmed by obtaining percentage differences within the range of -1% to 6% between the creatinine-to-IS ratio in the mixed samples and the theoretical value.

4.2.1.2 Linearity

The calibration curves demonstrated good linearity over the concentration ranges of 2.00–40.0 μg/mL for plasma and of 10.0–1000 μg/mL for urine. The correlation coefficients of the calibration curves were >0.99. Additionally, the linear regression equations for plasma and urine were calculated as follows: y = 0.0786x – 0.0149 (r^2 = 0.9977) and y = 0.0804x + 0.357 (r^2 = 0.9980), respectively.

4.2.1.3 Accuracy and precision

The REs for accuracy ranged from -14.8% to 13.0% in plasma and -13.2% to 11.0% in urine, while the CVs for precision ranged from 0.9% to 6.9% in plasma and 0.7% to 7.9% in urine. The mean REs and CVs for different concentration levels during intra- and inter-batch analyses are presented in Table 8.

Table 8 Intra- and inter-batch accuracy and precision.

Theoretical Concentration	Intra-batch accuracy (%)	Intra-batch CV (%)	Inter-batch accuracy (%)	Inter-batch CV (%)
Plasma				
LLOQ (2.00 μg/mL)	6.4	6.6	1.0	4.0
LQC (6.00 μg/mL)	5.7	4.6	1.9	4.3
MQC (15.0 μg/mL)	5.7	3.0	3.1	3.2
HQC (30.0 μg/mL)	5.6	5.7	4.6	0.9
Urine				
LLOQ (10.0 μg/mL)	-4.7	7.5	-5.3	0.5
LQC (30.0 μg/mL)	-6.0	5.3	-6.8	0.7
MQC (150 μg/mL)	10.3	1.8	6.6	2.8
HQC (750 μg/mL)	4.8	2.1	-0.3	4.2

LLOQ, lowest limit of quantification; LQC, lower quality control; MQC, middle quality control; HQC, higher quality control.

4.2.1.4 Recovery

The mean recoveries of creatinine were 87.4% and 99.1% in plasma and urine, respectively (Table 9).

Table 9 Recoveries for different concentration levels of quality control samples.

Matrix	Theoretical concentration	Peak area ratio (mean ± SD)		Recovery (%)
		Pre-extraction spiked	Post-extraction spiked	
Plasma	LQC (6.00 µg/mL)	1.15 ± 0.03	1.04 ± 0.01	90.6
	MQC (15.0 µg/mL)	2.00 ± 0.05	1.78 ± 0.02	88.8
	HQC (30.0 µg/mL)	3.38 ± 0.06	2.80 ± 0.03	82.7
Urine	LQC (30.0 µg/mL)	2.13 ± 0.04	2.09 ± 0.58	97.8
	MQC (150 µg/mL)	12.1 ± 0.2	11.3 ± 1.1	93.4
	HQC (750 µg/mL)	56.5 ± 0.9	59.9 ± 4.0	106

SD, standard deviation; LQC, lower quality control; MQC, middle quality control; HQC, higher quality control.

4.2.1.5 Stability

Creatinine in plasma and urine samples was stable at room temperature for 27 hours, in a refrigerator at -20°C, and after four freeze/thaw cycles between -20°C and room temperature (Table 10).

Table 10 Creatinine stability in different conditions.

Stability	Theoretical concentration	Measured Concentration (µg/mL)	Accuracy (%)	Precision (CV%)
Plasma				
Freeze-thaw	LQC (6.00 µg/mL)	6.01 ± 0.44	100	7.2
	HQC (30.0 µg/mL)	32.0 ± 0.9	107	2.7
Room temperature	LQC (6.00 µg/mL)	5.40 ± 0.10	89.6	2.2
	HQC (30.0 µg/mL)	29.7 ± 0.7	99.0	2.3
Short-term (-20°C)	LQC (6.00 µg/mL)	6.64 ± 1.40	111	6.0
	HQC (30.0 µg/mL)	33.1 ± 0.9	110	2.7
Urine				
Freeze-thaw	LQC (30.0 µg/mL)	28.2 ± 0.5	94.0	1.9
	HQC (750 µg/mL)	710 ± 14	94.6	2.0
Room temperature	LQC (30.0 µg/mL)	25.0 ± 0.7	96.7	2.7
	HQC (750 µg/mL)	654 ± 14	87.2	2.2
Short-term (-20°C)	LQC (30.0 µg/mL)	26.1 ± 0.6	86.9	2.1
	HQC (750 µg/mL)	748 ± 12	99.7	1.6

CV, coefficient of variation; LQC, lower quality control; MQC, middle quality control; HQC, higher quality control.

4.3 Retrospective analysis on creatinine data in patients following cardiac surgery using the established creatinine model

Estimates of CrCL and rCrCL% by the creatinine model are listed in Table 11. Correlation between post-hoc rCrCL% estimated by creatinine model and investigated factors for KCH and KMN studies are shown in Figure 6 and Figure 7, respectively. The covariate analysis results for all patients and investigated subgroups are listed in Table 12. In the KMN study, including f_{risk} and surgery duration as covariates on rCrCL% led to a reduction in OFV by -

9.79 and -4.84, respectively. However, the covariate of surgery duration was no longer significant after including the f_{risk}. Therefore, only the f_{risk} was retained in the final model.

Table 11 Estimates of creatinine clearance and factor by which creatinine clearance changes following surgery (rCrCL%) by creatinine model.

	KCH study		KMN study		
Parameter[a]	**Estimate**	**RSE (%)**[b]	**Estimate**		**RSE (%)**[b]
CrCL (L/h)	3.49	4.1	3.05		3.8
rCrCL%	-5.9	3.0	-2.1	($f_{risk} \leq 2$)	1.9
			-12.3	($f_{risk} > 2$)	3.0
V_d (L)	$28.9 \times \frac{TBW}{70}$				
CGR (mg/h)	$(140 - age) \times \frac{TBW}{72} \times 0.85(if\ female) \times 0.6$				
Inter-individual variability (%)					
CL	33.1 (7%)[c]	11.5	28.6 (10%)		10.4
rCrCL%	26.8 (2%)	26.5	7.6 (39%)		35.8
V_d			15.1 (fixed)		
CGR			12.7 (fixed)		
Residual variability					
Proportional error	6.8 (15%)[c]	10.0	8.5 (26%)[c]		

[a]CrCL, creatinine clearance; rCrCL%, relative change in creatinine clearance following surgery; f_{risk}, AKI risk factor; V_d, volume of distribution; TBW, total body weight; CGR, creatinine generation rate.
[b]RSE, relative standard error.
[c]Shrinkage estimates of random effects are shown in respective parentheses.

Calorie restriction was found a notably beneficial impact in the subgroup of patients with ≤2 f_{risk}, resulting in a significant reduction of 4.44 in the OFV when incorporated as a covariate on rCrCL% ($p < 0.05$). Following this, estimates of rCrCL% for DR group and control group were 1.0% and -6.2%, respectively.

The comparison between published findings and popPK results are listed in Table 13. Published findings were concluded based on change in creatinine concentrations 24 h and/or 48 h after surgery, and conclusions from popPK approach based on post-hoc estimate of rCrCL%. For the KCH study, no differences between groups were found via both methods. However, subgroup analysis in popPK approach did not show any significant impact of calorie restriction on rCrCL%. For the KMN study, the same findings were obtained for all patients and the subgroup of patients with ≤2 f_{risk}. Additionally, popPK analysis revealed a typical value of about 2.1-12.3% reduction in CrCL after surgery in both KCH and KMN studies. Moreover, there was an increase in rCrCL% in patients with f_{risk} more than 2 in the KMN study.

Table 12 Covariate analysis on the relative change in creatinine clearance following surgery (reflecting the degree of acute kidney injury).

Covariate	OFV decrease	
	KCH study	**KMN study**
All patients	**(*n* = 72)**	**(*n* = 74)**
Calorie restriction	-0.002	-0.483
Surgery duration	-0.206	-4.84*
Iohexol dose	-	-1.61
AKI risk factor	-	-9.79*
Subgroups	**Male (*n* = 57)**	**Risk factor ≤ 2 (*n* = 52)**
Calorie restriction	-0.0580	-4.44*
Subgroups	**Female (*n* = 15)**	**Risk factor > 2 (*n* = 22)**
Calorie restriction	-0.219	-0.991
Subgroups	**BMI > 25 (*n* = 49)**	**Iohexol dose ≤ 100 ml (*n* = 46)**
Calorie restriction	-0.0170	-1.79
Subgroups	**BMI ≤ 25 (*n* = 23)**	**Iohexol dose > 100 ml (*n* = 28)**
Calorie restriction	-0.0330	-1.15
Subgroups	**CKD stage = 1 (*n* = 28)**	
Calorie restriction	-0.475	
Subgroups	**CKD stage = 2 (*n* = 34)**	
Calorie restriction	-0.878	
Subgroups	**CKD stage = 3 (*n* = 9)**	
Calorie restriction	-0.922	

* ΔOFV ≤ -3.84 was considered as statistically significant ($p < 0.05$).

Table 13 Summary of the published findings and population pharmacokinetic results.

	Published findings	**popPK results**
KCH study		
All patients	No difference between two diet groups	No difference between groups
Male patients	Significant[a]	No difference between groups
Patients with BMI >25	Significant[a]	No difference between groups
Patients have CKD stage 1	Significant[a]	No difference between groups
KMN study		
All patients	No difference between two diet groups	No difference between groups
		AKI risk factor has significant impact on rCrCL%[c]
Patients with ≤2 risk factor	Significant[a, b]	Significant[c]
Patients received ≤100 ml iohexol	Significant[a]	No difference between groups

CKD, chronic kidney disease; rCrCL%, relative change in creatinine clearance following surgery.
[a]Statistical significance was achieved based on change in creatinine concentration from baseline to 48 hours.
[b]Statistical significance was achieved based on change in creatinine concentration from baseline to 24 hours.
[c]Statistical significance was achieved based on change in estimated creatinine clearance after surgery.

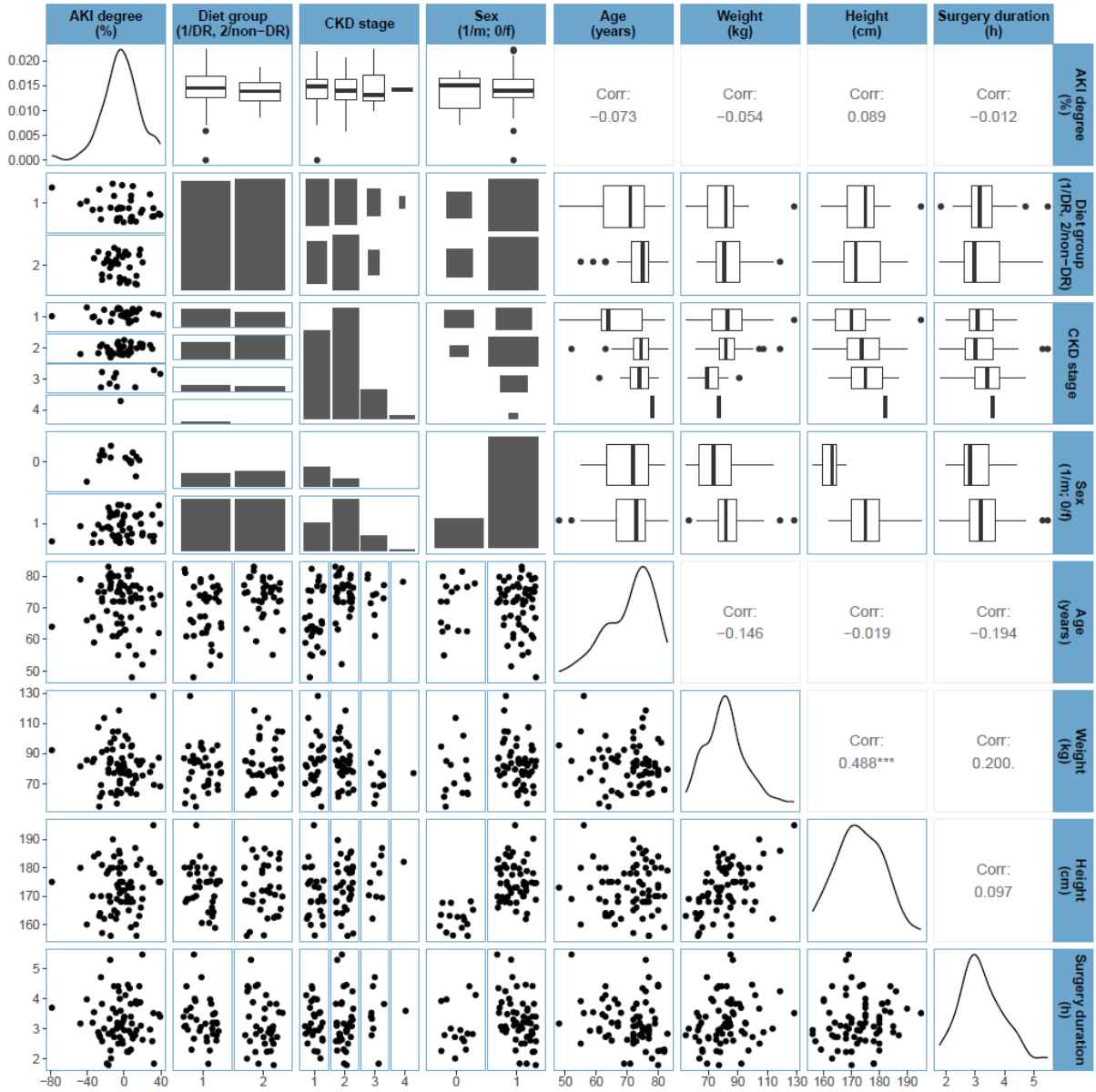

Figure 6 Correlation between AKI degree, indicated by the post-hoc relative change in creatinine clearance following surgery (rCrCL%), and investigated factors for KCH study (*n* = 72).

Upper right: correlation coefficient for continuous variables or bar charts for categorical variable (diet group, CKD stage, and sex); lower left: scatterplots for both continuous variables or density count for categorical variable; diagonal: kernel density estimation for continuous variables and normalized histogram statistics for categorical variable. DR, diet restriction; eGFR, estimated glomerular filtration rate by CKD-EPI (2009) equation. The first y-axis represents the density of variables for all plots on the diagonal, while the other y-axis and x-axis represent the numbers or the values of respective variables.

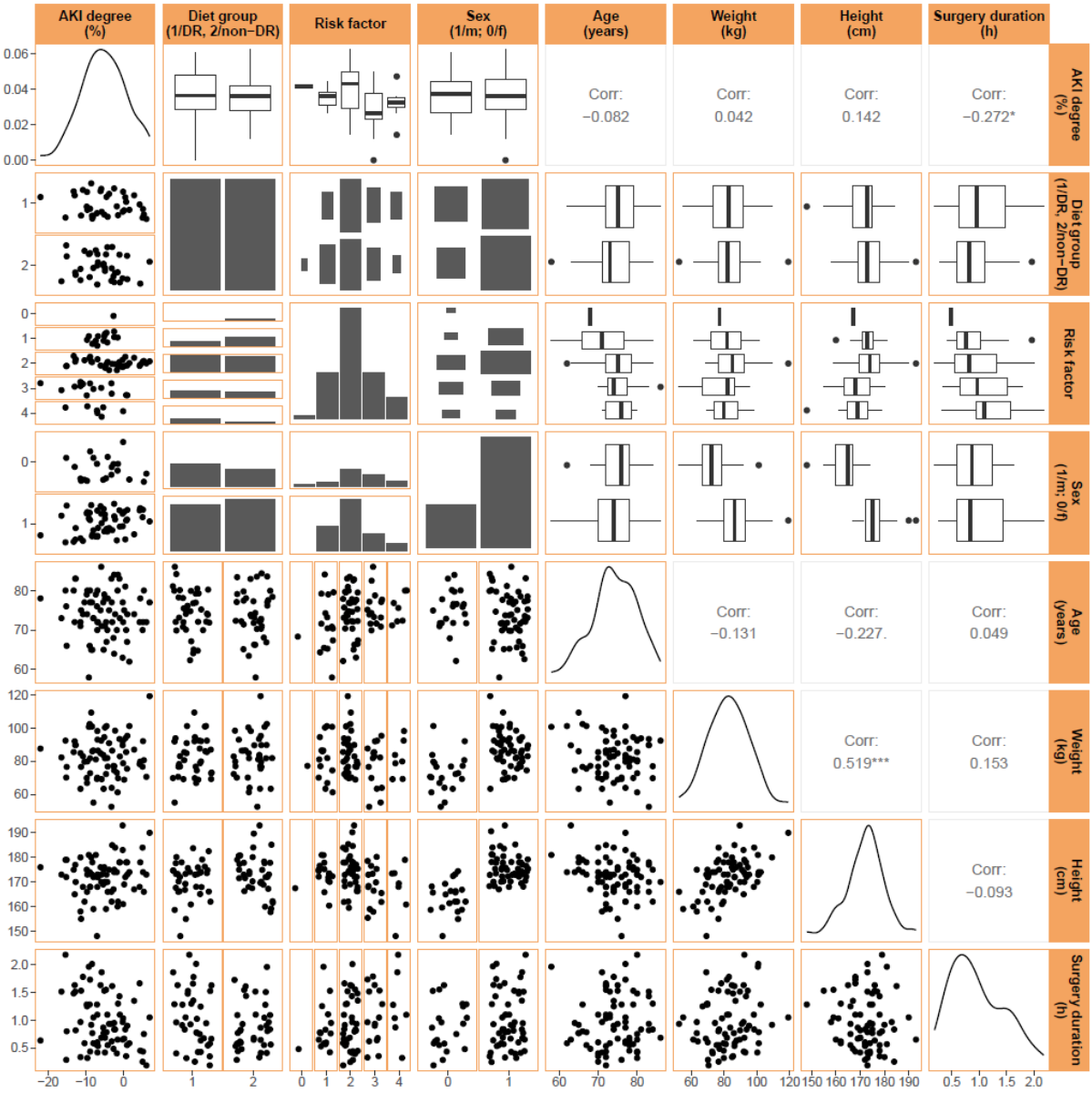

Figure 7 Correlation between AKI degree, indicated by the post-hoc relative change in creatinine clearance following surgery (rCrCL%), and investigated factors for KMN study (*n* = 74).

Upper right: correlation coefficient for continuous variables or bar charts for categorical variables (diet group, risk factor and sex); lower left: scatterplots for continuous variables or density count for categorical variables; diagonal: kernel density estimation for continuous variables and normalized histogram statistics for categorical variables. DR, diet restriction; eGFR, estimated glomerular filtration rate by CKD-EPI (2009) equation. Risk factor, represents the number of risk factors for AKI (factors including old age (>70 years), chronic kidney disease with a pre-existing serum creatinine above the normal range (i.e. >1.1 mg/dL in men, >0.9 mg/dL in women), diabetes mellitus, congestive heart failure, reduced left ventricular ejection fraction (<50%), or peripheral vascular disease). The first y-axis represents the density of variables for all plots on the diagonal, while the other y-axis and x-axis represent the numbers or the values of respective variables.

4.4 Plasma and cerebrospinal fluid population pharmacokinetics of vancomycin in patients with external ventricular drain

A three-compartment model with first-order elimination best described the vancomycin data. The estimated parameters included clearance (CL, 4.53 L/h), central compartment volume (V_c, 24.0 L), inter-compartmental clearance between central and peripheral compartments (Q_p, 5.69 L/h), peripheral compartment volume (V_p, 38.7 L), apparent CSF compartment volume (V_{CSF}, 0.445 L), and clearance between central and CSF compartments (Q_{CSF}, 0.00322 L/h and 0.00135 L/h for patients with and without primary CNS infection, respectively). CrCL was identified as a significant covariate affecting vancomycin CL. Three CSF-related covariates—CSF protein, glucose, and lactate concentrations—were found to significantly influence Q_{CSF}, with ΔOFV values of -29.8, -9.39, and -6.59, respectively. No significant difference was observed between samples collected from the proximal and distal ports.

Intermittent infusion and continuous infusion with a loading dose achieved CSF target concentrations more rapidly than continuous infusion alone. However, all infusion regimens ultimately reached similar CSF trough concentrations. In addition to dose adjustments based on renal function, initiating treatment with a loading dose is recommended for patients with primary CSF infection.

For comprehensive results of this study, please refer to the publication below.

Chen Z, Taubert M, Chen C, Dokos C, Fuhr U, Weig T, Zoller M, Heck S, Dimitriadis K, Terpolilli N, Kinast C, Scharf C, Lier C, Dorn C, Liebchen U. Plasma and cerebrospinal fluid population pharmacokinetics of vancomycin in patients with external ventricular drain. *Antimicrob Agents Chemother*. 2023. 67:e0024123. https://doi.org/10.1128/aac.00241-23

5 Summary

Creatinine is a widely used endogenous biomarker for eGFR and was studied through a refined popPK model that estimated CGR and Vd using data from retrospective and prospective studies. A key advancement of this work is the development of a joint creatinine/iohexol model, which enabled more precise assessment of renal function by incorporating nCTS as a parameter to evaluate OCT2/MATE-mediated tubular secretion. This approach may improve differentiation between glomerular and tubular function in clinical settings, offering a more accurate method for renal function assessment compared to traditional creatinine-based equations. However, the accuracy of the joint model remains constrained by external factors, such as uncertainties in creatinine absorption and the small clinical sample size.

The refined creatinine model was successfully applied to patients undergoing cardiac surgery to evaluate the degree of AKI and its association with potential contributing factors. However, the once-daily sampling schedule was not sufficient to generate substantial additional information on renal function using the model compared to raw concentration data. To enhance the utility of the model, more samples should be taken early after surgery, and it may be beneficial to administer iohexol before and shortly after surgery to assess AKI. Furthermore, the degree of AKI in these patients was limited in extent and duration, suggesting that more detailed monitoring may be relevant only in patients with risk factors.

Vancomycin is primarily excreted renally, making accurate renal function assessment crucial for optimizing dosing. This dissertation developed a vancomycin popPK model, incorporating estimated CrCL as a predictor for systemic clearance and CSF protein concentration as a predictor for CSF penetration. Monte Carlo simulations were employed to evaluate the probability of achieving PK/PD targets while ensuring systemic exposure remained within the therapeutic range across various dosing regimens. Additionally, the model confirmed the feasibility of using distal port CSF sampling for TDM in patients with EVDs. However, the study was limited by sparse sampling, small sample size, and absence of measured GFR, which restricted exploration of the relationship between renal function and vancomycin clearance.

Overall, this dissertation demonstrates the value of popPK modeling in improving renal function assessment and vancomycin dosing optimization, particularly through creatinine-based approaches. Future research should focus on refining these models with larger, more diverse datasets, and exploring simpler, more practical sampling strategies to improve accuracy and clinical applicability.

6 Zusammenfassung

Kreatinin ist ein weit verbreiteter endogener Biomarker zur Schätzung der glomerulären Filtrationsrate und wurde mithilfe eines verfeinerten populationspharmakokinetischen Modells untersucht, das die Kreatinin-Generationsrate und das Verteilungsvolumen anhand von Daten aus retrospektiven und prospektiven Studien schätzte. Ein wesentlicher Fortschritt dieser Arbeit ist die Entwicklung eines kombinierten Kreatinin-/Iohexol-Modells, das eine genauere Beurteilung der Nierenfunktion ermöglichte, indem die nicht-creatininvermittelte tubuläre Sekretion als Parameter zur Bewertung der Transporter-vermittelten tubulären Sekretion einbezogen wurde. Dieser Ansatz kann die Unterscheidung zwischen glomerulärer und tubulärer Funktion in klinischen Anwendungen verbessern und bietet eine genauere Methode zur Beurteilung der Nierenfunktion im Vergleich zu herkömmlichen kreatininbasierten Gleichungen. Die Genauigkeit des kombinierten Modells bleibt jedoch durch externe Faktoren eingeschränkt, beispielsweise durch Unsicherheiten bei der Absorption von Kreatinin und die geringe klinische Stichprobengröße.

Das verfeinerte Kreatininmodell wurde erfolgreich bei Patienten nach einer Herzoperation angewendet, um das Ausmaß der akuten Nierenschädigung und deren Zusammenhang mit möglichen beitragenden Faktoren zu bewerten. Der einmal tägliche Probenahmeplan war jedoch nicht ausreichend, um im Vergleich zu den reinen Konzentrationsdaten wesentliche zusätzliche Informationen über die Nierenfunktion zu generieren. Um den Nutzen des Modells zu erhöhen, sollten mehr Proben früh nach der Operation entnommen werden. Zudem könnte es vorteilhaft sein, Iohexol vor und kurz nach der Operation zu verabreichen, um Veränderungen der Nierenfunktion zu erfassen. Darüber hinaus war die akute Nierenschädigung bei diesen Patienten in Umfang und Dauer begrenzt, was darauf hindeutet, dass eine detailliertere Überwachung nur bei Patienten mit Risikofaktoren von Bedeutung ist.

Vancomycin wird hauptsächlich über die Niere ausgeschieden, was eine genaue Beurteilung der Nierenfunktion entscheidend für eine optimierte Dosierung macht. In dieser Dissertation wurde ein populationspharmakokinetisches Modell für Vancomycin entwickelt, das die geschätzte Kreatinin-Clearance als Prädiktor für die systemische Clearance sowie die Konzentration von Proteinen in der Rückenmarksflüssigkeit als Prädiktor für die Durchlässigkeit in dieses Kompartiment einbezieht. Monte-Carlo-Simulationen wurden eingesetzt, um die Wahrscheinlichkeit des Erreichens von pharmakokinetisch-pharmakodynamischen Zielwerten zu bewerten und gleichzeitig sicherzustellen, dass die systemische Exposition bei verschiedenen Dosierungsregimen im therapeutischen Bereich

blieb. Darüber hinaus bestätigte das Modell die Machbarkeit der therapeutischen Arzneimittelüberwachung durch Entnahme der Rückenmarksflüssigkeit über einen distalen Zugang bei Patienten mit externer Ventrikeldrainage. Die Aussagekraft der Studie war jedoch durch eine geringe Probenanzahl, eine kleine Stichprobengröße sowie das Fehlen gemessener glomerulärer Filtrationsraten eingeschränkt, was eine detaillierte Untersuchung des Zusammenhangs zwischen Nierenfunktion und Vancomycin-Clearance erschwerte.

Insgesamt zeigt diese Dissertation den Nutzen der populationspharmakokinetischen Modellierung zur Verbesserung der Beurteilung der Nierenfunktion und zur Optimierung der Vancomycin-Dosierung, insbesondere durch kreatininbasierte Ansätze. Zukünftige Forschung sollte sich auf die Verfeinerung dieser Modelle mit größeren und vielfältigeren Datensätzen konzentrieren sowie auf die Entwicklung einfacherer und praxisnaher Probenahmestrategien zur Verbesserung von Genauigkeit und klinischer Anwendbarkeit.

References

1. Hoenig MP, Hladik GA. 1 - Overview of kidney structure and function. In: Gilbert SJ, Weiner DE, editors. *National kidney foundation's primer on kidney diseases (seventh edition)*. Philadelphia: Elsevier; 2018. p. 2-18. https://doi.org/10.1016/B978-0-323-47794-9.00001-9

2. Inker LA, Levey AS. 3 - Assessment of kidney function in acute and chronic settings. In: Gilbert SJ, Weiner DE, editors. *National kidney foundation's primer on kidney diseases (seventh edition)*. Philadelphia: Elsevier; 2018. p. 26-32.e1. https://doi.org/10.1016/B978-0-323-47794-9.00003-2

3. Koopman MG, Koomen GCM, Krediet RT, *et al.* Circadian rhythm of glomerular filtration rate in normal individuals. *Clinical Science*. 1989. 77:105-11. http://doi.org/10.1042/cs0770105

4. Azevedo MJ, Padilha LM, Gross JL. A short-term low-protein diet reduces glomerular filtration rate in insulin-dependent diabetes mellitus patients. *Brazilian journal of medical and biological research*. 1990. 23:647-54. https://lume.ufrgs.br/bitstream/handle/10183/247450/000061265.pdf?sequence=1

5. Stevens PE, Ahmed SB, Carrero JJ, *et al.* KDIGO 2024 Clinical practice guideline for the evaluation and management of chronic kidney disease. *Kidney International*. 2024. 105:S117-S314. http://doi.org/10.1016/j.kint.2023.10.018

6. Vart P, Grams ME. Measuring and assessing kidney function. *Seminars in Nephrology*. 2016. 36:262-72. https://doi.org/10.1016/j.semnephrol.2016.05.003

7. Inker LA, Titan S. Measurement and estimation of GFR for use in clinical practice: core curriculum 2021. *American Journal of Kidney Diseases*. 2021. 78:736-49. http://doi.org/10.1053/j.ajkd.2021.04.016

8. Gaspari F, Perico N, Ruggenenti P, *et al.* Plasma clearance of nonradioactive iohexol as a measure of glomerular filtration rate. *Journal of the American Society of Nephrology*. 1995. 6 https://doi.org/10.1681/ASN.V62257

9. Berg UB, Bäck R, Celsi G, *et al.* Comparison of plasma clearance of iohexol and urinary clearance of inulin for measurement of GFR in children. *American Journal of Kidney Diseases*. 2011. 57:55-61. https://doi.org/10.1053/j.ajkd.2010.07.013

10. Barbour GL, Crumb CK, Boyd CM, *et al.* Comparison of inulin, iothalamate, and 99mTc-DTPA for measurement of glomerular filtration rate. *Journal of Nuclear Medicine*. 1976. 17:317. https://jnm.snmjournals.org/content/17/4/317.long

11. Brien TG, O'Hagan R, Muldowney FP. Chromium-51-EDTA in the determination of glomerular filtration rate. *Acta Radiologica: Therapy, Physics, Biology*. 1969. 8:523-9. https://doi.org/10.3109/02841866909134478

12. Soveri I, Berg UB, Björk J, *et al.* Measuring GFR: a systematic review. *American Journal of Kidney Diseases*. 2014. 64:411-24. https://doi.org/10.1053/j.ajkd.2014.04.010

13. Andersen TB, Jødal L, Nielsen NS, *et al.* Comparison of simultaneous plasma clearance of 99mTc-DTPA and 51Cr-EDTA: can one tracer replace the other? *Scandinavian Journal of Clinical and Laboratory Investigation*. 2019. 79:463-7. http://doi.org/10.1080/00365513.2019.1658217

14. Aburano T, Shuke N, Yokoyama K, *et al.* Renal perfusion with Tc-99m DTPA—simple noninvasive determination of extraction fraction and plasma flow. *Clinical Nuclear Medicine*. 1993. 18 http://doi.org/10.1097/00003072-199307000-00007

15. Cockcroft DW, Gault H. Prediction of creatinine clearance from serum creatinine. *Nephron*. 1976. 16:31-41. https://doi.org/10.1159/000180580

16. Levey AS, Bosch JP, Lewis JB, *et al.* A more accurate method to estimate glomerular filtration rate from serum creatinine: a new prediction equation. *Annals of Internal Medicine*. 1999. 130:461-70. http://doi.org/10.7326/0003-4819-130-6-199903160-00002

17. Juutilainen A, Kastarinen H, Antikainen R, *et al.* Comparison of the MDRD Study and the CKD-EPI study equations in evaluating trends of estimated kidney function at population level: findings from the national FINRISK Study. *Nephrology Dialysis Transplantation*. 2012. 27:3210-7. http://doi.org/10.1093/ndt/gfs047

18. Levey AS, Stevens LA, Schmid CH, *et al.* A new equation to estimate glomerular filtration rate. *Annals of Internal Medicine*. 2009. 150:604-12. https://doi.org/10.7326/0003-4819-150-9-200905050-00006

19. Matsushita K, Mahmoodi BK, Woodward M, *et al.* Comparison of risk prediction using the CKD-EPI equation and the MDRD study equation for estimated glomerular filtration rate. *JAMA*. 2012. 307:1941-51. https://doi.org/10.1001/jama.2012.3954

20. Schwartz GJ, Munoz A, Schneider MF, *et al.* New equations to estimate GFR in children with CKD. *Journal of the American Society of Nephrology*. 2009. 20:629-37. http://doi.org/10.1681/ASN.2008030287

21. Schaeffner ES, Ebert N, Delanaye P, *et al.* Two novel equations to estimate kidney function in persons aged 70 years or older. *Annals of Internal Medicine*. 2012. 157:471-81. https://doi.org/10.7326/0003-4819-157-7-201210020-00003

22. Pottel H, Hoste L, Dubourg L, *et al.* An estimated glomerular filtration rate equation for the full age spectrum. *Nephrology Dialysis Transplantation*. 2016. 31:798-806. https://doi.org/10.1093/ndt/gfv454

23. Ma Y, Shen X, Yong Z, *et al.* Comparison of glomerular filtration rate estimating equations in older adults: a systematic review and meta-analysis. *Archives of Gerontology and Geriatrics*. 2023. 114:105107. https://doi.org/10.1016/j.archger.2023.105107

24. Schaeffner ES, Martus P, Ebert N. External validation of the Berlin Initiative Equations. *American Journal of Kidney Diseases*. 2014. 64:658-9. https://doi.org/10.1053/j.ajkd.2014.04.037

25. Pottel H, Delanaye P, Cavalier E. Exploring renal function assessment: creatinine, cystatin C, and estimated glomerular filtration rate focused on the european kidney function consortium equation. *Ann Lab Med*. 2024. 44:135-43. https://doi.org/10.3343/alm.2023.0237

26. Screever EM, Kootstra-Ros JE, Doorn J, *et al.* Kidney function in patients with neuromuscular disease: creatinine versus cystatin C. *Frontiers in Neurology*. 2021. 12:688246. http://doi.org/10.3389/fneur.2021.688246

27. Matsuoka-Uchiyama N, Tsuji K, Takahashi K, *et al.* Association between urinary creatinine excretion and hypothyroidism in patients with chronic kidney disease. *Diagnostics*. 2023. 13:669. http://doi.org/10.3390/diagnostics13040669

28. Bragadottir G, Redfors B, Ricksten S-E. Assessing glomerular filtration rate (GFR) in critically ill patients with acute kidney injury - true GFR versus urinary creatinine clearance and estimating equations. *Critical Care*. 2013. 17:R108. http://doi.org/10.1186/cc12777

29. Lista AD, Sirimaturos M. Pharmacokinetic and pharmacodynamic principles for toxicology. *Critical Care Clinics*. 2021. 37:475-86. https://doi.org/10.1016/j.ccc.2021.03.001

30. Bardal SK, Waechter JE, Martin DS. Chapter 2 - Pharmacokinetics. In: Bardal SK, Waechter JE, Martin DS, editors. *Applied Pharmacology*. Philadelphia: W.B. Saunders; 2011. p. 17-34. https://doi.org/10.1016/B978-1-4377-0310-8.00002-6

31. Graham RC, Jr., Karnovsky MJ. Glomerular permeability: ultrastructural cytochemical studies using peroxidases as protein tracer. *Journal of Experimental Medicine*. 1966. 124:1123-34. https://doi.org/10.1084/jem.124.6.1123

32. Chaves. BJ, Tadi. P. *Gentamicin*. StatPearls: Treasure Island; 2023.

33. Correia CS, Bronander KA. Metformin-associated lactic acidosis masquerading as ischemic bowel. *The American Journal of Medicine*. 2012. 125:e9. https://doi.org/10.1016/j.amjmed.2011.11.012

34. Mutlu M, Aslan Y, Kader Ş, *et al.* Clinical signs and symptoms of toxic serum digoxin levels in neonates. *The Turkish Journal of Pediatrics*. 2019. 61:244-9. http://doi.org/10.24953/turkjped.2019.02.013

35. Pincus M. Management of digoxin toxicity. *Aust Prescr*. 2016. 39:18-20. http://doi.org/10.18773/austprescr.2016.006

36. Caroline Ashley AC. *The renal drug handbook*. 2nd ed. Radcliffe Medical Press, Oxford: 2004.

37. Manley HJ, Bailie GR, McClaran ML, *et al.* Gentamicin pharmacokinetics during slow daily home hemodialysis. *Kidney International*. 2003. 63:1072-78. https://doi.org/10.1046/j.1523-1755.2003.00819.x

38. Kuan IHS, Wilson LC, Leishman JC, *et al.* Metformin doses to ensure efficacy and safety in patients with reduced kidney function. *PLoS One*. 2021. 16:e0246247. http://doi.org/10.1371/journal.pone.0246247

39. Graham GG, Punt J, Arora M, *et al.* Clinical pharmacokinetics of metformin. *Clinical Pharmacokinetics*. 2011. 50:81-98. http://doi.org/10.2165/11534750-000000000-00000

40. King Edward Memorial Hospital Pharmacy Department. *Adult medication guideline - Digoxin*. https://www.kemh.health.wa.gov.au/~/media/HSPs/NMHS/Hospitals/WNHS/Documents/Clinical-guidelines/Obs-Gyn-MPs/Digoxin.pdf?thn=0 (2015). Accessed 13/03/2025.

41. Gheorghiade M, Adams KF, Colucci WS. Digoxin in the management of cardiovascular disorders. *Circulation*. 2004. 109:2959-64. https://doi.org/10.1161/01.CIR.0000132482.95686.87

42. Barras MA, Duffull SB, Atherton JJ, *et al.* Individualized Compared With Conventional Dosing of Enoxaparin. *Clinical Pharmacology & Therapeutics*. 2008. 83:882-8. https://doi.org/10.1038/sj.clpt.6100399

43. Green B, Greenwood M, Saltissi D, *et al.* Dosing strategy for enoxaparin in patients with renal impairment presenting with acute coronary syndromes. *British Journal of Clinical Pharmacology*. 2005. 59:281-90. https://doi.org/10.1111/j.1365-2125.2004.02253.x

44. Petersen JL, Mahaffey KW, Hasselblad V, *et al.* Efficacy and bleeding complications among patients randomized to enoxaparin or unfractionated heparin for antithrombin therapy in non–ST-segment elevation acute coronary syndromes a systematic overview. *JAMA*. 2004. 292:89-96. http://doi.org/10.1001/jama.292.1.89

45. Rybak MJ, Lomaestro BM, Rotscahfer JC, *et al.* Vancomycin therapeutic guidelines: a summary of consensus recommendations from the infectious diseases society of america, the american society of health-system pharmacists, and the society of infectious diseases pharmacists. *Clinical Infectious Diseases*. 2009. 49:325-7. https://doi.org/10.1086/600877

46. Scurt FG, Bose K, Mertens PR, *et al.* Cardiac surgery–associated acute kidney injury. *Kidney360*. 2024. 5 http://doi.org/10.34067/KID.0000000000000466

47. Gabrielle EH, John AH, Charles EW, *et al.* Importance of duration of acute kidney injury after severe trauma: a cohort study. *Trauma Surgery & Acute Care Open*. 2021. 6:e000689. http://doi.org/10.1136/tsaco-2021-000689

48. Peerapornratana S, Manrique-Caballero CL, Gómez H, *et al.* Acute kidney injury from sepsis: current concepts, epidemiology, pathophysiology, prevention and treatment. *Kidney International*. 2019. 96:1083-99. https://doi.org/10.1016/j.kint.2019.05.026

49. Odutayo A, Wong CX, Farkouh M, *et al.* AKI and long-term risk for vardiovascular rvents and mortality. *Journal of the American Society of Nephrology*. 2017. 28:377-87. http://doi.org/10.1681/ASN.2016010105

50. Perazella MA, Rosner MH. Drug-induced acute kidney injury. *Clinical Journal of the American Society of Nephrology*. 2022. 17:1220-33. http://doi.org/10.2215/CJN.11290821

51. Levey AS, Inker LA. Assessment of glomerular filtration rate in health and disease: a state of the art review. *Clinical Pharmacology & Therapeutics*. 2017. 102:405-19. https://doi.org/10.1002/cpt.729

52. Cheruku SR, Raphael J, Neyra JA, *et al.* Acute kidney injury after cardiac surgery: prediction, prevention, and management. *Anesthesiology*. 2023. 139:880-98. https://doi.org/10.1097/ALN.0000000000004734

53. Khwaja A. KDIGO clinical practice guidelines for acute kidney injury. *Nephron Clinical Practice*. 2012. 120:c179-c84. https://doi.org/10.1159/000339789

54. Türk D, Müller F, Fromm MF, *et al.* Renal transporter-mediated drug-biomarker interactions of the endogenous substrates creatinine and N1-methylnicotinamide: a PBPK modeling approach. *Clinical Pharmacology & Therapeutics*. 2022. 112:687-98. https://doi.org/10.1002/cpt.2636

55. Ullah S, Zoller M, Jaehde U, *et al.* A model-based approach to assess unstable creatinine clearance in critically Ill patients. *Clinical Pharmacology & Therapeutics*. 2021. 110:1240-9. https://doi.org/10.1002/cpt.2341

56. Yin J, Wang J. Renal drug transporters and their significance in drug–drug interactions. *Acta Pharmaceutica Sinica B*. 2016. 6:363-73. https://doi.org/10.1016/j.apsb.2016.07.013

57. Sato M, Mamada H, Anzai N, *et al.* Renal secretion of uric acid by organic anion transporter 2 (OAT2/SLC22A7) in human. *Biological and Pharmaceutical Bulletin*. 2010. 33:498-503. https://doi.org/10.1248/bpb.33.498

58. Urakami Y, Kimura N, Okuda M, *et al.* Creatinine transport by basolateral organic cation transporter hOCT2 in the human kidney. *Pharmaceutical Research*. 2004. 21:976-81. https://doi.org/10.1023/B:PHAM.0000029286.45788.ad

59. VanWert AL, Bailey RM, Sweet DH. Organic anion transporter 3 (OAT3/SLC22A8) knockout mice exhibit altered clearance and distribution of penicillin G. *American Journal of Physiology-Renal Physiology*. 2007. 293:F1332-F41. https://doi.org/10.1152/ajprenal.00319.2007

60. Odlind B, Beermann B. Renal tubular secretion and effects of furosemide. *Clinical Pharmacology & Therapeutics*. 1980. 27:784-90. https://doi.org/10.1038/clpt.1980.111

61. Koren G. Clinical pharmacokinetic significance of the renal tubular secretion of digoxin. *Clinical Pharmacokinetics*. 1987. 13:334-43. https://doi.org/10.2165/00003088-198713050-00004

62. Bodemar G, Norlander B, Walan A. Pharmacokinetics of cimetidine after single doses and during continuous treatment. *Clinical Pharmacokinetics*. 1981. 6:306-15. http://doi.org/10.2165/00003088-198106040-00005

63. Kearney BP, Yale K, Shah J, *et al.* Pharmacokinetics and dosing recommendations of tenofovir disoproxil fumarate in gepatic or renal impairment. *Clinical Pharmacokinetics*. 2006. 45:1115-24. http://doi.org/10.2165/00003088-200645110-00005

64. Bourke RS, Chheda G, Bremer A, *et al.* Inhibition of Renal Tubular Transport of Methotrexate by Probenecid1. *Cancer Research*. 1975. 35:110-6.

65. El Masri AER, Tobler C, Willemijn B, *et al.* Case report: hepatotoxicity and nephrotoxicity induced by methotrexate in a paediatric patient, what is the role of precision medicine in 2023? *Frontiers in Pharmacology*. 2023. 14:1130548. https://doi.org/10.3389/fphar.2023.1130548

66. Wilson RC, Riezk A, Arkell P, *et al.* Towards pharmacokinetic boosting of phenoxymethylpenicillin (penicillin-V) using probenecid for the treatment of bacterial infections. *Scientific Reports*. 2024. 14:16762. http://doi.org/10.1038/s41598-024-67354-6

67. Suchy-Dicey AM, Laha T, Hoofnagle A, *et al.* Tubular secretion in CKD. *Journal of the American Society of Nephrology*. 2016. 27 http://doi.org/10.1681/ASN.2014121193

68. Bullen AL, Ascher SB, Scherzer R, *et al.* Markers of kidney tubular secretion and risk of adverse events in SPRINT participants with CKD. *Journal of the American Society of Nephrology*. 2022. 33:1915-26. http://doi.org/10.1681/ASN.2022010117

69. Thompson LE, Joy MS. Endogenous markers of kidney function and renal drug clearance processes of filtration, secretion, and reabsorption. *Current Opinion in Toxicology*. 2022. 31:100344. https://doi.org/10.1016/j.cotox.2022.03.005

70. Chen Y, Zelnick LR, Wang K, *et al.* Kidney clearance of secretory solutes is associated with progression of CKD: the CRIC study. *Journal of the American Society of Nephrology*. 2020. 31:817-27. http://doi.org/10.1681/ASN.2019080811

71. Wang K, Zelnick LR, Hoofnagle AN, *et al.* Differences in proximal tubular solute clearance across common etiologies of chronic kidney disease. *Nephrology Dialysis Transplantation*. 2020. 35:1916-23. http://doi.org/10.1093/ndt/gfz144

72. Nigam SK, Bush KT, Martovetsky G, *et al.* The organic anion transporter (OAT) family: a systems biology perspective. *Physiological Reviews*. 2015. 95:83-123. http://doi.org/10.1152/physrev.00025.2013

73. Shen H, Holenarsipur VK, Mariappan TT, *et al.* Evidence for the validity of pyridoxic acid (PDA) as a plasma-based endogenous probe for OAT1 and OAT3 function in healthy subjects. *Journal of Pharmacology and Experimental Therapeutics*. 2019. 368:136. http://doi.org/10.1124/jpet.118.252643

74. Liu R, Hao J, Zhao X, *et al.* Characterization of elimination pathways and the feasibility of endogenous metabolites as biomarkers of organic anion transporter 1/3 inhibition in cynomolgus monkeys. *Drug Metabolism and Disposition*. 2023. 51:844. http://doi.org/10.1124/dmd.123.001277

75. Müller F, Hohl K, Keller S, *et al.* N-methylnicotinamide as biomarker for MATE-mediated renal drug–drug interactions: impact of cimetidine, rifampin, verapamil, and probenecid. *Clinical Pharmacology & Therapeutics*. 2023. 113:1070-9. https://doi.org/10.1002/cpt.2849

76. Orlando R, Floreani M, Napoli E, *et al.* Renal clearance of N1-methylnicotinamide: a sensitive marker of the severity of liver dysfunction in cirrhosis. *Nephron*. 2000. 84:32-9. http://doi.org/10.1159/000045536

77. Levey AS, Perrone RD, Madias NE. Serum creatinine and renal function. *Annual Review of Medicine*. 1988. 39:465-90. https://doi.org/10.1146/annurev.me.39.020188.002341

78. Ma Y, Ran F, Xin M, *et al.* Albumin-bound kynurenic acid is an appropriate endogenous biomarker for assessment of the renal tubular OATs-MRP4 channel. *Journal of Pharmaceutical Analysis*. 2023. 13:1205-20. https://doi.org/10.1016/j.jpha.2023.05.007

79. Mathialagan S, Feng B, Rodrigues AD, *et al.* Drug-drug interactions involving renal OCT2/MATE transporters: clinical risk assessment may require endogenous biomarker-informed approach. *Clinical Pharmacology & Therapeutics*. 2021. 110:855-9. https://doi.org/10.1002/cpt.2089

80. Cundy KC, Barditch-Crovo P, Walker RE, *et al.* Clinical pharmacokinetics of adefovir in human immunodeficiency virus type 1-infected patients. *Antimicrobial Agents and Chemotherapy*. 1995. 39:2401-5. http://doi.org/10.1128/aac.39.11.2401

81. Trueck C, Hsin C-h, Scherf-Clavel O, *et al.* A clinical drug-drug interaction study assessing a novel drug transporter phenotyping cocktail with adefovir, sitagliptin, metformin, pitavastatin, and digoxin. *Clinical Pharmacology & Therapeutics*. 2019. 106:1398-407. https://doi.org/10.1002/cpt.1564

82. Vance-Bryan K, Guay DRP, Rotschafer JC. Clinical pharmacokinetics of ciprofloxacin. *Clinical Pharmacokinetics*. 1990. 19:434-61. http://doi.org/10.2165/00003088-199019060-00003

83. Webb DB, Roberts DE, Williams JD, *et al.* Pharmacokinetics of ciprofloxacin in healthy volunteers and patients with impaired kidney function. *Journal of Antimicrobial Chemotherapy*. 1986. 18:83-7. http://doi.org/10.1093/jac/18.Supplement_D.83

84. VanWert AL, Srimaroeng C, Sweet DH. Organic anion transporter 3 (oat3/slc22a8) interacts with carboxyfluoroquinolones, and deletion increases systemic exposure to ciprofloxacin. *Molecular Pharmacology*. 2008. 74:122. http://doi.org/10.1124/mol.107.042853

85. Scheen AJ. Clinical pharmacokinetics of metformin. *Clinical Pharmacokinetics*. 1996. 30:359-71. http://doi.org/10.2165/00003088-199630050-00003

86. Gong L, Goswami S, Giacomini KM, *et al.* Metformin pathways: pharmacokinetics and pharmacodynamics. *Pharmacogenetics and Genomics*. 2012. 22:820-7. http://doi.org/10.1097/FPC.0b013e3283559b22

87. U.S. Food and Drug Administration. *FDA's examples of drugs that interact with CYP enzymes and transporter systems*. https://www.fda.gov/drugs/drug-interactions-

labeling/healthcare-professionals-fdas-examples-drugs-interact-cyp-enzymes-and-transporter-systems (2024). Accessed 13/03/2025.

88. Hagos FT, Daood MJ, Ocque JA, *et al.* Probenecid, an organic anion transporter 1 and 3 inhibitor, increases plasma and brain exposure of N-acetylcysteine. *Xenobiotica*. 2017. 47:346-53. http://doi.org/10.1080/00498254.2016.1187777

89. Ito S, Kusuhara H, Yokochi M, *et al.* Competitive inhibition of the luminal efflux by multidrug and toxin Extrusions, but not basolateral uptake by organic cation transporter 2, is the likely mechanism underlying the pharmacokinetic drug-drug Interactions caused by cimetidine in the kidney. *Journal of Pharmacology and Experimental Therapeutics*. 2012. 340:393. http://doi.org/10.1124/jpet.111.184986

90. Tran K-N, Rybak Michael J. β-Lactam combinations with vancomycin show synergistic activity against vancomycin-susceptible staphylococcus aureus, vancomycin-intermediate S. aureus (VISA), and heterogeneous VISA. *Antimicrobial Agents and Chemotherapy*. 2018. 62:e00157-18. http://doi.org/10.1128/aac.00157-18

91. Stogios PJ, Savchenko A. Molecular mechanisms of vancomycin resistance. *Protein Science*. 2020. 29:654-69. https://doi.org/10.1002/pro.3819

92. Ma P, Ma H, Liu R, *et al.* Prediction of vancomycin plasma concentration in elderly patients based on multi-algorithm mining combined with population pharmacokinetics. *Scientific Reports*. 2024. 14:27165. https://doi.org/10.1038/s41598-024-78558-1

93. David MZ, Daum RS. Treatment of Staphylococcus aureus infections. In: Bagnoli F, Rappuoli R, Grandi G, editors. *Staphylococcus aureus: Microbiology, Pathology, Immunology, Therapy and Prophylaxis*. Cham: Springer International Publishing; 2017. p. 325-83. https://doi.org/10.1007/82_2017_42

94. Rao S, Kupfer Y, Pagala M, *et al.* Systemic absorption of oral vancomycin in patients with Clostridium difficile infection. *Scandinavian Journal of Infectious Diseases*. 2011. 43:386-8. https://doi.org/10.3109/00365548.2010.544671

95. Libuit J, Whitman A, Wolfe R, *et al.* Empiric vancomycin use in febrile neutropenic oncology patients. *Open Forum Infectious Diseases*. 2014. 1:ofu006. http://doi.org/10.1093/ofid/ofu006

96. Nguyen CT, Baccile R, Brown AM, *et al.* When is vancomycin prophylaxis necessary? Risk factors for MRSA surgical site infection. *Antimicrobial Stewardship & Healthcare Epidemiology*. 2024. 4:e10. http://doi.org/10.1017/ash.2024.7

97. Hermsen ED, Hanson M, Sankaranarayanan J, *et al.* Clinical outcomes and nephrotoxicity associated with vancomycin trough concentrations during treatment of deep-seated infections. *Expert Opinion on Drug Safety*. 2010. 9:9-14. http://doi.org/10.1517/14740330903413514

98. Wunderink RG, Niederman MS, Kollef MH, *et al.* Linezolid in methicillin-resistant staphylococcus aureus nosocomial pneumonia: a randomized, controlled study. *Clinical Infectious Diseases*. 2012. 54:621-9. http://doi.org/10.1093/cid/cir895

99. Forouzesh A, Moise Pamela A, Sakoulas G. Vancomycin ototoxicity: a reevaluation in an era of increasing doses. *Antimicrobial Agents and Chemotherapy*. 2009. 53:483-6. http://doi.org/10.1128/aac.01088-08

100. Moellering RC, Jr. Pharmacokinetics of vancomycin. *Journal of Antimicrobial Chemotherapy*. 1984. 14:43-52. https://doi.org/10.1093/jac/14.suppl_D.43

101. Rodvold KA, Blum RA, Fischer JH, *et al.* Vancomycin pharmacokinetics in patients with various degrees of renal function. *Antimicrobial Agents and Chemotherapy*. 1988. 32:848-52. https://doi.org/10.1128/aac.32.6.848

102. Matzke GR, Zhanel GG, Guay DRP. Clinical pharmacokinetics of vancomycin. *Clinical Pharmacokinetics*. 1986. 11:257-82. https://doi.org/10.2165/00003088-198611040-00001

103. Giuliano C, Haase KK, Hall R. Use of vancomycin pharmacokinetic–pharmacodynamic properties in the treatment of MRSA infections. *Expert Review of Anti-infective Therapy*. 2010. 8:95-106. http://doi.org/10.1586/eri.09.123

104. Rybak MJ, Le J, Lodise TP, *et al.* Therapeutic monitoring of vancomycin for serious methicillin-resistant staphylococcus aureus infections: a revised consensus guideline and review by the american society of health-system pharmacists, the infectious diseases society of america, the pediatric infectious diseases society, and the society of infectious fiseases pharmacists. *American Journal of Health-System Pharmacy*. 2020. 77:835-64. http://doi.org/10.1093/ajhp/zxaa036

105. Aljefri DM, Avedissian SN, Rhodes NJ, *et al.* Vancomycin area under the curve and acute kidney injury: a meta-analysis. *Clinical Infectious Diseases*. 2019. 69:1881-7. http://doi.org/10.1093/cid/ciz051

106. Liu C, Bayer A, Cosgrove SE, *et al.* Clinical practice guidelines by the infectious diseases society of america for the treatment of methicillin-resistant staphylococcus aureus infections in adults and children. *Clinical Infectious Diseases*. 2011. 52:e18-e55. https://doi.org/10.1093/cid/ciq146

107. Udy AA, Baptista JP, Lim NL, *et al.* Augmented renal clearance in the ICU: results of a multicenter observational study of renal function in critically ill patients with normal plasma creatinine concentrations. *Critical Care Medicine*. 2014. 42:520-7. https://doi.org/10.1097/CCM.0000000000000029

108. Assadoon MS, Pearson JC, Kubiak DW, *et al.* Evaluation of vancomycin accumulation in patients with obesity. *Open Forum Infectious Diseases*. 2022. 9:ofac491. https://doi.org/10.1093/ofid/ofac491

109. Allegaert K, Verbesselt R, Naulaers G, *et al.* Developmental pharmacology: neonates are not just small adults. *Acta Clinica Belgica*. 2008. 63:16-24. https://doi.org/10.1179/acb.2008.003

110. Nahata MC. Vancomycin dosage regimens for pediatric patients. *The Journal of Pediatric Pharmacology and Therapeutics*. 2009. 14:64-5. https://doi.org/10.5863/1551-6776-14.2.64

111. Kang J-S, Lee M-H. Overview of therapeutic drug monitoring. *Korean J Intern Med*. 2009. 24:1-10. https://doi.org/10.3904/kjim.2009.24.1.1

112. Aljutayli A, Marsot A, Nekka F. An update on population pharmacokinetic analyses of vancomycin, part I: in adults. *Clinical Pharmacokinetics*. 2020. 59:671-98. https://doi.org/10.1007/s40262-020-00866-2

113. Albanell-Fernández M, Rodríguez-Reyes M, Bastida C, *et al.* A review of vancomycin, gentamicin, and amikacin population pharmacokinetic models in neonates and infants. *Clinical Pharmacokinetics*. 2025. 64:1-25. https://doi.org/10.1007/s40262-024-01459-z

114. Jarugula P, Akcan-Arikan A, Munoz-Rivas F, *et al.* Optimizing vancomycin dosing and monitoring in neonates and infants using population pharmacokinetic modeling. *Antimicrobial Agents and Chemotherapy*. 2022. 66:e01899-21. https://doi.org/doi:10.1128/aac.01899-21

115. Polaskova L, Murinova I, Gregorova J, *et al.* Vancomycin population pharmacokinetics and dosing proposal for the initial treatment in obese adult patients. *Front Pharmacol*. 2024. 15:1364681. https://doi.org/10.3389/fphar.2024.1364681

116. Ben Romdhane H, Woillard JB, Ben Fadhel N, *et al.* Population pharmacokinetic of vancomycin administered by continuous infusion in critically ill patients. *Pharmacology*. 2024.65-76. https://doi.org/10.1159/000539866

117. Kim D-J, Lee D-H, Ahn S, *et al.* A new population pharmacokinetic model for vancomycin in patients with variable renal function: therapeutic drug monitoring based on extended covariate model using CKD-EPI estimation. *Journal of Clinical Pharmacy and Therapeutics*. 2019. 44:750-9. https://doi.org/10.1111/jcpt.12995

118. Monteiro JF, Hahn SR, Gonçalves J, *et al.* Vancomycin therapeutic drug monitoring and population pharmacokinetic models in special patient subpopulations. *Pharmacology Research & Perspectives*. 2018. 6:e00420. https://doi.org/10.1002/prp2.420

119. Ling J, Yang X, Dong L, *et al.* Utility of cystatin C and serum creatinine-based glomerular filtration rate equations in predicting vancomycin clearance: a population pharmacokinetics analysis in elderly chinese patients. *Biopharmaceutics & Drug Disposition*. 2024. 45:58-68. https://doi.org/10.1002/bdd.2383

120. Frymoyer A, Schwenk HT, Zorn Y, *et al.* Model-informed precision dosing of vancomycin in hospitalized children: implementation and adoption at an academic children's hospital. *Frontiers in Pharmacology*. 2020. 11:551. https://doi.org/10.3389/fphar.2020.00551

121. Oliver MB, Boeser KD, Carlson MK, *et al.* Considerations for implementation of vancomycin Bayesian software monitoring in a level IV NICU population within a multisite health system. *American Journal of Health-System Pharmacy*. 2023. 80:670-7. https://doi.org/10.1093/ajhp/zxad048

122. Schneider F, Gessner A, El-Najjar N. Efficacy of vancomycin and meropenem in central nervous system infections in children and adults: current update. *Antibiotics*. 2022. 11:173. https://doi.org/10.3390/antibiotics11020173

123. Beer R, Lackner P, Pfausler B, *et al.* Nosocomial ventriculitis and meningitis in neurocritical care patients. *Journal of Neurology*. 2008. 255:1617-24. https://doi.org/10.1007/s00415-008-0059-8

124. Beach JE, Perrott J, Turgeon RD, *et al.* Penetration of vancomycin into the cerebrospinal fluid: a systematic review. *Clinical Pharmacokinetics*. 2017. 56:1479-90. https://doi.org/10.1007/s40262-017-0548-y

125. Lutsar I, McCracken GH, Jr., Friedland IR. Antibiotic pharmacodynamics in cerebrospinal fluid. *Clinical Infectious Diseases*. 1998. 27:1117-29. https://doi.org/10.1086/515003

126. Rybak MJ. The pharmacokinetic and pharmacodynamic properties of vancomycin. *Clinical Infectious Diseases*. 2006. 42:S35-S9. https://doi.org/10.1086/491712

127. Popa D, Loewenstein L, Lam SW, *et al.* Therapeutic drug monitoring of cerebrospinal fluid vancomycin concentration during intraventricular administration. *Journal of Hospital Infection*. 2016. 92:199-202. https://doi.org/10.1016/j.jhin.2015.10.017

128. Li X, Wu Y, Sun S, *et al.* Population pharmacokinetics of vancomycin in postoperative neurosurgical patients. *Journal of Pharmaceutical Sciences*. 2015. 104:3960-7. https://doi.org/10.1002/jps.24604

129. Li X, Wu Y, Sun S*, et al.* Population pharmacokinetics of vancomycin in postoperative neurosurgical patients and the application in dosing recommendation. *Journal of Pharmaceutical Sciences*. 2016. 105:3425-31. https://doi.org/10.1016/j.xphs.2016.08.012

130. Jalusic KO, Hempel G, Arnemann P-H*, et al.* Population pharmacokinetics of vancomycin in patients with external ventricular drain-associated ventriculitis. *British Journal of Clinical Pharmacology*. 2021. 87:2502-10. https://doi.org/10.1111/bcp.14657

131. Mayersohn M, Conrad K, Achari R. The influence of a cooked meat meal on creatinine plasma concentration and creatinine clearance. *British Journal of Clinical Pharmacology*. 1983. 15:227-30. https://doi.org/10.1111/j.1365-2125.1983.tb01490.x

132. Thakare R, Chhonker YS, Gautam N*, et al.* Quantitative analysis of endogenous compounds. *Journal of Pharmaceutical and Biomedical Analysis*. 2016. 128:426-37. https://doi.org/10.1016/j.jpba.2016.06.017

133. Sun N, Li Q, Zhao L*, et al.* Simultaneous quantitative analysis of phosphocreatine, creatine and creatinine in plasma of children by HPLC–MS/MS method: application to a pharmacokinetic study in children with viral myocarditis. *Biomedical Chromatography*. 2019. 33:e4558. https://doi.org/10.1002/bmc.4558

134. Grundmann F, Müller RU, Reppenhorst A*, et al.* Preoperative short-term calorie restriction for prevention of acute kidney injury after cardiac surgery: a randomized, controlled, open-label, pilot trial. *Journal of the American Heart Association*. 7:e008181. http://doi.org/10.1161/JAHA.117.008181

135. Grundmann F, Müller R-U, Hoyer-Allo KJR*, et al.* Dietary restriction for prevention of contrast-induced acute kidney injury in patients undergoing percutaneous coronary angiography: a randomized controlled trial. *Scientific Reports*. 2020. 10:5202. http://doi.org/10.1038/s41598-020-61895-2

136. Kinast CB, Paal M, Liebchen U. Comparison of cerebrospinal fluid collection through the proximal and distal port below the overflow system from an external ventricular drain. *Neurocritical Care*. 2022. 37:775-8. https://doi.org/10.1007/s12028-022-01615-y

137. Blassmann U, Hope W, Roehr AC*, et al.* CSF penetration of vancomycin in critical care patients with proven or suspected ventriculitis: a prospective observational study. *Journal of Antimicrobial Chemotherapy*. 2019. 74:991-6. https://doi.org/10.1093/jac/dky543

Declaration of contributions

I declare that, in accordance with the provisions of the doctoral regulations, all the included publications will be used solely by myself in a cumulative dissertation. Furthermore, I hereby declare my contributions, as well as those of all co-authors, to the publications related to the projects included in my dissertation.

Publication 1:

ZC (Zhendong Chen) and CC (Chunli Chen) developed the model and drafted the manuscript. Specifically, ZC carried out these two tasks while CC supported the process with her advice. MM (Michael Mayersohn) performed the clinical trial and provided the data. UF (Uwe Fuhr) and MT (Max Taubert) designed and guided the research.

Publication 2:

ZC, UF, and MT wrote the manuscript. Specifically, ZC drafted the manuscript, while UF and MT provided revisions and helped ZC finalize it. ZC and QD (Qian Dong) developed the clinical protocol with input, suggestions, and revisions from UF and MT. ZC, QD, CD (Charalambos Dokos), JB (Jana Boland), and UF performed the research; ZC, QD, and MT analyzed the data. Specifically, ZC developed and tested the models with guidance and comments from QD and MT.

Publication 3:

ZC drafted the manuscript, while UF and UL (Uwe Liebchen) provided revisions and helped ZC finalize it. ZC analyzed the data and tested the models with input and suggestions from UF and UL. CC and CD supervised the data analysis. TW (Thomas Weig), MZ (Michael Zoller), SH (Suzette Heck), KD (Konstantinos Dimitriadis), NT (Nicole Terpolilli), CK (Christina Kinast), CS (Christina Scharf), and UL designed the research and conducted the clinical study. CL (Constantin Lier) and CD performed the measurements.

PhD candidate, Zhendong Chen

Supervisor, Univ.-Prof. Dr. med. Uwe Fuhr

Acknowledgments

First and foremost, I want to thank my supervisor, Professor Uwe Fuhr, for guiding me through my PhD journey. I'm deeply grateful he accepted me as his student even though my academic background didn't perfectly match his research field. Throughout my studies, he was endlessly patient - teaching me at my own pace and giving me room to grow. His constant encouragement built my confidence, while his trust allowed me to work independently. I especially appreciate how he always valued my ideas and opinions. More than just an advisor, he helped me become both a better researcher and a better person.

I would also like to sincerely thank my tutors, Professor Thomas Streichert and Professor Paul Brinkkötter, for their helpful advice and support during my studies, and for their time and effort during the regular tutor meetings.

Special thanks to Dr. Max Taubert and Dr. Chunli Chen for patiently teaching me population pharmacokinetics when I was just starting out. Your clear explanations of complex topics gave me the foundation I needed.

Thank my colleagues for preparing and conducting our clinical studies together. Your professionalism in patient recruitment, data collection, and problem-solving during challenges made our collaborative work both productive and enjoyable.

I'm truly thankful to Professor Dafang Zhong for encouraging me to pursue research in Germany, and for making my study abroad possible. My heartfelt thanks go to Dr. Yifan Zhang for her continuous guidance - her thoughtful mentorship and our academic discussions have contributed immensely to my growth as a researcher.

Finally, to my beloved parents and dearest friends: your unwavering emotional support, understanding during my absences, and constant encouragement carried me through this entire journey. This achievement belongs as much to you as it does to me.

I gratefully acknowledge the China Scholarship Council for their financial support during my PhD studies.

Curriculum Vitae

Name: Zhendong Chen

Education background

University of Cologne Cologne, Germany

PhD. student, Supervisor: Professor Uwe Fuhr 10/2021 - present

Major: Clinical pharmacology and pharmacometrics

Shanghai Institute of Materia Medica (SIMM), Chinese Academy of Sciences Shanghai, China

Master's Degree, Supervisor: Professor Dafang Zhong 09/2017 - 07/2020

Major: Drug metabolism and pharmacokinetics

Sichuan University Chengdu, China

Bachelor's Degree, West China school of pharmacy 09/2013 - 06/2017

Major: Pharmacy

Publications

Chen Z, Qian D, Dokos C, *et al*. A joint pharmacometric model of iohexol and creatinine administered through a meat meal to assess GFR and renal OCT2/MATE activity. *Clin Pharmacol Ther*. 2025. Epub ahead of print.

Chen Z, Taubert M, Chen C, *et al*. A semi-mechanistic population pharmacokinetic model of noscapine in healthy subjects considering hepatic first-pass extraction and *CYP2C9* genotypes. *Drugs R D*. 2024. 24:187-199.

Chen Z, Taubert M, Chen C, *et al*. Plasma and cerebrospinal fluid population pharmacokinetics of vancomycin in patients with external ventricular drain. *Antimicrob Agents Chemother*. 2023. 67:e0024123

Chen Z, Chen C, Taubert M, *et al*. A population pharmacokinetic model for creatinine with and without ingestion of a cooked meat meal. *Eur J Clin Pharmacol*. 2022. 78:1945-1947.

Chen Z, Gao Y, Xue H, *et al*. Pharmacokinetics of FGF21-164 fusion protein in mice using UHPLC-MS/MS method. *Acta Pharmaceutica Sinica*. 2021. 56:2372-2377.

Chen Z, Zhang Y, Zhu Y, *et al*. Effects of food on the pharmacokinetic properties and mass balance of henagliflozin in healthy male volunteers. *Clin Ther*. 2021. S0149-2918:00252-6.

Chen Z, Li L, Zhan Y, *et al*. Characterization of henagliflozin metabolism and quantitative determination of its major metabolites in humans. *J Pharm Biomed Anal*. 2021. 192:113632.

Chen Z, Gao Y, Zhong D. Technologies to improve the sensitivity of existing chromatographic methods used for bioanalytical studies. *Biomed chromatogr*, 2020. 34:e4798.

27.06.2025 Zhendong Chen

Date Signature

Erklärung

Hiermit versichere ich an Eides statt, dass ich die vorliegende Dissertationsschrift selbststandig und ohne die Benutzung anderer als der angegebenen Hilfsmittel angefertigt habe. Alle Stellen - einschlieslich Tabellen, Karten und Abbildungen -, die wortlich oder sinngemas aus veroffentlichten und nicht veroffentlichten anderen Werken im Wortlaut oder dem Sinn nach entnommen sind, sind in jedem Einzelfall als Entlehnung kenntlich gemacht. Ich versichere an Eides statt, dass diese Dissertationsschrift noch keiner anderen Fakultät oder Universität zur Prufung vorgelegen hat; dass sie - abgesehen von unten angegebenen Teilpublikationen - noch nicht veröffentlicht worden ist sowie, dass ich eine solche Veröffentlichung vor Abschluss der Promotion nicht ohne Genehmigung der / des Vorsitzenden des IPHS-Promotionsausschusses vornehmen werde. Die Bestimmungen dieser Ordnung sind mir bekannt. Die von mir vorgelegte Dissertation ist von Prof. Dr. med. Uwe Fuhr betreut worden.

Daruber hinaus erklare ich hiermit, dass ich die Ordnung zur Sicherung guter wissenschaftlicher Praxis und zum Umgang mit wissenschaftlichem Fehlverhalten der Universitat zu Koln gelesen und sie bei der Durchfuhrung der Dissertation beachtet habe und verpflichte mich hiermit, die dort genannten Vorgaben bei allen wissenschaftlichen Tatigkeiten zu beachten und umzusetzen.

Übersicht der Publikationen

1. Chen Z, Chen C, Taubert M, *et al*. A population pharmacokinetic model for creatinine with and without ingestion of a cooked meat meal. *Eur J Clin Pharmacol*. 2022. 78:1945-1947.
2. Chen Z, Dong Q, Dokos C, *et al*. A joint pharmacometric model of iohexol and creatinine administered through a meat meal to assess GFR and renal OCT2/MATE activity. *Clin Pharmacol Ther*. 2025. Epub ahead of print.
3. Chen Z, Taubert M, Chen C, *et al*. Plasma and cerebrospinal fluid population pharmacokinetics of vancomycin in patients with external ventricular drain. *Antimicrob Agents Chemother*. 2023. 67:e0024123.

Ich versichere, dass ich alle Angaben wahrheitsgemas nach bestem Wissen und Gewissen gemacht habe und verpflichte mich, jedmogliche, die obigen Angaben betreffenden Veranderungen, dem IPHS-Promotionsausschuss unverzuglich mitzuteilen.

27.06.2025	Zhendong Chen
Datum	Unterschrift

Appendix (copies of publications)

European Journal of Clinical Pharmacology (2022) 78:1945–1947
https://doi.org/10.1007/s00228-022-03398-9

RESEARCH

A population pharmacokinetic model for creatinine with and without ingestion of a cooked meat meal

Zhendong Chen[1] · Chunli Chen[1,2] · Max Taubert[1] · Michael Mayersohn[3] · Uwe Fuhr[1]

Received: 5 September 2022 / Accepted: 29 September 2022 / Published online: 10 October 2022

Keywords Creatinine · Population pharmacokinetic model · Volume of distribution · Creatinine generation rate

To the Editor,

Commonly used equations for estimating creatinine clearance (CL) and/or glomerular filtration rate (GFR) from serum creatinine are based on steady-state assumptions regarding creatinine formation and elimination and are therefore less applicable to patients with unstable renal function [1–3]. A compartmental creatinine model that can describe the dynamics in creatinine parameters over time was previously introduced by Ullah et al. to estimate creatinine clearance [4]. In this model, volume of distribution (V_d) of creatinine was fixed at 60% of total body weight, corresponding to total body water (TBW). This approximation ignores variability, which may lead to biased estimates of other pharmacokinetic (PK) parameters [4]. Therefore, there is a need to enrich the estimation of creatinine PK parameters with experimental data, in the case of V_d including exogenous administration of creatinine. Creatinine PK profiles in healthy subjects with and without ingestion of a cooked meat meal as a creatinine source were previously reported by Mayersohn et al. [5]. Data from this study were reanalyzed using a population pharmacokinetic (PPK) approach to estimate PK parameters for creatinine, refine the dynamic creatinine model, and reduce bias in the estimation of other kinetic parameters.

A one-compartment PK model with linear elimination, first-order absorption, and zero-order creatinine generation was constructed based on the dataset composed of 133 serial creatinine plasma concentrations and 11 creatinine amounts excreted in urine during 24 h. Exponential models were most suitable to describe inter-individual variability (IIV), while two separate proportional errors were best to describe residual variability of plasma concentrations and amounts excreted in urine, respectively. The individual bioavailable creatinine dose for each subject was estimated using a pre-defined arbitrary population dose (180 mg) multiplied by individual post hoc estimates for apparent bioavailability (F1). Both the goodness of fit and visual predictive check plots (Supplemental Figs. 1 and 2) and the bootstrap results showed that the final model was reliable and stable.

Table 1 lists the PK parameters estimated from the final model and the 95% confidence intervals derived from 994 successful bootstrap samples. The typical values for CL and V_d of creatinine were estimated to be 7.92 L/h and 53.9 L (73.8% of the total body weight), which were similar to the reported values [5–7]. Incorporating variability on CL and V_d did not significantly improve the model, which may be attributable to the relative homogeneity of the small population studied. As a comparison, when fixing the value of V_d to the estimated TBW, which is 43.8 L (60% of 73 kg), the OFV will increase by 3.230, which does not represent a significant difference, while values of other parameters do not change much. Deciding between various error models was not straightforward due to the limited number of data points, but the point estimates for pharmacokinetic parameters remained essentially unchanged regardless of the error model chosen and are therefore considered as reliable.

✉ Zhendong Chen
zhendong.chen@uk-koeln.de

1 Department I of Pharmacology, Center for Pharmacology, Faculty of Medicine and University Hospital Cologne, University of Cologne, Gleueler Straße 24, Cologne 50931, Germany

2 Heilongjiang Key Laboratory for Animal Disease Control and Pharmaceutical Development, College of Veterinary Medicine, Northeast Agricultural University, Changjiang Road 600, Xiangfang District, Harbin 150030, People's Republic of China

3 College of Pharmacy, University of Arizona, Tucson, AZ, USA

Table 1 Parameter estimates obtained from the final model and bootstrap statistics ($n = 1000$)

	Final model		994 successful bootstrap runs	
Parameter	**Estimates**	**RSE (%)**	**Median**	**95% CI**
Ka (1/h)	1.76	26.7	1.60	0.715–3.34
CL (L/h)	7.59	6.4	7.59	6.71–8.48
V_d (L)	53.9	20.0	53.0	31.2–72.0
F1	1.57	21.1	1.60	1.04–2.07
CGR (mg/h)	67.9	6.9	67.9	59.4–76.3
Lag time (h)	0.344	4.7	0.344	0.297–0.370
IIV				
Ka (CV%)	55.3 (1.6%)	37.7	55.4	3.8–83.1
F1 (CV%)	24.6 (0.1%)	20.3	24.0	15.0–30.0
CGR (CV%)	3.9 (0.1%)	25.8	3.5	1.1–4.7
Residual variability				
Proportional error, % (plasma)	3.9 (7.0)	10.0	3.8	3.2–4.5
Proportional error, % (urine)	15.5 (0.2)	21.8	14.7	6.4–19.7

For IIV, the corresponding shrinkage estimates are shown in parentheses

Ka apparent absorption rate constant, *CL* renal clearance, V_d the volume of distribution, *F1* dose correction factor, *CGR* creatinine generation rate

The typical value of the creatinine generation rate (CGR) in healthy volunteers was 68.0 mg/h, which is consistent with the value of 65.8 mg/h (male, 31 years, 73 kg) calculated based on the reported equation [2], but higher than the value of 42.8 mg/h and 43.8 mg/h in patients reported by Ullah et al. and Daugirdas et al., respectively [5, 8]. The estimated dose (293 ± 62.0 mg, $n = 6$) was not fully consistent with the increased creatinine amount excreted in urine after beef ingestion (180 ± 102 mg, $n = 5$). This does not exclude the possibility that these discrepancies are related to the accuracy of the raw data; furthermore, no demographic information is available in the publication to better define the PPK model.

In this evaluation, a PPK creatinine model was developed using creatinine data with and without ingestion of boiled beef in healthy volunteers. Reasonable parameter estimates including CGR and V_d were obtained from the final well-structured model. The model is a useful starting point for further experimental approaches to improve the understanding of creatinine kinetics, which may involve creatinine "dosing" accompanied by independent methods to assess GFR, e.g., by a test dose of iohexol.

Supplementary Information The online version contains supplementary material available at https://doi.org/10.1007/s00228-022-03398-9.

Acknowledgements China Scholarship council is greatly acknowledged for providing a PhD scholarship to Mr. Zhendong Chen.

Author contribution ZC and CC developed the model and drafted the manuscript. MM performed the clinical trial and provided the data. UF and MT designed and guided the research. All authors contributed to the final version of the manuscript.

Funding Open Access funding enabled and organized by Projekt DEAL. The authors received no external funding for this work. Zhendong Chen received a scholarship from the China Scholarship Council (CSC) for support of his PhD studies. The funder had no role in design, collection, analysis and interpretation of data, and writing and publication of the manuscript.

Data availability The data that support the findings of this study are available from the corresponding author upon reasonable request.

Declarations

Conflict of interest The authors declare no competing interests.

References

1. Bragadottir G, Redfors B, Ricksten SE (2013) Assessing glomerular filtration rate (GFR) in critically ill patients with acute kidney injury–true GFR versus urinary creatinine clearance and estimating equations. Crit Care 17(3):R108. https://doi.org/10.1186/cc12777

2. Cockcroft DW, Gault MH (1976) Prediction of creatinine clearance from serum creatinine. Nephron 16(1):31–41. https://doi.org/10.1159/000180580
3. Scappaticci GB, Regal RE (2017) Cockcroft-Gault revisited: new deliverance on recommendations for use in cirrhosis. World J Hepatol 9(3):131–138. https://doi.org/10.4254/wjh.v9.i3.131
4. Ullah S, Zoller M, Jaehde U et al (2021) A model-based approach to assess unstable creatinine clearance in critically ill patients. Clin Pharmacol Ther 110(5):1240–1249. https://doi.org/10.1002/cpt.2341
5. Mayersohn M, Conrad KA, Achari R (1983) The influence of a cooked meat meal on creatinine plasma concentration and creatinine clearance. Br J Clin Pharmacol 15(2):227–230. https://doi.org/10.1111/j.1365-2125.1983.tb01490.x
6. Pickering JW, Ralib AM, Endre ZH (2013) Combining creatinine and volume kinetics identifies missed cases of acute kidney injury following cardiac arrest. Crit Care 17(1):R7. https://doi.org/10.1186/cc11931
7. Bjornsson TD (1979) Use of serum creatinine concentrations to determine renal function. Clin Pharmacokinet 4(3):200–222. https://doi.org/10.2165/00003088-197904030-00003
8. Daugirdas JT, Depner TA (2017) Creatinine generation from kinetic modeling with or without postdialysis serum creatinine measurement: results from the HEMO study. Nephrol Dial Transplant 32(11):1926–1933. https://doi.org/10.1093/ndt/gfx320

A Joint Pharmacometric Model of Iohexol and Creatinine Administered through a Meat Meal to Assess GFR and Renal OCT2/MATE Activity

Zhendong Chen*, Qian Dong, Charalambos Dokos, Jana Boland, Uwe Fuhr and Max Taubert

Accurately assessing glomerular filtration rate (GFR) from plasma creatinine concentrations is challenging in patients with unstable renal function. This study aimed to refine the understanding of creatinine kinetics for more reliable assessments of GFR and net creatinine tubular secretion (nCTS) via OCT2/MATE in humans. In a clinical study of 14 healthy volunteers, iohexol was administered intravenously as a reference GFR marker, and creatinine was introduced through a meat meal. A joint pharmacometric model was developed using dense plasma and urine sampling. Simulations were used to evaluate the effect of different creatinine volume of distribution (V_d) values on GFR estimation after acute kidney injury (AKI) and to assess the impact of limited sampling strategies on GFR and nCTS estimation. Pharmacokinetic parameters for iohexol and creatinine aligned with reported values, but a lower V_d of 41% of total body weight and a nCTS fraction of 31% relative to overall creatinine clearance were observed. Commonly used equations based on single-point creatinine measurement all overestimated GFR, with the Modification of Diet in Renal Disease (MDRD) equation performing best, followed by Chronic Kidney Disease Epidemiology Collaboration (CKD-EPI) 2009 equation. Simulations demonstrate the effect of V_d estimate accuracy on detecting AKI from creatinine plasma concentrations only. Following low-dose iohexol administration, a single plasma sample at 5 hours and a urine sample from 0 to 5 hours provided accurate estimates of both GFR and nCTS using the joint model and enabled adequate correction for incomplete urine collection. This approach shows promise for assessing renal transporter activity based on estimated nCTS.

Study Highlights

WHAT IS THE CURRENT KNOWLEDGE ON THE TOPIC?

☑ Creatinine volume of distribution (V_d) plays a key role in estimating unstable glomerular filtration rate and is typically assumed to be 60% of total body weight (TBW), but was estimated at 73.8% of TBW in a previous study. Apart from glomerular filtration, creatinine undergoes tubular secretion via OCT2/MATE and tubular reabsorption. The net creatinine tubular secretion (nCTS) accounts for 10–40% of its renal excretion and has the potential for assessing renal transporter activity.

WHAT QUESTION DID THIS STUDY ADDRESS?

☑ What is the true value of V_d, and to what extent does it affect the estimation of unstable renal function? Additionally, how many samples are required to accurately estimate both GFR and nCTS following a low-dose iohexol administration?

WHAT DOES THIS STUDY ADD TO OUR KNOWLEDGE?

☑ A joint pharmacometric model of iohexol and creatinine was developed and validated, confirming key pharmacokinetic parameters but identifying a lower V_d of 41.3% of total body weight and a higher nCTS fraction of 31% relative to creatinine clearance. The model demonstrated that varying V_d values can introduce significant bias in GFR estimation. Using a single plasma sample at 5 hours and a urine sample from 0 to 5 hours after low-dose iohexol administration, the joint model accurately predicted both GFR and nCTS.

HOW MIGHT THIS CHANGE CLINICAL PHARMACOLOGY OR TRANSLATIONAL SCIENCE?

☑ The joint model of iohexol and creatinine can serve as an effective tool for estimating unstable GFR and nCTS, with nCTS potentially acting as a marker for assessing renal OCT2/MATE activity.

Department I of Pharmacology, Center for Pharmacology, Faculty of Medicine and University Hospital Cologne, University of Cologne, Cologne, Germany.
*Correspondence: Zhendong Chen (zhendong.chen@uk-koeln.de)

Received November 16, 2024; accepted February 5, 2025. doi:10.1002/cpt.3612

Estimated creatinine clearance (CrCL) and/or estimated glomerular filtration rate (eGFR) based on serum creatinine are commonly used in clinical laboratories to assess kidney function and guide drug dosing adjustments in chronic renal impairment.[1] However, these estimates assume steady-state conditions for creatinine formation and elimination, making them less reliable for patients with fluctuating renal function.[2–4] Although measured CrCL using a collection of urine can be used when a steady state has not been reached and there is no change in kinetics, it assumes that the observed data are free of error and ignores common mistakes in urine collection.[5] A study by van Acker et al. showed a circadian rhythm in GFR, with higher rates during the day and lower rates at night, which cannot be detected from relatively stable creatinine plasma concentrations.[6] A slight post-meal decrease in creatinine at 1.5 hours aligns with previously reported intra-individual creatinine variation throughout the day.[7–9] Therefore, GFR estimates based on a single time-point creatinine plasma concentration under non-steady-state conditions are expected to be biased.

In contrast, compartmental nonlinear mixed-effects modeling offers a feasible method to more accurately assess unstable CrCL and account for measurement errors. Ullah et al. proposed a compartmental creatinine model using plasma and urine creatinine data from critically ill patients, effectively describing renal function changes and outperforming standard methods.[10] However, further evaluation of this model through an independent assessment of GFR is desirable before application. Additionally, the study assumed a creatinine volume of distribution (V_d) of 60% of total body weight (TBW),[10] which neglected variability and may result in biased estimates of other kinetic parameters. The magnitude of creatinine V_d is important because it determines how fast changes in CrCL are reflected by changes in plasma concentrations. Our prior analysis of published creatinine data in healthy volunteers, both with and without the ingestion of cooked meat,[11] yielded an estimation of creatinine V_d close to total body water.[12] It also provided an approximate estimate of the creatinine generation rate (CGR) consistent with reported values for healthy individuals. However, the absence of demographic information in this study limited further investigation into creatinine pharmacokinetics (PK).

Beyond the use of creatinine to assess global renal function, it may also serve as an endogenous marker to assess transporter activity. It is well-known that creatinine is eliminated not only through glomerular filtration but also undergoes tubular secretion and reabsorption. The net contribution of tubular secretion, accounting for reabsorption, represents 10–40% of its total renal excretion.[13] The transporter chain mediating this secretion has been identified as basolateral organic cation transporter 2 (OCT2) and apical multidrug and toxin extrusion proteins (MATE1 and MATE2-K) by *in vitro* experiments as well as by clinical studies with the selective inhibitors cimetidine (MATEs), trimethoprim (MATEs), dolutegravir (OCT2) and pyrimethamine (OCT2 and MATEs).[14] The effects of these inhibitors were much larger on renal metformin excretion, a drug also secreted by OCT2/MATE, because the fraction of metformin eliminated by tubular secretion is also much larger.[14] Therefore, using overall renal excretion of creatinine to assess OCT2/MATE activity *in vivo* is not very informative.[15] Still, when assessing net creatinine tubular secretion (nCTS) separately instead of overall excretion,[16] creatinine may provide valuable information on renal OCT2/MATE activity including its inhibition by drug–drug interactions (DDIs).

The present study aims at improving the description of creatinine kinetics as a prerequisite for a more reliable creatinine-based assessment of renal function and/or OCT/MATE activity in humans. To this end, we evaluated a dynamic creatinine model in a clinical trial in healthy volunteers by analyzing creatinine data from dense plasma and urine sampling and comparing the results to those obtained with iohexol as an independent GFR probe. The importance of correct creatinine V_d estimates was investigated by simulations. Finally, a limited sampling strategy was evaluated for simultaneous assessment of GFR and nCTS.

METHODS

Ethical approval

The clinical study was registered with the German Clinical Trials Register under the identification code DRKS00029908 and approved by the Ethics Committee of the Faculty of Medicine at the University of Cologne, Germany, on November 21, 2022 (No. 22-1347_1). The study was conducted in accordance with Good Clinical Practice guidelines and the Declaration of Helsinki (64th WMA General Assembly, Brazil, October 2013).[17] All volunteers provided informed written consent.

Study design

Pilot study. A pilot study was conducted with two healthy adult participants, aged over 18 years with a body mass index (BMI) ranging from 18.5 to 30 kg/m^2, to assess the feasibility of administering creatinine via cooked beef. Participants were enrolled after a pre-screening evaluation of their health status. Key exclusion criteria included hypersensitivity to iohexol, previous reactions to contrast media, any relevant clinical or laboratory abnormality, concurrent medication use, smoking, drug addiction, and pregnancy or breastfeeding.

A two-period crossover design was used, with participants receiving either 259 mg iohexol intravenously without food (test period) or 250 g cooked beef as a breakfast 25 minutes after intravenous administration of 259 mg iohexol (meat period). Beef was vacuum-sealed and cooked at 70°C for 1.5 hours. Approximately 200 mg of cooked beef was collected in three aliquots for the measurement of creatinine content. Both participants received lunch (13.2 g non-meat protein) and dinner (11.3 g non-meat protein), and approximately 240 ml of plain water before and after urine collection. For pharmacokinetic analysis, blood samples were collected using EDTA-K tubes at baseline and 0.17, 0.33, 0.5, 0.75, 1, 1.5, 2, 3, 4, 5, 6, 8, 10, 12, 16, 20, and 24 hours after iohexol administration in the non-meat period. In the meat period, additional blood samples were obtained at 1.25, 2.5, 28, 32, and 36 hours post-iohexol administration. Urine samples were collected during intervals of 0–2, 2–4, 4–6, 6–8, 8–10, 10–12, 12–16, 16–20, 20–24 hours in the non-meat period, with additional samples at 24–28, 28–32, and 32–36 hours in the meat period. The wash-out period was at least 7 days.

Main study. Twelve additional volunteers were included based on the same inclusion/exclusion criteria as the pilot study. The main study used a crossover design with six random sequences, where participants received three treatments: 3,235 mg iohexol under fasting conditions

(reference period); 259 mg iohexol under fasting conditions (test period); and 3,235 mg iohexol with 250 g cooked beef (meat period). The inclusion of two iohexol dose levels aimed to assess a possible dose effect on iohexol clearance (IoCL); however, it is not the primary objective of this study and will be reported separately.[18] The beef steak was minced in a blender and then vacuum-sealed in a plastic bag. The minced beef was cooked in a water bath at 90°C for 1.5 hours to generate a significant amount of creatinine. All other conditions and procedures were identical with those employed in the pilot study. Quantification methods for iohexol and creatinine are available in the **supplementary materials**.

Population pharmacokinetic analysis

Population pharmacokinetic (popPK) modeling was conducted using a nonlinear mixed-effects approach with NONMEM version 7.4.0 (ICON Development Solutions, USA), Perl-speaks-NONMEM (PsN) version 5.3.0 (Uppsala University, Sweden), using the first-order conditional estimation with interaction (FOCE-I) method throughout model development. Post-processing and plotting of NONMEM data were done using R version 4.3.0 (https://www.R-project.org/). To compare nested models differing by one parameter, a statistical criterion of 3.84 in the objective function value (OFV) was used (equivalent to $P < 0.05$). The final model was evaluated using goodness-of-fit (GOF) plots, non-parametric bootstrap analysis, and prediction-corrected visual predictive check (pcVPC). Model estimates were compared to non-compartmental analysis results (method described in **supplementary material**) to ensure no bias in parameter estimates.

The following assumptions were made for all participants: (1) no changes in the typical value of IoCL, CrCL, and CGR throughout the study; (2) iohexol and creatinine are solely eliminated via kidney; and (3) the circadian rhythms of iohexol and CrCL follow a consistent sine function pattern within a day.[6]

Joint population pharmacokinetic model for iohexol and creatinine. Based on prior knowledge, iohexol was modeled using a three-compartment linear elimination model, and creatinine with a one-compartment model.[10,12,19] A first-order process with lag time and a zero-order process described creatinine uptake from meat and endogenous production, respectively.[12] Different settings for creatinine dose assessment/bioavailability (F1) and creatinine V_d were evaluated for model performance and physiological plausibility (**Table 1**). After establishing stable models for iohexol and creatinine, a joint model was developed where IoCL represented GFR and CrCL represented the sum of GFR and nCTS. The inter-individual variability (IIV) and inter-occasion variability (IOV) for PK parameters were modeled exponentially as the following equation: $\theta_i = \theta \times e^{\eta_i}$, where θ_i represents the value of the individual parameter value, θ represents the population point estimate, and η_i is a normally distributed random variable with a mean of 0 and variance of ω^2. Four independent proportional residual error models were used for plasma and urine data of iohexol and creatinine.

Covariate model. The circadian rhythm of both GFR and nCTS was first using the joint model based on the following equation:

$$CL = CL_{TV} \times \left(1 + \sin\left(\frac{\text{time}}{\text{interval}} \times \pi\right) \times \theta_{\text{daytime/night}}\right)$$

where CL represents GFR or nCTS, CL_{TV} is the typical value of GFR or nCTS, "time" was adjusted to start as 0, and "interval" is 14 hours for daytime and 10 hours for night. The food effect was assessed using a proportional model at 2-hour intervals after a non-meat protein meal. PK parameters were allometrically scaled to a TBW of 70 kg, using a power of 0.75 for GFR, nCTS, and inter-compartmental clearances of iohexol (Q_{p1} and Q_{p2}) and of 1.0 for iohexol central compartment volume (V_c), creatinine V_d, and iohexol peripheral compartment volumes (V_{p1} and V_{p2}).[20] In comparison, using other body size-related covariates or estimating scaling factors for clearance and volume were subsequently assessed. The estimation of CGR was replaced by the Cockcroft-Gault equation.[3] Subsequent covariate analysis employed forward addition and backward elimination methods, with significance levels of 0.05 (ΔOFV <= −3.84) and 0.01 (ΔOFV <= −6.63), respectively. The effects of sex, age, height, TBW, BMI, lean body mass,[21] estimated total body water,[22] and plasma albumin concentration from laboratory test results on appropriate PK parameters were

Table 1 Different settings for creatinine dose, bioavailability (F1), and volume of distribution (V_d) as well as the parameter estimates and objective function value (OFV) from the respective models

	Dose input in the dataset		F1		V_d		CL	CGR	
Model	Setting	Mean (mg)	Setting	Value	Setting	Mean (L)	Value (mL/min)	Value (mg/h)	OFV
1	Creatinine content in ingested beef	401	Fixed	100%	Estimated	76.6	136	67.9	3,809
2	Individual differences in creatinine excretion over 24 h between meat and non-meat periods	335	Fixed	100%	Estimated	53.4	136	67.7	3,536
3	Individual differences in creatinine excretion over 16 h between meat and non-meat periods	273	Fixed	100%	Estimated	44.7	135	67.8	3,502
4	Creatinine content in ingested beef	401	Estimated	61.9%	Fixed at "individual estimated total body weight ×0.6"	47.1	134	67.3	3,461
5	Creatinine content in ingested beef	401	Estimated	57.9%	Fixed at "individual estimated total body water"[22]	42.3	133	67.1	3,418
6	Creatinine content in ingested beef	401	Estimated	48.7%	Estimated	27.1	132	66.7	3,364

investigated. Covariate relationships were modeled based on the following equations:

(1)Continuous covariate:

$$P_i = P_{TV} \times \left(\frac{C_{ij}}{mean\left(C_j\right)} \right)^{\theta}$$

(2) Categorical covariate:

$$P_i = P_{TV} \times \theta^{C_{ij}}$$

where P_{TV} represents the typical value of parameter, C_{ij} represents the covariate value of participant i for parameter P, and $mean\left(C_j\right)$ represents the mean of covariate j in the investigated population.

Simulation of creatinine profiles after presumed AKI

Creatinine plasma concentration profiles were simulated in 1000 virtual patients using the final model, with reductions in both GFR and nCTS evenly distributed from 25% to 75% across the population. Circadian rhythms of GFR and nCTS were not taken into account. The simulation data were subsequently re-analyzed with different settings for creatinine V_d (from 41.3% to 73.8% of TBW).[10,11] For early diagnosis of acute kidney injury (AKI), estimating the changed GFR using first 1, 2, or 3 concentrations (assuming hourly sampling post-AKI), as well as concentrations measured after 24 and 48 hours, were compared using the different V_d values described above. While using 41.3% as a reference, the relative error (RE) was calculated by the following equation:

$$\mathrm{RE}(\%) = \left(\frac{\text{Estimated changed GFR}}{\text{True changed GFR}} - 1 \right) \times 100\,\%$$

Creatinine plasma concentrations following a 75% reduction in both GFR and nCTS were simulated for an individual with median dataset covariates, using three different settings for creatinine V_d. Based on the RIFLE (Risk, Injury, Failure, Loss of kidney function, and End-stage kidney disease) classification for AKI definition, the times when plasma concentrations reach 1.5-fold (risk), 2.0-fold (injury), and 3.0-fold (failure) of baseline level after AKI were calculate for each model.[23]

Limited sampling strategy

Iohexol and creatinine plasma concentrations, along with amounts excreted in urine (A_e), were simulated in 1,000 virtual individuals following a 259 mg intravenous dose of iohexol, using final model estimates of GFR and nCTS with a predefined 30% coefficient of variation. A random 10%–50% urine loss was applied to both iohexol and urine data over the 0–5 hours interval post-dose, generating datasets (urine.loss) with incomplete urine collection. Various limited sampling strategies for estimating GFR were evaluated, based on 1 to 4 plasma samples collected at 10 minutes, 30 minutes, 2 hours, and 5 hours, with later samples included as sample numbers were reduced.[24] The respective individual GFR estimates were then used to predict iohexol A_e over the 0–5 hours post-dose interval. To account for incomplete urine collection, creatinine A_e was corrected by multiplying it by the ratio of predicted to incomplete iohexol A_e, generating datasets (urine.corrected) with correction. Finally, iohexol plasma data, creatinine plasma data, and corrected urine data were used to estimate GFR and nCTS using the final model. The RE and root mean squared error (RMSE) of GFR and nCTS were calculated for each model.

RESULTS

Demographics

Fourteen participants, mean age 33 years (range: 23–48), were enrolled, including two in the pilot and 12 in the main study. The dataset includes 771 iohexol and 826 creatinine plasma concentrations, and 439 measurements for both iohexol and creatinine in urine. Observations with missing data (< 5%) were discarded. Detailed demographics and baseline characteristics are provided in **Table 2**.

Population pharmacokinetic analysis

A three-compartment model for iohexol and a one-compartment model for creatinine fitted the data well. No further refinement was explored for the iohexol model since it provided a fully adequate description of the data. **Table 1** lists the parameter

Table 2 Demographics and baseline characteristics of enrolled participants

	Male	Female	All	
Demographics/Characteristic	Mean (SD)	Mean (SD)	Mean (SD)	Range
Number	9	5	14	–
Age (years)	31 (6)	37 (8)	33 (8)	23–48
Height (cm)	183 (6)	169 (6)	178 (9)	163–196
Total body weight (kg)	86.2 (7.1)	64.5 (4.7)	78.5 (12.2)	59.1–95.8
Body mass index (kg/m^2)	25.9 (2.1)	22.6 (0.9)	24.7 (2.4)	21.2–28.9
Body surface area (m^2)	2.08 (0.10)	1.74 (0.09)	1.96 (0.19)	1.63–2.22
Plasma albumin (g/L)	45.7 (1.6)	45.4 (3.6)	45.6 (2.5)	40.0–50.0
Plasma creatinine concentration (mg/dL)[a]	1.00 (0.08)	0.73 (0.09)	0.90 (0.15)	0.60–1.17
Estimated creatinine generation rate (mg/h)[3]	78.4 (7.2)	48.0 (4.9)	67.3 (16.3)	41.0–92.6
Estimated lean body mass (kg)[21]	64.6 (3.7)	47.8 (3.7)	58.6 (8.9)	43.7–69.7
Estimated total body water (L)[22]	48.1 (2.6)	31.9 (1.7)	42.3 (8.1)	29.9–52.5
Estimated glomerular filtration rate (mL/min/1.73 m^2)[27]	101 (9)	104 (12)	102 (10)	80.0–116

[a]Creatinine plasma concentration was measured from a laboratory test at the screening visit.

estimates and OFV for models tested with different dose inputs (written in the datasets), F1, and creatinine V_d. The creatinine amount in beef (mean: 401 mg) was higher than the differences in creatinine excretion between non-meat and meat periods over 24 h (mean: 335 mg) or 16 h (mean: 273 mg), indicating less than 100% bioavailability. Meanwhile, a high correlation of 0.96 was observed between estimates of the calculated dose (dose input × F1) and creatinine V_d. The creatinine model estimating both F1 and V_d yielded the best performance compared with other models, which all overestimated plasma concentrations during the meat period (**Figure S1**). This model provided estimates of F1 and V_d with low relative standard errors (RSE) of 9% and 6%, respectively, while the point estimates of CrCL and CGR remained stable across all tested models. IOV for CrCL and CGR was estimated at 3.1% and 3.3%, respectively, and was not included in the final model due to a lack of clinical significance.

In the joint model, all estimates of iohexol and creatinine PK parameters were consistent with those from separate models (**Table S1**). The schematic diagram of the joint model is presented in **Figure S2**. Circadian rhythms of GFR and nCTS were merged, resulting in better estimations with lower RSEs and enhanced model stability compared to estimating them separately. Subsequently, circadian rhythms during daytime and nighttime were assessed using the joint model, reducing OFV by 53.5 and 29.7, respectively. IIV on GFR, iohexol V_c, nCTS, and creatinine V_d were estimated at 14.6%, 18.7%, 43.6%, and 18.4%, respectively. After including TBW as a covariate for all parameters by standard allometric scaling,[20] IIV decreased to 11.8%, 14.5%, 32.3%, and 15.4%, respectively. Additional tests using other body size-related covariates or estimating scaling factors for clearance and volume did not show significant improvement and thus standard allometric scaling was kept (**Table S2**). Replacing CGR with the Cockcroft-Gault equation decreased the OFV by 21.5 and reduced the IIV for CGR by 17.6%, from 30.4% to 12.8%. Further covariate analysis found that sex significantly affected nCTS, reducing the OFV by 7.48.

GOF plots (**Figures S3 and S4**) suggest that the final model fits the iohexol and creatinine data well overall, despite some slight overestimation in both creatinine plasma and urine data at early time points. Creatinine plasma data were better captured by the model with circadian rhythm. The pcVPC (**Figure S5**) also indicates a good fit for both iohexol and creatinine data. Estimates of all PK parameters in the final model, along with the 95% confidence intervals from bootstrap results, are listed in **Table 3**. Fixed and random effects showed sufficient precision, with RSEs below 21.0% and 63.9%, respectively.

Final estimates for GFR (IoCL) and CrCL (GFR plus nCTS), scaled to the mean weight of 78.5 kg, were 94.8 mL/min and 138 mL/min, respectively. These estimates are consistent with non-compartmental analysis results (results shown in **supplementary material**). In healthy participants, GFR accounted for approximately 69% of total CrCL, with 31% mediated by nCTS. Due to circadian rhythm, GFR and nCTS fluctuated between 104% and 91.6% of the mean over 24 hours. Creatinine V_d was estimated at 28.9 L, accounting for 41.3% of TBW in the investigated population.

Comparison of post hoc estimates of IoCL and CrCL with eGFR using different equations, including Cockcroft-Gault equation,[3] CKD-EPI 2021 (creatinine and cystatin C),[25] CKD-EPI 2012 (creatinine and cystatin C),[26] CKD-EPI 2021 (creatinine only), CKD-EPI 2009 (creatinine only),[27] and four-variable modification of diet in renal disease (MDRD) equation,[28] is presented in **Figure 1**. The eGFRs based on single time-point concentration prior to administration from commonly used equations all overestimate GFR, with the MDRD equation performing best, followed by CKD-EPI 2009. Conversely, CKD-EPI 2021 (creatinine and cystatin C) and Cockcroft-Gault equations provided the closest CrCL estimates.

AKI simulation for different creatinine V_d values

The final model was used to generate the simulation data for patients with sudden AKI. Prediction accuracy for different creatinine V_d settings and with 1–3 initial samples post-AKI onset is shown in **Figure 2a**. When using the reference value of 41.3%, the model captured the overall trend but was less accurate and precise with fewer concentrations. In contrast, models with V_d values of 60.0% and 73.8% of total body weight underestimated GFR by 35.7% and 65.7% with one concentration, by 32.2% and 59.4% with two concentrations, and by 28.9% and 53.3% with three concentrations. However, when using 2 concentrations after 24 hours and 48 hours, models showed minor differences in prediction accuracy with mean RE <1%. Concentration-time curves following a reduction of 75% in both GFR and nCTS in one individual are illustrated in **Figure 2b**. The timing of AKI diagnosis based on RIFLE criteria corresponds to the used values of creatinine V_d in ascending order, and the ratio of the times is approximately equal to the ratio of V_d used. Therefore, the timing to diagnose AKI risk (from 4.1 to 6.5 h after onset of AKI) is less dependent on the values for creatinine V_d, but it significantly varies for definitely diagnosing kidney failure (from 19.6 to 34.0 h after onset of AKI).

Limited sampling strategy

Figure 3 illustrates prediction accuracy for GFR and nCTS across models with varying numbers of plasma concentrations, with and without urine data. Including urine data and using more than a single plasma sample at 5 h post-dose provided only minor improvements in GFR estimation (mean RE: −0.3 to 1.2%). However, urine data were critical for nCTS prediction accuracy, with mean RE for nCTS at −19.2% when 10–50% random urine loss occurred. Based on these findings, individual eGFR estimates derived from a single plasma sample at 5 h post-dose were used to predict iohexol A_e and calculate correction factors for incomplete urine collection. Applying the correction factor to creatinine A_e improved nCTS prediction accuracy and reduced RMSE compared to using uncorrected "urine.loss" data.

DISCUSSION

In this study, the dynamic creatinine model reliably described the kinetics of creatinine and essentially confirmed previous evaluations, while a lower V_d of 41.3% of TBW was found. Simulations to assess the impact of different V_d values illustrated the relevance of a proper V_d estimate to accurate diagnosis of AKI. nCTS,

Table 3 Parameter estimates and bootstrap (n = 1,000) results for creatinine and iohexol

Parameters	Estimate	RSE (%)	95% confidence interval	CV (%)	Shrinkage (%)
Fixed effect					
Iohexol					
GFR (mL/min)	87.0	3.4	(81.0, 92.7)	–	–
V_c (L)	8.69	4.7	(7.91, 9.54)	–	–
Q_{p1} (L/h)	0.131	9.2	(0.107, 0.163)	–	–
V_{p1} (L)	1.15	5.2	(1.05, 1.33)	–	–
Q_{p2} (L/h)	4.01	8.0	(3.37, 4.78)	–	–
V_{p2} (L)	4.22	3.1	(3.93, 4.53)	–	–
Creatinine					
K_a (1/h)	1.71	13.3	(1.35, 2.19)	–	–
nCTS (mL/min)	39.7	10.2	(31.2, 46.8)	–	–
V_d (L)	28.9	6.5	(25.6, 33.4)	–	–
F1 (%)	52.3	5.2	(47.7, 58.4)	–	–
Lag time (h)	0.291	3.0	(0.277, 0.308)	–	–
CGR (mg/h)	(140–age)×TBW/72×0.85 (if female)×60/100			–	–
Covariates					
Circadian rhythm during daytime (%)	3.70	21.0	(2.12, 5.72)	–	–
Circadian rhythm during nighttime (%)	8.42	17.7	(5.10, 11.1)	–	–
SEX on CTS[a]	0.627	15.0	(0.455, 0.857)	–	–
TBW on GFR, Q_{p1}, Q_{p2}, and nCTS	0.75 FIX	–		–	–
TBW on iohexol V_c and creatinine V_d	1 FIX	–		–	–
Random effect (IIV)					
Iohexol					
GFR	0.0226	43.6	(0.00379, 0.0246)	11.9	0.1
V_c	0.0211	38.2	(0.00585, 0.0390)	14.6	18.8
V_{p1}	0.0121	63.9	(0.00164, 0.0259)	11.0	6.2
V_{p2}	0.0113	33.8	(0.00304, 0.0187)	10.7	9.7
Creatinine					
nCTS	0.0506	56.7	(0.00333, 0.102)	23.1	10.6
V_d	0.0211	40.7	(0.00284, 0.0375)	15.1	2.3
CGR	0.0163	31.2	(0.00710, 0.0278)	12.7	0.7
F1	0.00810	53.5	(0.00145, 0.0205)	10.4	22.8
Random effect (RV)					
Iohexol					
Plasma concentration	0.0171	18.4	(0.0118, 0.0240)	13.3	2.6
Excreted amount in urine	0.0617	27.2	(0.0330, 0.0970)	25.2	0.7
Creatinine					
Plasma concentration	0.00255	7.3	(0.00221, 0.00291)	5.1	1.8
Excreted amount in urine	0.0413	41.4	(0.0142, 0.0770)	20.5	1.2

GFR, iohexol clearance was assumed as GFR; nCTS, net tubular secretion part of creatinine clearance; V_c, iohexol central compartment volume; Q_{p1}, inter–compartment clearance between central and first peripheral compartment; V_{p1} first peripheral compartment volume; Q_{p2}, inter–compartment clearance between central and second peripheral compartment; K_a, apparent absorption rate; V_d, creatinine volume of distribution; CGR, creatinine generation rate; F1, bioavailability; TBW, total body weight; RSE, relative standard error; CV, coefficient variance; IIV, inter-individual variability; RV, residual variability.
[a]SEX is a categorical covariate of 0 for male and 1 for female.

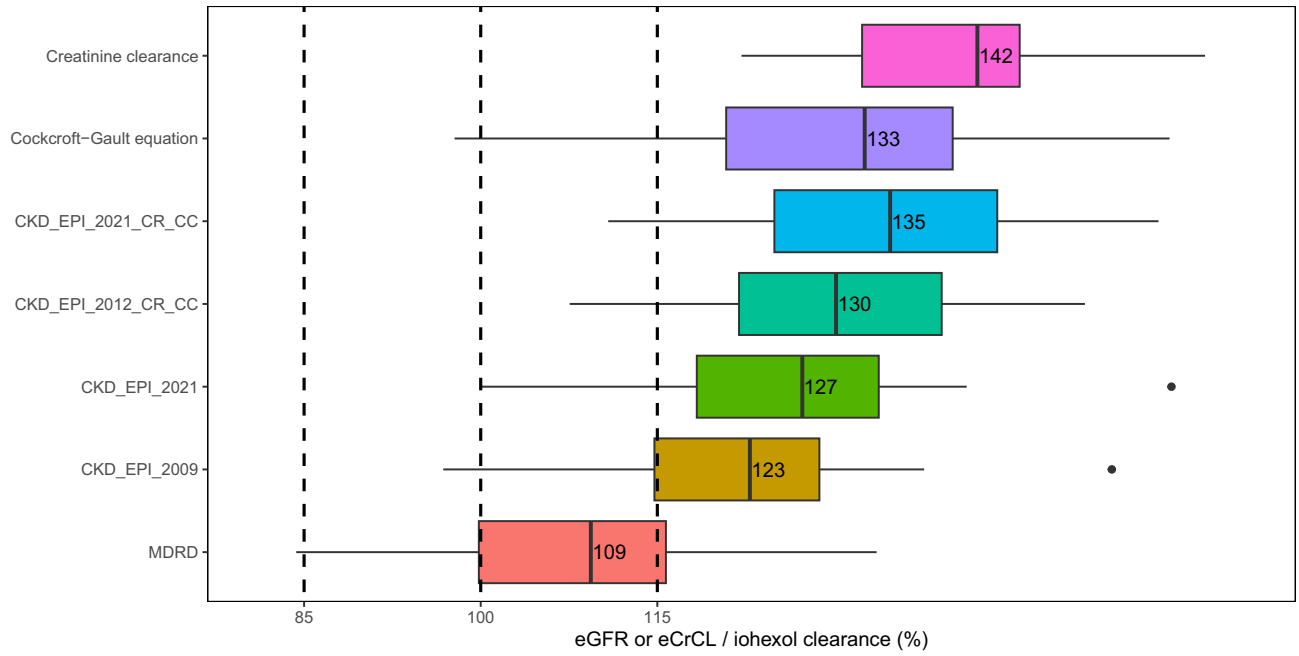

Figure 1 Comparison between post hoc estimates of iohexol clearance ("true GFR") and creatinine clearance in the present model, estimated GFR (eGFR) or estimated creatinine clearance (eCrCL) calculated using commonly used equations ($n = 14$). All individual values were normalized by dividing eGFR/eCrCL by iohexol clearance. From top to bottom, the items are creatinine clearance using the popPK approach, eCrCL by Cockcroft-Gault equation, eGFR by CKD-EPI 2021 (based on creatinine and cystatin C), CKD-EPI 2012 (based on creatinine and cystatin C), CKD-EPI 2021 (based on creatinine only), CKD-EPI 2009 (based on creatinine only), and MDRD equation.

quantified by the joint creatinine/iohexol model, accounted for 31% of renal CrCL and shows promise as a tool for assessing OCT2/MATE activity *in vivo* at least in healthy individuals.

A primary objective of this study was to precisely estimate creatinine V_d in order to refine the creatinine PK model. Based on previous studies,[11,12] boiled beef was selected as an external source of oral creatinine to induce a perturbation in creatinine PK away from the steady-state baseline (as with the usual single-point method), and with frequent sampling, to allow modeling the time course of creatinine PK. Fitting the creatinine time-course profile in plasma, along with the amounts excreted in urine, informed the estimation of the absorption rate, bioavailability, and V_d, based on the assumption that all systemically available creatinine is excreted renally. An overall recovery of 104% for iohexol over 24-hours post-dose (data will be reported separately) indicated the completeness of the urine collection.[18] However, determining the true creatinine dose was challenging due to the incomplete absorption of creatinine from beef and inconsistent differences in creatinine excretion between meat and non-meat periods of this study over 16 and 24 hours. This discrepancy may be due to the significant interference from the large amount of endogenous creatinine. Even a small fraction of daily creatinine production (~2000 mg) could introduce substantial errors in estimating the external creatinine dose, especially when the external amount is as low as ~300 mg. Given lower residual errors in plasma data compared to urine data, simultaneous estimation of F1 and V_d provided the best model fit.

In the covariate assessment, TBW and estimates of the Cockcroft-Gault equation were included as covariates based on prior knowledge.[20] Additionally, sex was identified as a statistically significant covariate on nCTS, potentially due to a higher abundance and expression of transporters in males compared to females.[29] However, the effect of sex on nCTS remains uncertain, as the small sample size in this study limits the robustness of this finding. Age is used as a key factor in eGFR equations but was not identified as significant in this study, likely because of the small sample size and the limited age range.[30] The food effect on GFR and nCTS was not significant, possibly due to the limited amounts of non-meat protein in the meals provided. A lower serum albumin level corresponding to a higher level of nCTS was observed in previous studies.[31,32] However, it was not found as a significant covariate on nCTS maybe due to only healthy participants included in the current study.

The estimated nCTS in this study accounts for approximately 31% of the total CrCL, which falls within the reported range of 10–40%.[13] The ratios of 32.0% and 4.8% have been reported in healthy individuals in rehydrated and dehydrated states, respectively.[33] To stimulate urine production, 240 mL of water was administered during every urine collection interval in this study, which may have kept participants in a rehydrated state and thus led to a relatively high contribution of nCTS to CrCL.

Among evaluated eGFR equations, including cystatin C did not improve predictive performance compared to creatinine-only equations, thus failing to provide additional evidence to support the broader use of cystatin C. A possible explanation for this finding is that the study included only healthy Caucasian participants because Cystatin C has shown a greater sensitivity in patients with impaired kidney function and is less influenced by race.[34,35]

The assumption that creatinine V_d equals to total body water (60% of TBW) has been widely used in creatinine models.[10,36–38] In contrast, the previous analysis estimated it at 73.8%,[12] while the current study estimated it at 41.3%. These results suggested a close

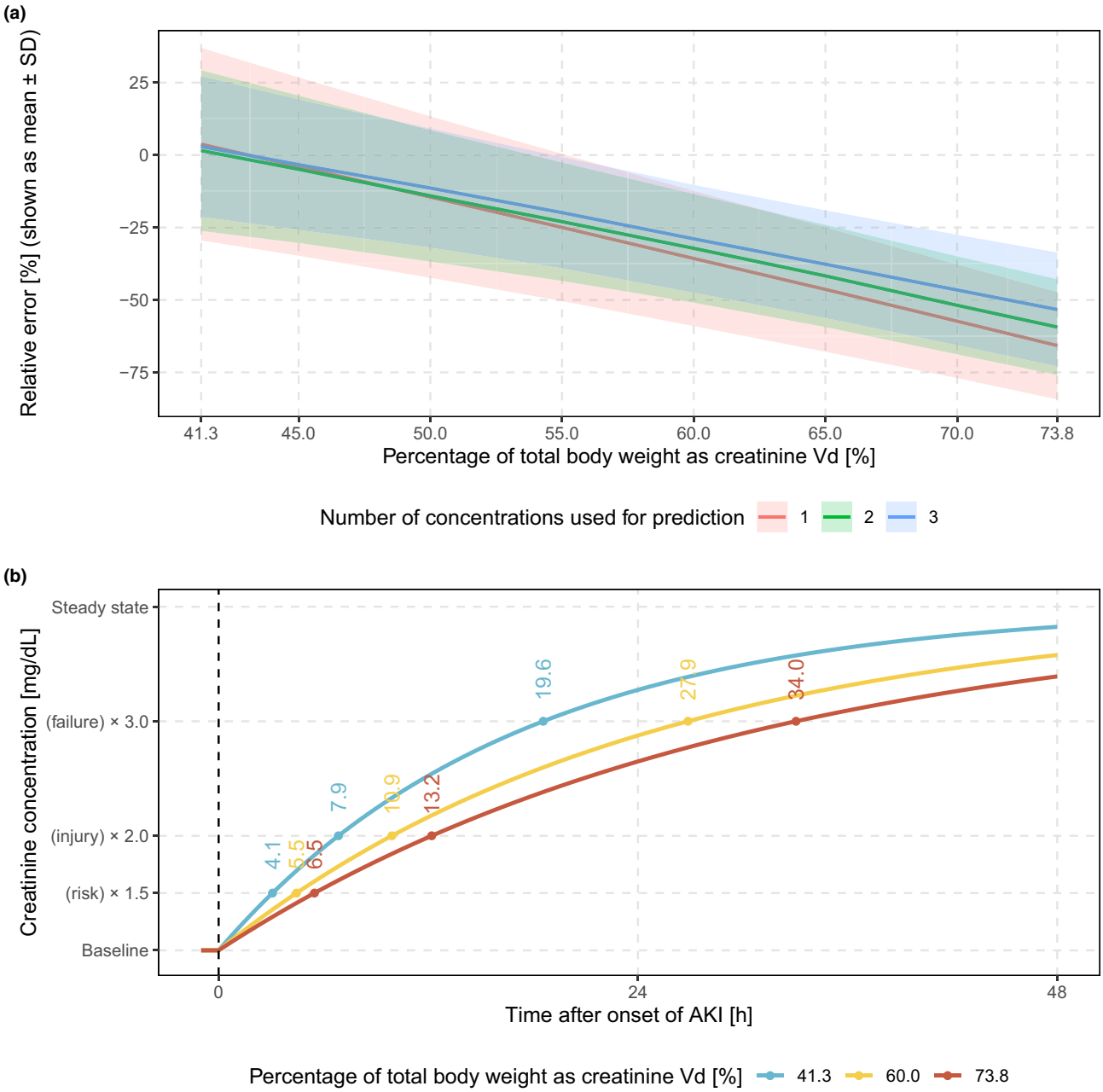

Figure 2 Simulations for AKI diagnosis using different values for creatinine volume of distribution (V_d). (**a**) prediction accuracy of changed GFR after onset of acute kidney injury (AKI) comparing models with different number of concentrations. (**b**) concentration-time curves following a 75% reduction in both GFR and nCTS and the timing to diagnose AKI risk, injury, and failure based on RIFLE criteria.

relationship between assumed and true values, but also highlighted potential discrepancies. Simulations (**Figure 3**) using a final model with different V_d values (41.3% as a reference value) revealed significant uncertainty in predicting GFR following AKI, with substantial discrepancies observed when using "biased" V_d values, such as 60% or 73.8%. This highlights the critical importance of accurately selecting the V_d, underscoring the need for caution when assuming a value for creatinine V_d.

Previous studies have shown that 1 to 4 plasma samples within 5 hour post-dose are sufficient to accurately estimate IoCL following a 3,235 mg iohexol dose.[24,39,40] However, incomplete urine collection may result in an underestimation of CrCL, thus leading to an underestimation of nCTS.[41] Applying a correction factor based on the ratio of predicted to observed iohexol excretion can resolve this discrepancy. This study demonstrated the feasibility of a joint model for iohexol and creatinine, using a single plasma sample at 5 hours and a urine sample from the 0–5-hour interval after a 259 mg iohexol dose, to accurately predict both GFR and nCTS. Therefore, this approach also shows the potential for assessing renal OCT2/MATE activity based on estimated nCTS.

Apart from the limitations discussed above, renal elimination was assumed to be the sole pathway for creatinine, though minor pathways such as gut metabolism may exist.[42] The small sample size and the narrow range of demographics in this study in healthy

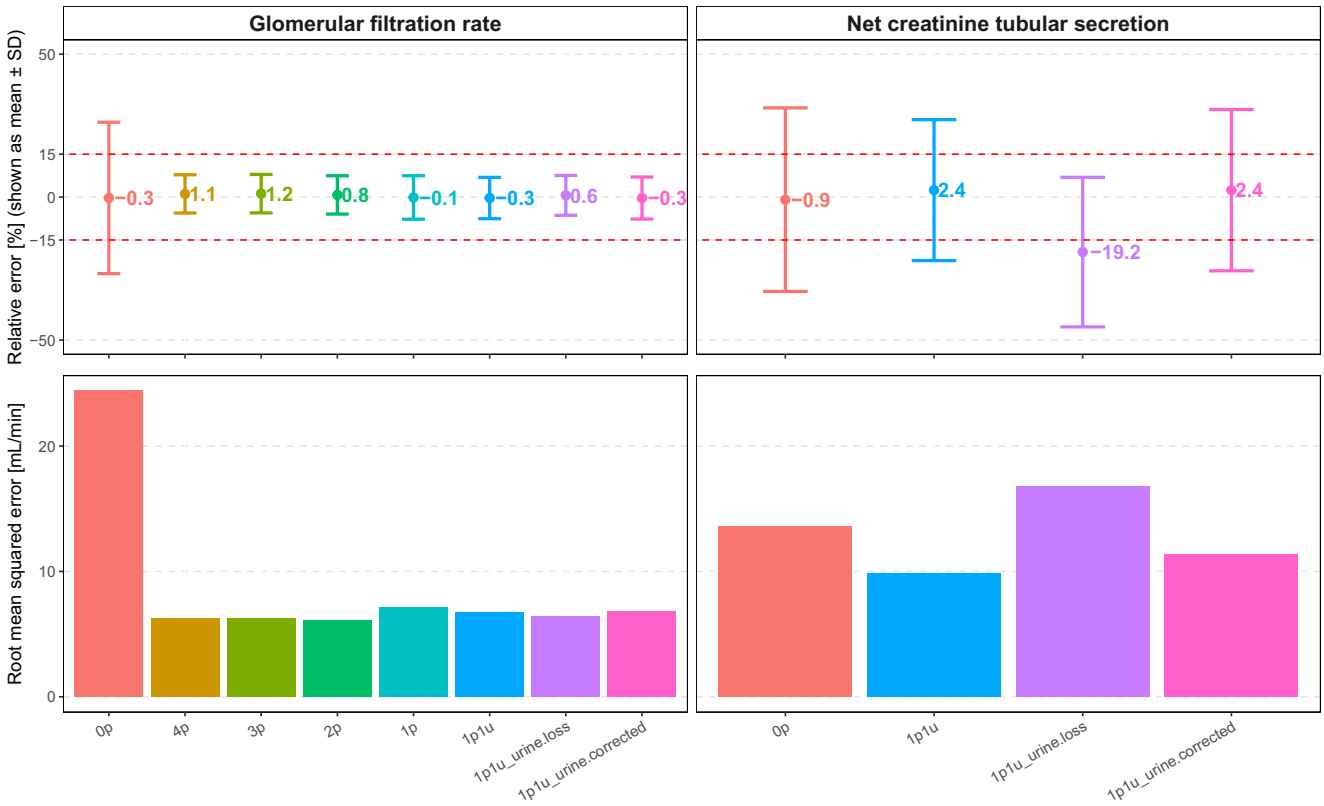

p: plasma sample (10 min, 30 min, 2 h, and 5 h postdose; later samples were kept if sample number reduced);
u: urine sample (0–5 h interval postdose);
urine.loss: random loss of 10–50% of urine;
urine.corrected: incomplete creatinine excreted amount was corrected using the individual ratio of predicted to incomplete iohexol excreted amount.

Figure 3 Comparison of prediction accuracy for GFR and nCTS between models using different numbers of plasma concentrations with or without urine data.

volunteers limited the ability to accurately assess covariate relationships and to extrapolate the results to other populations, such as the elderly or those with impaired kidney function. Early in each study period, highly variable plasma concentrations and unexplained outliers in urinary excretion were observed, likely due to the study design requiring early morning arrival at the ward, potentially sustaining elevated physiological activity. A proportional error model best fit creatinine plasma data measured via LC–MS/MS but may not apply to clinical samples measured using the Jaffe method, leading to potential bias in simulated data versus real-world data.

In conclusion, the joint model for iohexol and creatinine, incorporating CrCL as the sum of GFR (equivalent to IoCL) and nCTS, while accounting for TBW effects and circadian variation, accurately described plasma and urine concentrations. The estimated creatinine V_d was 28.9 L or 41.3% of TBW. Simulations revealed significant differences in predicting GFR changes after AKI based on varying creatinine V_d, emphasizing the importance of careful selection. Following a low-dose iohexol administration, a single plasma and urine sample was proven sufficient to predict GFR and nCTS even for incomplete urine collection, demonstrating potential use in assessing renal OCT2/MATE activity.

SUPPORTING INFORMATION

Supplementary information accompanies this paper on the *Clinical Pharmacology & Therapeutics* website (www.cpt-journal.com).

ACKNOWLEDGMENTS

We appreciate our colleagues from the Department of Pharmacology, Center for Pharmacology, Faculty of Medicine, and University Hospital Cologne, University of Cologne, for their support during the study. We extend our gratitude to Yali Wu, Chunli Chen, Muhammad Bilal, Jil Hennig, Svenja Flögel, Chiara Mandl, Sylvia Goitzsch, Samira Boussettaoui, Simone Kalis, and Kathi Krüsemann. We also thank the volunteers who participated in this study. Open Access funding enabled and organized by Projekt DEAL.

FUNDING

No funding was received for this project. Zhendong Chen and Qian Dong received scholarships from the China Scholarship Council to support their PhD studies.

CONFLICTS OF INTEREST

The authors declared no competing interests for this work.

AUTHOR CONTRIBUTIONS

Z.C., U.F., and M.T. wrote the manuscript; U.F., Z.C., Q.D., and M.T. designed the research; Z.C., Q.D., C.D., J.B., and U.F. performed the research; Z.C., Q.D., and M.T. analyzed the data.

1. Stevens, L.A. & Levey, A.S. Measured GFR as a confirmatory test for estimated GFR. *J. Am. Soc. Nephrol.* **20**, 2305–2313 (2009).
2. Bragadottir, G., Redfors, B. & Ricksten, S.E. Assessing glomerular filtration rate (GFR) in critically ill patients with acute kidney injury–true GFR versus urinary creatinine clearance and estimating equations. *Crit. Care* **17**, R108 (2013).
3. Cockcroft, D.W. & Gault, M.H. Prediction of creatinine clearance from serum creatinine. *Nephron* **16**, 31–41 (1976).
4. Scappaticci, G.B. & Regal, R.E. Cockcroft-Gault revisited: new de-liver-ance on recommendations for use in cirrhosis. *World J. Hepatol.* **9**, 131–138 (2017).
5. Prowle, J.R., Kolic, I., Purdell-Lewis, J. *et al*. Serum creatinine changes associated with critical illness and detection of persistent renal dysfunction after AKI. *Clin. J. Am. Soc. Nephrol.* **9**, 1015–1023 (2014).
6. Koopman, M.G., Koomen, G.C., Krediet, R.T. *et al*. Circadian rhythm of glomerular filtration rate in normal individuals. *Clin. Sci. (Lond.)* **77**, 105–111 (1989).
7. Preiss, D.J., Godber, I.M., Lamb, E.J. *et al*. The influence of a cooked-meat meal on estimated glomerular filtration rate. *Ann. Clin. Biochem.* **44**, 35–42 (2007).
8. Larsson, A., Akerstedt, T., Hansson, L.O. & Axelsson, J. Circadian variability of cystatin C, creatinine, and glomerular filtration rate (GFR) in healthy men during normal sleep and after an acute shift of sleep. *Chronobiol. Int.* **25**, 1047–1061 (2008).
9. Morrison, B., Shenkin, A., McLelland, A. *et al*. Intra-individual variation in commonly analyzed serum constituents. *Clin. Chem.* **25**, 1799–1805 (1979).
10. Ullah, S., Zoller, M., Jaehde, U. *et al*. A model-based approach to assess unstable creatinine clearance in critically ill patients. *Clin. Pharmacol. Ther.* **110**, 1240–1249 (2021).
11. Mayersohn, M., Conrad, K.A. & Achari, R. The influence of a cooked meat meal on creatinine plasma concentration and creatinine clearance. *Br. J. Clin. Pharmacol.* **15**, 227–230 (1983).
12. Chen, Z., Chen, C., Taubert, M. *et al*. A population pharmacokinetic model for creatinine with and without ingestion of a cooked meat meal. *Eur. J. Clin. Pharmacol.* **78**, 1945–1947 (2022).
13. Levey, A.S., Perrone, R.D. & Madias, N.E. Serum creatinine and renal function. *Annu. Rev. Med.* **39**, 465–490 (1988).
14. Mathialagan, S., Feng, B., Rodrigues, A.D. & Varma, M.V.S. Drug-drug interactions involving renal OCT2/MATE transporters: clinical risk assessment may require endogenous biomarker-informed approach. *Clin. Pharmacol. Ther.* **110**, 855–859 (2021).
15. Gessner, A., Müller, F., Wenisch, P. *et al*. A metabolomic analysis of sensitivity and specificity of 23 previously proposed biomarkers for renal transporter-mediated drug–drug interactions. *Clin. Pharmacol. Ther.* **114**, 1058–1072 (2023).
16. Trueck, C., Hsin, C.H., Scherf-Clavel, O. *et al*. A clinical drug–drug interaction study assessing a novel drug transporter phenotyping cocktail with adefovir, sitagliptin, metformin, pitavastatin, and digoxin. *Clin. Pharmacol. Ther.* **106**, 1398–1407 (2019).
17. World Medical Association. *The Declaration of Helsinki, as Established by the 18th WMA General Assembly, Helsinki, Finland, June 1964 and Amended by the 64th WMA General Assembly* (World Medical Association, Fortaleza (Brazil), 2013). <https://www.wma.net/policies-post/wma-declaration-of-helsinki-ethical-principles-for-medical-research-involving-human-subjects/>.
18. Dong, Q., Chen, Z., Boland, J. *et al*. Validating low-dose iohexol as a marker for glomerular filtration rate by in vitro and in vivo studies. *Clin. Transl. Sci.* **18**, e70141 (2025).
19. Taubert, M., Ebert, N., Martus, P. *et al*. Using a three-compartment model improves the estimation of iohexol clearance to assess glomerular filtration rate. *Sci. Rep.* **8**, 17723 (2018).
20. González-Sales, M., Holford, N., Bonnefois, G. & Desrochers, J. Wide size dispersion and use of body composition and maturation improves the reliability of allometric exponent estimates. *J. Pharmacokinet. Pharmacodyn.* **49**, 151–165 (2022).
21. Boer, P. Estimated lean body mass as an index for normalization of body fluid volumes in humans. *Am. J. Phys.* **247**(4 Pt 2), F632–F636 (1984).
22. Watson, P.E., Watson, I.D. & Batt, R.D. Total body water volumes for adult males and females estimated from simple anthropometric measurements. *Am. J. Clin. Nutr.* **33**, 27–39 (1980).
23. Bellomo, R., Ronco, C., Kellum, J.A. *et al*. Acute renal failure – definition, outcome measures, animal models, fluid therapy and information technology needs: the second international consensus conference of the acute dialysis quality initiative (ADQI) group. *Crit. Care* **8**, R204–R212 (2004).
24. Åsberg, A., Bjerre, A., Almaas, R. *et al*. Measured GFR by utilizing population pharmacokinetic methods to determine iohexol clearance. *Kidney Int. Rep.* **5**, 189–198 (2019).
25. Inker, L.A., Eneanya, N.D., Coresh, J. *et al*. New creatinine- and cystatin C-based equations to estimate GFR without race. *N. Engl. J. Med.* **385**, 1737–1749 (2021).
26. Inker, L.A., Schmid, C.H., Tighiouart, H. *et al*. Estimating glomerular filtration rate from serum creatinine and cystatin C. *N. Engl. J. Med.* **367**, 20–29 (2012).
27. Levey, A.S., Stevens, L.A., Schmid, C.H. *et al*. A new equation to estimate glomerular filtration rate. *Ann. Intern. Med.* **150**, 604–612 (2009).
28. Levey, A.S., Coresh, J., Greene, T. *et al*. Using standardized serum creatinine values in the modification of diet in renal disease study equation for estimating glomerular filtration rate. *Ann. Intern. Med.* **145**, 247–254 (2006).
29. McDonough, A.A., Harris, A.N., Xiong, L.I. & Layton, A.T. Sex differences in renal transporters: assessment and functional consequences. *Nat. Rev. Nephrol.* **20**, 21–36 (2024).
30. Michels, W.M., Grootendorst, D.C., Verduijn, M. *et al*. Performance of the Cockcroft-Gault, MDRD, and new CKD-EPI formulas in relation to GFR, age, and body size. *Clin. J. Am. Soc. Nephrol.* **5**, 1003–1009 (2010).
31. Branten, A.J., Vervoort, G. & Wetzels, J.F. Serum creatinine is a poor marker of GFR in nephrotic syndrome. *Nephrol. Dial. Transplant.* **20**, 707–711 (2005).
32. Horio, M., Imai, E., Yasuda, Y. *et al*. Lower serum albumin level is associated with higher fractional excretion of creatinine. *Clin. Exp. Nephrol.* **18**, 469–474 (2014).
33. Sjöström, P.A., Odlind, B.G. & Wolgast, M. Extensive tubular secretion and reabsorption of creatinine in humans. *Scand. J. Urol. Nephrol.* **22**, 129–131 (1988).
34. Chen, D.C., Potok, O.A., Rifkin, D. & Estrella, M.M. Advantages, limitations, and clinical considerations in using cystatin C to estimate GFR. *Kidney360* **3**, 1807–1814 (2022).
35. Spencer, S., Desborough, R. & Bhandari, S. Should cystatin C eGFR become routine clinical practice? *Biomol. Ther.* **13**, 1075 (2023).
36. Bjornsson, T.D. Use of serum creatinine concentrations to determine renal function. *Clin. Pharmacokinet.* **4**, 200–222 (1979).
37. Pickering, J.W., Ralib, A.M. & Endre, Z.H. Combining creatinine and volume kinetics identifies missed cases of acute kidney injury following cardiac arrest. *Crit. Care* **17**, R7 (2013).
38. Takita, H., Scotcher, D., Chinnadurai, R. et al. Physiologically-based pharmacokinetic modelling of creatinine-drug interactions in the chronic kidney disease population. *CPT Pharmacometrics Syst. Pharmacol.* **9**, 695–706 (2020).
39. Taubert, M., Schaeffner, E., Martus, P. *et al*. Advancement of pharmacokinetic models of iohexol in patients aged 70 years or older with impaired kidney function. *Sci. Rep.* **11**, 22656 (2021).
40. Delanaye, P., Flamant, M., Dubourg, L. *et al*. Single- versus multiple-sample method to measure glomerular filtration rate. *Nephrol. Dial. Transplant.* **33**, 1778–1785 (2018).
41. Mann, S.J. & Gerber, L.M. Addressing the problem of inaccuracy of measured 24-hour urine collections due to incomplete collection. *J. Clin. Hypertens. (Greenwich)* **21**, 1626–1634 (2019).
42. Kallner, A. Creatinine clearance, measurement, metabolism. In *Encyclopedia of Intensive Care Medicine* (eds. Vincent, J.L. & Hall, J.B.) (Springer, Berlin, Heidelberg, 2012).

AMERICAN SOCIETY FOR MICROBIOLOGY | Antimicrobial Agents and Chemotherapy®

PHARMACOLOGY

Plasma and Cerebrospinal Fluid Population Pharmacokinetics of Vancomycin in Patients with External Ventricular Drain

Zhendong Chen,[a] Max Taubert,[a] Chunli Chen,[a,b] Charalambos Dokos,[a] Uwe Fuhr,[a] Thomas Weig,[c] Michael Zoller,[c] Suzette Heck,[d] Konstantinos Dimitriadis,[d,e] Nicole Terpolilli,[e,f] Christina Kinast,[c] Christina Scharf,[c] Constantin Lier,[g] Christoph Dorn,[g] Uwe Liebchen[c]

[a]Department I of Pharmacology, Center for Pharmacology, Faculty of Medicine and University Hospital Cologne, University of Cologne, Cologne, Germany
[b]Heilongjiang Key Laboratory for Animal Disease Control and Pharmaceutical Development, College of Veterinary Medicine, Northeast Agricultural University, Harbin, People's Republic of China
[c]Department of Anesthesiology, University Hospital, Ludwig Maximilians University of Munich, Munich, Germany
[d]Department of Neurology, University Hospital, Ludwig Maximilian University, Munich, Germany
[e]Institute for Stroke and Dementia Research (ISD), University Hospital, Ludwig Maximilians University, Munich, Germany
[f]Department of Neurosurgery, Munich University Hospital, Munich, Germany
[g]Institute of Pharmacy, Faculty of Chemistry and Pharmacy, University of Regensburg, Regensburg, Germany

ABSTRACT Vancomycin is a commonly used antibacterial agent in patients with primary central nervous system (CNS) infection. This study aims to examine predictors of vancomycin penetration into cerebrospinal fluid (CSF) in patients with external ventricular drainage and the feasibility of CSF sampling from the distal drainage port for therapeutic drug monitoring. Fourteen adult patients (9 with primary CNS infection) were treated with vancomycin intravenously. The vancomycin concentrations in blood and CSF (from proximal [CSF_P] and distal [CSF_D] drainage ports) were evaluated by population pharmacokinetics. Model-based simulations were conducted to compare various infusion modes. A three-compartment model with first-order elimination best described the vancomycin data. Estimated parameters included clearance (CL, 4.53 L/h), central compartment volume (V_c, 24.0 L), apparent CSF compartment volume (V_{CSF}, 0.445 L), and clearance between central and CSF compartments (Q_{CSF}, 0.00322 L/h and 0.00135 L/h for patients with and without primary CNS infection, respectively). Creatinine clearance was a significant covariate on vancomycin CL. CSF protein was the primary covariate to explain the variability of Q_{CSF}. There was no detectable difference between the data for sampling from the proximal and the distal port. Intermittent infusion and continuous infusion with a loading dose reached the CSF target concentration faster than continuous infusion only. All infusion schedules reached similar CSF trough concentrations. Beyond adjusting doses according to renal function, starting treatment with a loading dose in patients with primary CSF infection is recommended. Occasionally, very high and possibly toxic doses would be required to achieve adequate CSF concentrations, which calls for more investigation of direct intraventricular administration of vancomycin. (This study has been registered at ClinicalTrials.gov under registration no. NCT04426383).

KEYWORDS vancomycin, population pharmacokinetics model, distal port, CSF protein, central nervous system infection, ventriculitis

External ventricular drainage (EVD) is a common procedure in neurocritical care units to monitor and treat intracranial pressure by draining cerebrospinal fluid (CSF) (1). However, an EVD-associated infection is a serious nosocomial complication and is associated with significant morbidity and mortality in neurocritical patients (1). Insufficient penetration of antimicrobials into the CSF after intravenous administration could contribute to therapeutic failure (2). This often results in the selection of high doses, which in turn

Address correspondence to Zhendong Chen, zhendong.chen@uk-koeln.de.

The authors declare no conflict of interest.

Received 22 February 2023
Returned for modification 21 March 2023
Accepted 15 April 2023

increases the risk for systemic adverse effects. It is therefore particularly important in patients suffering from EVD-related infections to individualize the dose of antibiotics to achieve a timely effective concentration in the CSF.

Due to the occurrence of Gram-positive penicillin-resistant pathogens, vancomycin is a standard therapy for central nervous system (CNS) infections, specifically, nosocomial infections (3). Nowadays, the plasma pharmacokinetics (PK) of vancomycin have been well investigated by many studies (4–9), and various population pharmacokinetics (PopPK) models based on plasma concentrations have also been reported for different populations, including adults, critically ill patients, pediatric patients, neonate patients, etc. (10). In most of these models, total body weight (TBW) and/or creatinine clearance (CrCL) were confirmed as significant covariates on vancomycin clearance, since vancomycin is primarily eliminated by the kidney in unchanged form (10). Therefore, predictable vancomycin plasma concentrations can be obtained using these models (11).

However, vancomycin cannot easily penetrate the blood-brain barrier (BBB) into the CSF due to its pronounced hydrophilicity and high molecular weight (12). Vancomycin CSF concentrations are highly variable and unpredictable in most cases, because the extent of vancomycin penetration depends greatly on the integrity of the BBB (13–15). BBB damage caused by inflamed meninges has also been proven to enhance the penetration of vancomycin into the CSF. So far, only a few studies have investigated the pharmacokinetics of vancomycin, reporting several validated PopPK models in which CSF albumin or lactate concentrations were related to the distribution of vancomycin into the CSF, thus helping to predict CSF concentrations after intravenous administration (16–18). The available data in individual studies are sparse, the validation of developed predictors is limited, and there is still insufficient knowledge about vancomycin CSF penetration and the respective covariates in neurological/neurosurgical patients. Therefore, the main aim of this study was to investigate predictors for vancomycin penetration into CSF. To this end, a new PopPK model was developed and validated based on vancomycin plasma and CSF data from patients who had an EVD. The feasibility of collecting CSF samples at the distal port of the EVD system for therapeutic drug monitoring (TDM) was assessed using this new PopPK model. Finally, the benefits of different infusion modes and dosages were examined through model-based simulations.

RESULTS

Patient characteristics. A total of 190 plasma samples and 232 CSF samples, including 22 samples taken from the proximal port (CSF_P) and 210 samples taken from the distal port (CSF_D), were collected from 14 patients with EVDs in this study (for an illustration of the drainage system, see reference 19). Among the 14 patients, 9 with CNS infection and 5 without primary CNS infection, 11 were men and 3 were women, with a mean age of 52 years (range, 22 to 77 years). The main patient characteristics are shown in Table 1. Detailed information on disease for each patient, as well as the vancomycin infusion mode and additional covariate values, including the values for unbound fraction (f_u), albumin, bilirubin, C-reactive protein, leukocytes, and interleukin 6 and ferritin (CSF), erythrocytes (CSF), cell count (CSF), and interleukin 6 (CSF), are shown in Tables S1 and S2 in the supplemental material.

Population pharmacokinetics model. A two-compartment model with first-order elimination and proportional residual error best described the vancomycin plasma data. The base plasma model was parameterized by vancomycin clearance (CL), central compartment volume (V_c), intercompartment clearance (Q_p), and peripheral compartment volume (V_p). Before the inclusion of any covariates, the interindividual variables (IIVs) of CL, Q_p, and V_p were estimated to be 38.5%, 93.7%, and 53.8%, respectively. Significant effects of CrCL on CL (change in objective function value [ΔOFV] = −4.073) and of age on Q_p (ΔOFV = −10.585) were found, resulting in reductions of IIVs to 30.8% and 35.1% for CL and Q_p, respectively. Other clinical characteristics, including sex, weight, height, body surface area (BSA), estimated glomerular filtration rate (eGFR), and f_u, were eliminated due to showing no significant contribution to ΔOFV.

On the basis of the final plasma model, two different CSF models, including the transit compartment model and the bulk flow model, were compared to fit the vancomycin CSF

TABLE 1 Demographics and covariates of subjects

Characteristic[a]	No. or mean value (SD) for patients:	
	With primary CNS infection	Without primary CNS infection
Demographics		
Male	7	4
Female	2	1
Age (yr)	59.7 (11.8)	37.0 (10.2)
Body wt (kg)	84.2 (25.0)	88.6 (16.6)
Ht (cm)	174 (6)	179 (9)
Covariates		
In plasma		
Creatinine (mg/dL)	0.671 (0.138)	0.693 (0.287)
CrCL (mL/min)	142 (57)	194 (41)
In CSF		
Protein (mg/dL)	108 (53)	27.4 (29.0)
S100 protein (μg/L)	3.88 (2.13)	30.0 (0.0)
Glucose (mg/dL)	51.4 (21.7)	80.4 (13.5)
NSE (μg/L)	15.6 (4.9)	326 (199)
Lactate (mmol/L)	4.63 (0.98)	1.78 (0.43)

[a]CrCL, creatinine clearance estimated by the Cockcroft-Gault equation; NSE, neuron-specific enolase concentration. For further parameters, see Table S2.

data separately. Little difference was found in either goodness-of-fit (GOF) plots or change in Akaike information criterion (ΔAIC) (1.711) between two different CSF models, which were subsequently analyzed for CSF-related covariates in parallel. However, the bulk flow model showed better correlations between Q_{CSF} and all covariates than the transit compartment model, and it had a lower AIC when including a particular Q_{CSF}-related covariate. Therefore, the bulk flow model was ultimately chosen for the base CSF model.

Five CSF-related covariates, including CSF protein, S100 protein, glucose, neuron-specific enolase (NSE), and lactate concentrations in CSF, were found to have significant effects on Q_{CSF} separately, and the ΔOFVs were −29.755, −9.868, −9.394, −7.582, and −6.587, respectively. The regression plots of the Q_{CSF} versus the concentrations of each CSF-related covariate are shown in Fig. S1. Due to the multicollinearity and reasonable physiological considerations, only the CSF protein concentration was included in the final CSF model, which led to a decrease from 165.6% to 36.6% in the IIV of Q_{CSF}. Primary CNS infection was found to be a significant covariate both for Q_{CSF} and the protein covariate effect, resulting in decreases in the OFVs of 5.152 and 6.959, respectively. Therefore, two separate equations were generated to estimate the vancomycin penetration in patients with and without primary CNS infection. The relationships between random effects (η) and the significant covariates in the base model and the final model are shown in Fig. S2.

All parameter estimates remained essentially unchanged after the exclusion of CSF_P data (not shown). The proportional residual errors for CSF_P and CSF_D samples were estimated to be 25.2% and 27.8%, respectively, and the separation of the error models for each of them did not improve the CSF model fitting (ΔOFV = −0.256). This indicated little difference in the accuracy of vancomycin concentrations between the two types of CSF samples. Therefore, only one proportional residual error model was used for both the CSF_P and CSF_D samples in the final CSF model. The final model equations for CL, Q_p, and Q_{CSF} are presented below:

$$\mathrm{CL} = \left(\frac{\mathrm{CrCL}}{170}\right)^{0.461} \times \mathrm{TVCL} \times e^{\eta_1}$$

$$Q_p = \left(\frac{\mathrm{age}}{48}\right)^{2.61} \times \mathrm{TVQ}_p \times e^{\eta_2}$$

For patients with primary CNS infection,

TABLE 2 Parameter estimates and bootstrap results from the final model

	Value(s) for:			
	Final model		927 successful bootstrap runs (n = 1,000)	
Parameter[a]	Estimate	RSE (%)[b]	Median	95% CI[c]
CL (L/h)	4.53	7.5	4.52	3.74–5.29
V_c (L)	24.0	8.6	23.3	16.6–27.0
Q_p (L/h)	5.69	12.2	5.70	4.43–8.64
V_p (L)	38.7	16.5	39.7	27.9–59.1
Q_{CSF}_1 (L/h)	0.00322	5.6	0.00331	0.00263–0.00390
Q_{CSF}_2 (L/h)	0.00135	29.9	0.00129	0.000938–0.00383
V_{CSF} (L)	0.445	14.7	0.465	0.244–0.883
Covariates				
CrCL on CL	0.453	27.6	0.452	0.150–0.830
Age on Q_p	2.69	24.4	2.84	1.37–4.74
Protein (CSF) on Q_{CSF}_1	1.09	6.0	1.10	0.808–1.67
Protein (CSF) on Q_{CSF}_2	0.575	21.9	0.575	0.203–1.03
Interindividual variability (%)				
CL	29.5 (0.1)[d]	18.7	27.9	15.9–38.1
V_p	54.3 (20.6)	25.1	54.9	21.4–93.7
Q_{CSF}	19.8 (17.7)	20.8	13.6	4.7–25.1
V_{CSF}	94.2 (10.1)	20.8	105.0	36.1–175.7
Residual variability (proportional error) (%)[e]				
Plasma	15.9 (5.3)[d]	15.5	15.4	10.7–20.4
CSF	27.5 (3.8)	5.6	26.5	17.3–34.7

[a]CL, clearance; V_c, central compartment volume; Q_p, intercompartment clearance between central and peripheral compartments; V_p, peripheral compartment volume; Q_{CSF}_1, intercompartment clearance between plasma and CSF compartment in patients with primary CNS infection; Q_{CSF}_2, intercompartment clearance between plasma and CSF compartment in patients without primary CNS infection; V_{CSF}, CSF compartment volume; CrCL, creatinine clearance.
[b]RSE, relative standard error.
[c]CI, confidence interval.
[d]Shrinkage estimates of interindividual variability (IIV) and residual variability are shown in parentheses.
[e]Proportional residual error is expressed as the coefficient of variation (CV).

$$Q_{CSF} = \left(\frac{\text{CSF protein}}{84}\right)^{1.09} \times \text{TVQ}_{CSF}\_1 \times e^{\eta_3}$$

For patients without primary CNS infection,

$$Q_{CSF} = \left(\frac{\text{CSF protein}}{84}\right)^{0.575} \times \text{TVQ}_{CSF}\_2 \times e^{\eta_3}$$

where TVCL, TVQ_p, TVQ_{CSF}_1, and TVQ_{CSF}_2 are the typical population values for CL, Q_p, Q_{CSF}_1, and Q_{CSF}_2, respectively.

The final model parameter estimates and the 95% confidence intervals for the results of 1,000 bootstrap analyses are displayed in Table 2. As shown, all relative standard errors (RSEs) for PK parameters were less than 30%, which demonstrated acceptable precision. The IIV shrinkages of CL, V_p, Q_{CSF}, and V_{CSF} both in the base model and the final model (Table 2) were all below 30%, which was considered acceptable. The consistency between original parameter estimates and median values estimated from the bootstrap analysis proved the model was stable. The GOF plots for model diagnosis are displayed in Fig. 1. The inclusion of covariates significantly improved the model diagnostic plots. A satisfactory fit was subsequently obtained between observed and predicted values, with no trends of conditional weighted residuals over time for either plasma or CSF samples. Figure 2 shows the prediction-corrected visual predictive checks (pcVPCs) of the final model, which indicated that the model captured the central tendency and distribution of most observed data points both in plasma and CSF. However, the 95% percentile observed in the CSF lies at the inner boundary of the

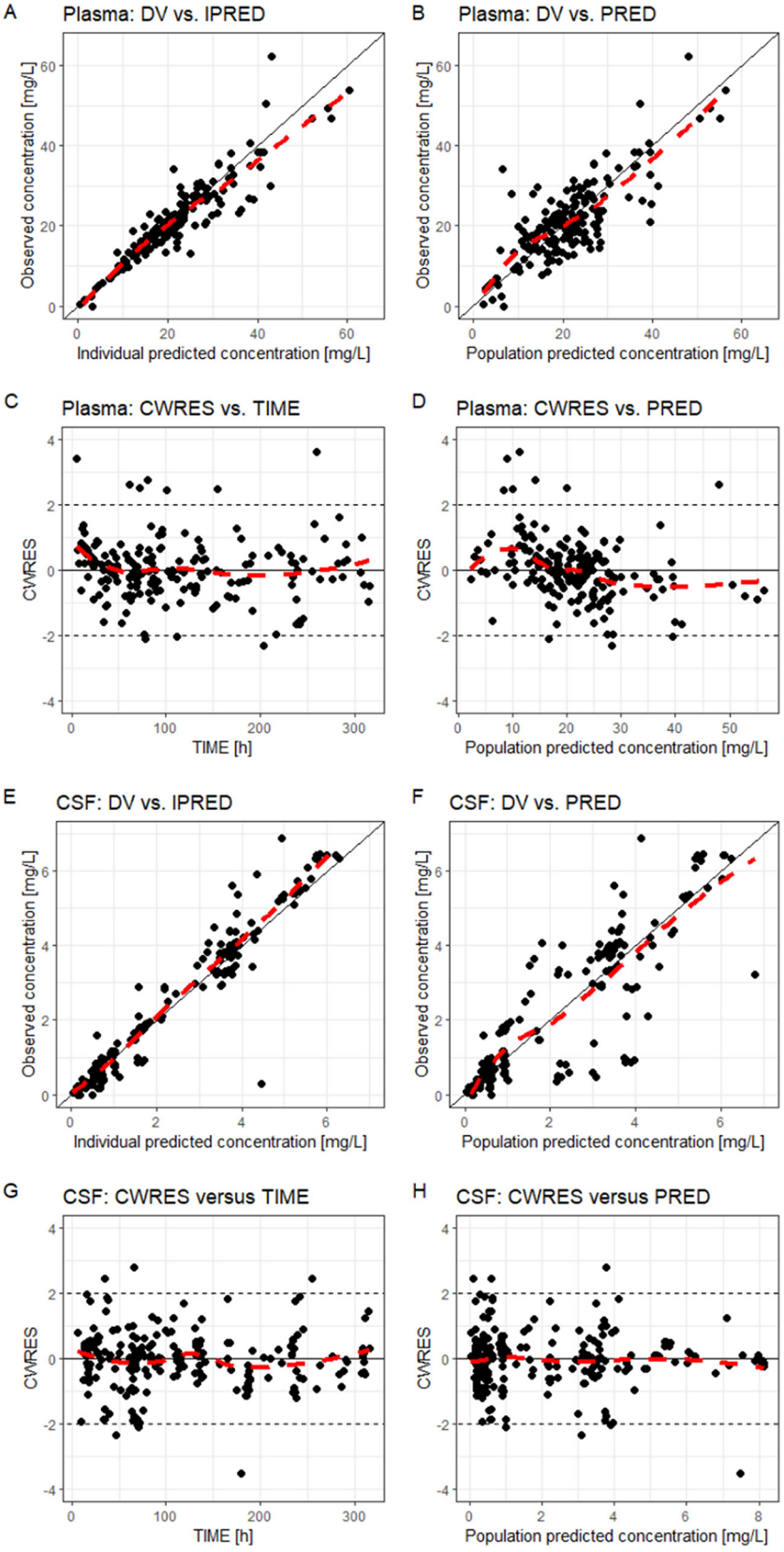

FIG 1 Combined goodness-of-fit plots of the final model for vancomycin plasma (A to D) and CSF (E to H) concentrations. DV, observed concentrations; IPRED, individual predicted concentrations; PRED, population predicted concentrations; CWRES, conditional weighted residuals; TIME, time after the first dose. Red lines show the local polynomial regression fit.

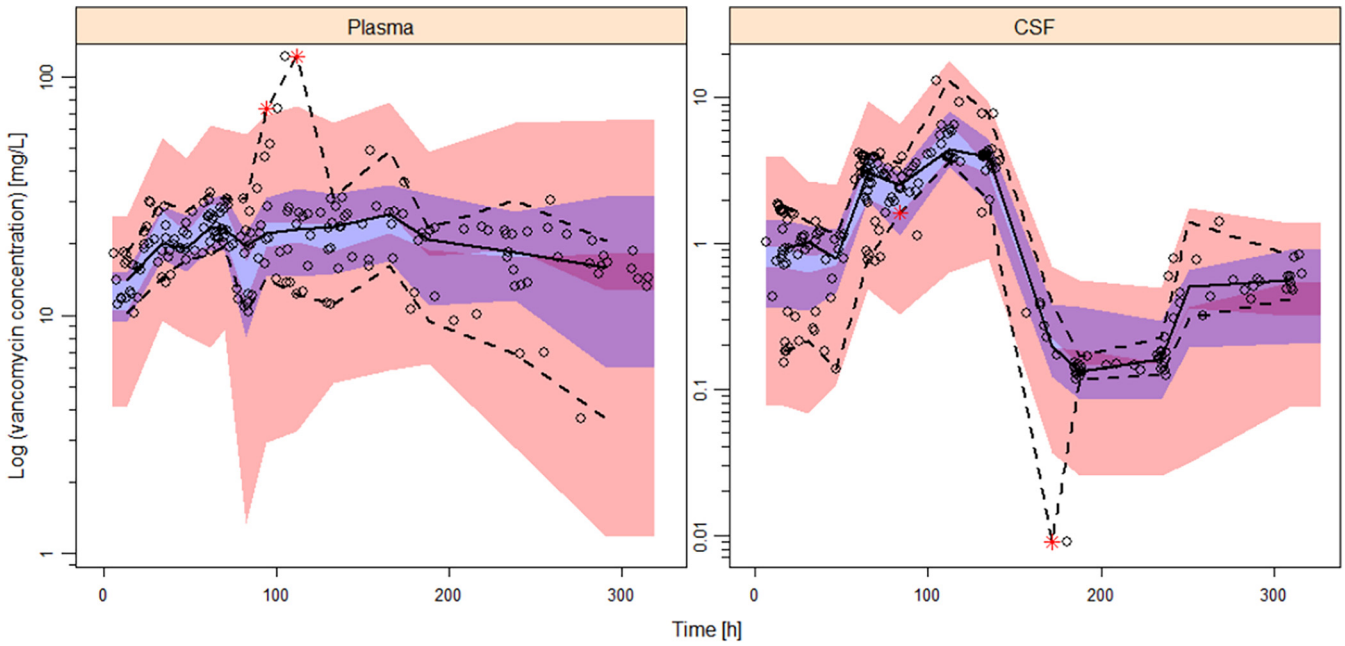

FIG 2 Confidence interval prediction-corrected visual predictive check (n = 1,000) for the final model for plasma and CSF. Dots represent observed concentrations. Black solid lines represent the median values, while dashed lines show the 5th and 95th percentiles of observed concentrations. Shaded areas are the model-predicted 95% confidence intervals for the 5th (red), 50th (blue), and 95th (red) percentiles from 1,000 simulated data sets.

respective confidence intervals, which may be due to the large variability of the V_{CSF}. Individual plots of observed concentrations and concentrations predicted by the final model in plasma and CSF are displayed in Fig. S3 and S4, respectively.

Comparisons of parameter estimates and calculations of probability of target attainment (PTA) for the sensitivity analysis with individual adjustment of CSF_D sampling times are shown in Tables S3 and S4. The parameter estimates remained nearly unchanged except for V_{CSF}, which had a lower estimate when using earlier sampling times for CSF_D samples. The PTA ratios for both plasma and CSF targets between the two models ranged from 0.83 to 1.29, indicating no relevant difference. When assuming a uniform CSF flow rate of 12 or 36 mL/min (20), the respective adjustments in sampling times had essentially no effect on any parameter estimates or on PTA calculations (data not shown). Therefore, the uncertainty of the CSF flow rate and the related time delay for CSF_D samples is irrelevant for the model's application, and assuming no delay between CSF_P and CSF_D samples in this study is justifiable.

Simulations. Changes in the vancomycin plasma area under the concentration-time curve over 24 h (AUC_{24}) and CSF trough concentration (C_{trough}) in patients with different CrCL values and concentrations of CSF protein under different dosing regimens are shown in Fig. S5 and S6, respectively. The simulation results suggested that CrCL showed a moderate effect on CL but CSF protein had a large effect on Q_{CSF}. The multitude of covariates did not allow standard dosing recommendations in this study.

The probabilities of target attainment (PTA) in simulated patients with primary CNS infection after different dosing regimens of vancomycin are listed in Table 3. On the first day of vancomycin treatment, there were only minor differences in plasma AUC_{24} values between intermittent infusion and continuous infusion with a loading dose, but there were relatively lower plasma AUC_{24} values for continuous infusion without a loading dose. A daily dose of 2 g vancomycin was sufficient to achieve the target plasma ratio of AUC_{24} to MIC (AUC_{24}/MIC = 400) at MICs of $\leq$0.5 mg/L in $>$90% of simulated patients, regardless of the renal function, whether administration was by intermittent infusion or continuous infusion with a loading dose. If the MIC was 1 mg/L, a daily dose of 3 g was sufficient for 84.4% of simulated patients with CrCL of $<$150 mL/min, whereas patients with CrCL of $>$150 mL/min might require a daily dose of 4 g, which was the recommended

TABLE 3 Probability of target attainment in simulated patients with primary central nervous system infection after different dosing regimens of vancomycin

	Values [day 1 (steady state)] for indicated type and amt (g) of dose/24 h[b]								
	II (q12h)			CI_L			CI		
PK/PD target[a]	2	3	4	2	3	4	2	3	4
Plasma AUC_{24} (mg · h/L)									
>200	96.0 (98.8)	99.9 (99.9)	100 (100)	94.5 (98.7)	99.9 (100)	100 (100)	84.1 (99.0)	99.7 (100)	100 (100)
>400	12.0 (56.9)	72.4 (91.3)	96.0 (98.8)	11.3 (59.6)	67.1 (92.1)	94.5 (98.7)	0.7 (61.7)	36.1 (92.7)	84.1 (99.0)
>600	0.1 (15.5)	12.0 (56.9)	54.0 (85.6)	0 (17.0)	11.3 (59.6)	48.2 (85.8)	0 (17.7)	0.7 (61.7)	17.3 (87.3)
CSF C_{trough} (mg/L)									
>0.5	87.5 (98.4)	94.0 (99.7)	96.7 (100)	87.1 (99.0)	94.1 (99.9)	96.8 (100)	86.4 (99.3)	93.4 (99.9)	96.6 (100)
>1.0	64.2 (89.2)	80.7 (96.0)	87.5 (98.4)	62.5 (92.0)	78.7 (97.4)	87.1 (99.1)	64.3 (92.4)	78.7 (97.8)	86.4 (99.3)
>2.0	27.6 (63.7)	49.9 (81.4)	64.2 (89.2)	23.5 (70.3)	47.6 (85.7)	62.5 (92.0)	29.7 (70.1)	51.0 (85.8)	64.3 (92.4)

[a]AUC_{24}, daily area under the curve; C_{trough}, the concentration at 24 h or 120 h after the first dose for day 1 or steady state, respectively.
[b]II, intermittent infusion; CI_L, continuous infusion with a loading dose same as the first does of II; CI, continuous infusion without a loading dose.

daily dose for continuous infusion by Jalusic et al. (18) For different known pathogens, the daily dose could be optimized to adapt the respective target AUC_{24}/MIC for all populations.

Simulated time-concentration profiles in plasma and CSF after different dosing regimens over 5 days are displayed in Fig. 3. The three infusion modes with the same daily dose resulted in similar levels of C_{trough} in CSF on day 1 and at steady state, but intermittent infusion and continuous infusion with a loading dose allowed the presumed same target concentrations in CSF to be reached faster than continuous infusion without a loading dose did. In contrast, continuous infusion could keep plasma concentrations relatively low during the therapy. Therefore, continuous infusion, especially at high doses, is recommended to avoid higher vancomycin plasma concentrations, which may help reduce renal toxicity (21). If the target C_{trough} in CSF was 1 mg/L, adjustment of doses according to CSF protein concentrations of ≥150, <150 and ≥100, and <100 mg/dL resulted in daily doses of 2, 3, and 4 g vancomycin, which were then linked to PTAs of 90.4%, 90.8%, and 69.6%, respectively, in simulated patients. As a concern for patients with primary CNS infection, a daily dose of 4 g vancomycin would cause at least 17.3% of patients to face a potential plasma AUC_{24} above 600 mg · h/L, which may lead to a higher risk of acute kidney injury (AKI) (22). Excessive systemic exposure would also prohibit using even higher vancomycin doses in order to achieve higher CSF PTAs in patients with low CSF protein concentrations.

DISCUSSION

In the present study, a PopPK model of vancomycin was successfully developed based on 14 patients with EVDs to examine potential surrogate parameters for the vancomycin penetration rate from plasma to CSF. The time courses of the plasma and CSF concentrations of vancomycin were best described by a linear three-compartment model (contains a CSF compartment). The difference in residual unexplained variability of CSF samples collected at the proximal and the distal port of the EVD system as assessed by residual error models showed that sampling at the distal port is feasible. The probability of PK/pharmacodynamics (PD) target attainment by AUC_{24}/MIC or MIC was subsequently evaluated across different dosing regimens with Monte Carlo simulations.

The plasma PK of vancomycin in different populations have been well investigated by a number of studies. Compared with the published models, the parameter estimate for CL (4.54 L/h) in our model was consistent with reported values, and in accordance with previous studies, CrCL showed a significant effect on CL (16–18, 23, 24). In addition, an additional finding of this study was that age was well correlated with Q_p, suggesting faster distribution of vancomycin into tissues with increasing age. The difference from the published models lies in the V_p, which was estimated at 38.6 L in this study, and no significant covariate on V_p was found. In similar studies about PopPK models in patients who underwent EVD, Li reported a value of 19.8 L for V_p and Jalusic fixed the value at

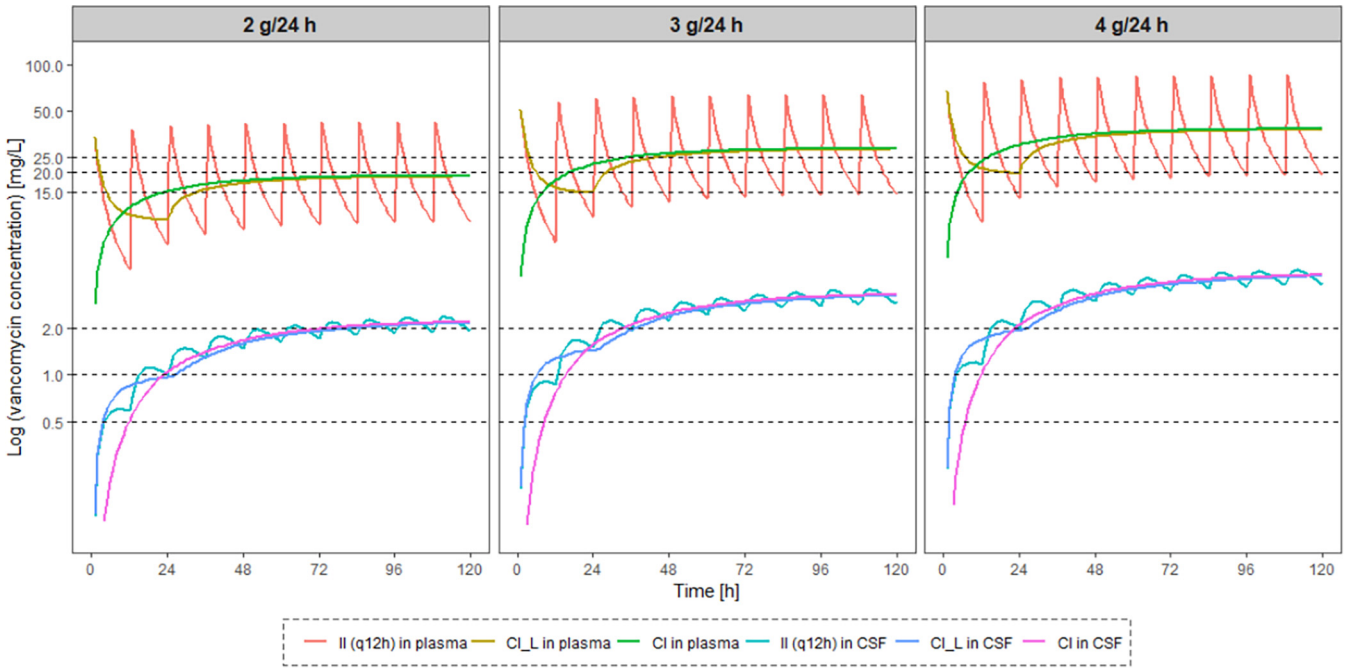

FIG 3 Median concentration-versus-time curves simulated in plasma and CSF after different dosing regimens of vancomycin over 5 days in patients with CNS infection. II, intermittent infusion; q12h, every 12 h; CI_L, continuous infusion with a loading dose same as the first dose of q12h; CI, continuous infusion without a loading dose.

86.2 L in their final model (17, 18). This discrepancy might be due to the different distributions of sampling points in different studies (17). Compared with Jalusic's model, more time points close to the peak were used to build the model in this study, and thus, the estimation of V_p may be closer to the true value.

In addition to the reported CSF lactate concentration, four additional potential surrogate parameters, CSF protein, S100 protein, glucose, and NSE, were identified as showing good correlations with vancomycin penetration from plasma to CSF using the bulk flow model. In accordance with the previous finding, the elevation of CSF protein and lactate concentrations, as well as the reduction of CSF glucose concentration, can suggest CNS infection with BBB damage, which could lead to easier penetration of vancomycin into CSF (18, 25, 26). However, the correlations of increased CSF S100 protein and NSE concentrations to decreased Q_{CSF} are not in agreement with other findings, where higher CSF S100 protein and NSE concentrations were found in patients with CNS infection (27, 28). This discrepancy may be due to the small sample size of this study or limitations of the structural CSF model.

Typically, it is common to collect CSF samples at the proximal port of the EVD system, which is closest to the head. In contrast, collecting CSF samples via a distal overflow system is easier and safer for minimizing the infection risk (19, 29) but will cause a time delay in drug concentrations for TDM. No delay between CSF_P and CSF_D samples was assumed in the present study because the spaces were not fully separated and diffusion might play a role in the propagation of vancomycin concentrations, in addition to flow rate. Moreover, the concentration measured in a CSF_D sample represents an average concentration over a period instead of the concentration at a certain time. Kinast et al. and Wong confirmed no significant differences in the concentrations of substances, including total protein, glucose, and lactate, between the CSF samples from the two sites (19, 29). To our knowledge, no such studies so far have investigated the feasibility of using CSF_D samples for TDM of vancomycin or other drugs. In this study, the residual errors of CSF_P and CSF_D samples were compared using separate proportional residual error models, and no statistically significant difference was found. In addition, the sensitivity analyses assuming various degrees of delay for CSF_D samples showed no meaningful

impact of the CSF sampling site. Therefore, collecting CSF samples at the distal port of the EVD system for TDM or Bayesian dosing approaches of vancomycin could be a valuable choice in the future. It is worth noting that careful documentation of the start and end times of collecting CSF_D samples is critical to calculating the applicable time, thus reducing potential error (30).

A previous PK/PD target tentatively suggested for vancomycin TDM was a plasma C_{trough} of 15 to 20 mg/L for adult patients, but data supporting this target are very limited (31). Recent evidence shows that a more reliable PK/PD target in plasma is an AUC_{24}/MIC of ≥400, taking into account efficacy and safety (22), as the AKI risk was significantly less with AUC-guided monitoring than with C_{trough}-guided monitoring (32). Furthermore, there are also studies evaluating the relationship between the daily vancomycin AUC and AKI, and these suggested that the AUC_{24} in plasma should be maintained between 400 and 600 mg · h/L to maximize efficacy and minimize toxicity (22). However, an AUC_{24}/MIC of ≥400 in CSF is hardly achievable, due to the limited vancomycin penetration from plasma to CSF. Monitoring the AUC in CSF by a rich sampling strategy during TDM is also cumbersome in practice for intermittent infusions, and an AUC_{24} of ≥400 is not achievable in most cases (33). At the same time, no such relevant PK/PD target in CSF was defined so far for optimizing dosing regimens for patients with CNS infection (34). Therefore, simulations in this study were performed using both the AUC_{24} in plasma and the C_{trough} in CSF as PK/PD targets to obtain PTA in different dosing regimens. Because there was no significant difference in vancomycin CL between patients with and without primary CNS infection, subsequent simulations were only conducted in patients with primary CNS infection. The reported protein binding (PB) of vancomycin in plasma is approximately 50% (3), while the mean PB of the 14 subjects in the present study was 70.1% (63.9 to 82.7%) and was highly variable. The inclusion of individual f_u as a covariate for the CSF volume of distribution or Q_{CSF} did not help to improve the model fit and was therefore not considered. The PB of vancomycin in CSF was also not taken into account, because the highest CSF protein concentration (2.26 mg/mL) reported in the present study is still far from the normal protein concentration in plasma (60 to 70 mg/mL) (35), suggesting that the total CSF concentrations of vancomycin are essentially equal to the unbound concentrations.

Based on our simulation results, a starting daily dose of 2, 3, or 4 g was recommended for patients with a CSF protein concentration of ≥150, <150 and ≥100, or <100 mg/dL, respectively. In the meantime, continuous infusion with a loading dose of vancomycin is recommended for patients with CNS infection. On the first day of the treatment, intermittent infusion could lead to a steep increase in the vancomycin concentration in CSF, which is helpful to achieve a target concentration in CSF faster than by continuous infusion. Afterwards, continuous infusion could be used to maintain an adequate plasma concentration, to avoid potential AKI and nephrotoxicity (21, 34). In addition, a dose of vancomycin such as 4 g/24 h was recommended for achieving an adequate CSF vancomycin concentration in other studies, but this dose resulted in a plasma AUC_{24} exceeding 600 mg · h/L on day 1 and at steady state in at least 17.3% and 85.6% of simulated patients, respectively. Therefore, it is recommended that dose adjustment should be made in a timely manner after adequate CSF concentrations have been obtained, based on TDM results and Bayesian predictions via the PopPK method. The proposed final model in this study could be employed after external evaluation and software integration.

For the treatment of patients with CNS infection, combined intravenous (i.v.) and intraventricular (i.v.t.) administration of vancomycin is becoming increasingly popular for first applications (22). The doses for i.v.t. reported in the literature ranged from 0.075 to 50 mg/day, and the CSF vancomycin concentrations varied widely, from 1.1 to 812.6 mg/L (36). Tentatively, simulations using the same dosages as reported in the literature were performed using our model established herein. The results showed that the predicted plasma concentrations for combined administration at most time points were close to the reported values, but the predicted CSF concentrations at all points in time were less than the reported values. This underestimation may be caused by the predicted (empirical) V_{CSF}

(0.445 L) in this study being larger than the actual human V_{CSF} (approximately 0.15 L). Obstruction of CSF circulation due to hydrocephalus or surgery may also result in CSF concentrations in actual CSF samples being higher than expected if vancomycin was evenly distributed in the CSF (36, 37). Therefore, our model using only data after intravenous administration was unable to predict CSF concentrations after combined i.v. and i.v.t. administration (36, 38). Despite the apparent underprediction of CSF concentrations compared to those obtained with real combined i.v./i.v.t. administration, our predicted CSF C_{trough} would exceed 10 mg/L in most patients after 20 mg i.v.t. with 2 g i.v. every 24 h, while the predicted plasma AUC would remain at a safe and effective level. This indicates that the combined administration could be a better choice to improve the outcome of patients with CNS infection in the future and should be further investigated.

Several limitations remain in this study. Only 14 patients were included and not all covariates were available for all patients, and thus, correlations between different CSF-related covariates and Q_{CSF} could not be compared. In addition, the small sample size precluded the use of a more stringent backward-elimination strategy for the covariance model. The final model still retains unexplained IIVs of 19.8% and 94.2% for Q_{CSF} and V_{CSF}, respectively. Relatively limited data for CSF_P samples were supported to compare the residual error of CSF_P and CSF_D samples. No vancomycin data for i.v.t. administration were available to refine the PopPK model and, thus, more precisely predict the CSF concentration after i.v.t. administration of vancomycin. In this study, standard dosing recommendations for all populations are unrealistic due to the multitude of covariates, but dosing adjustment based on Bayesian prediction via the PopPK model might be a better option.

In this study, a PopPK model for vancomycin was successfully established using data from patients with EVD. Three substances quantified in CSF were identified as predictors associated with vancomycin CSF concentrations, and the relationship with CSF protein was the closest. The model fully supported the feasibility of collecting CSF samples at the distal port of the EVD system for TDM. Recommendations on dosing regimen for patients with CNS infection were provided according to different CSF protein levels. Beyond adjusting doses according to renal function, starting treatment with a loading dose in patients with primary CSF infection was recommended.

MATERIALS AND METHODS

Ethical approval. This study protocol was approved by the Institutional Review Board of the Medical Faculty of the Ludwig-Maximilians-Universität München (Munich, Germany) (approval number 20-169). The study is registered at ClinicalTrials.gov under registration no. NCT04426383. Written informed consent was obtained from all patients or their health care proxies.

Study design and data organization. This study was conducted at University Hospital of Munich, Germany. Adult patients who underwent EVD due to, e.g., ventriculitis, traumatic brain injury, or subarachnoid hemorrhage and who received vancomycin were recruited from August 2020 to September 2021. EVD systems remained open and, thus, provided continuous CSF draining. Patients were classified according to whether the primary infection was a CNS infection or not. Vancomycin was administered by intermittent infusion and/or continuous infusion (with or without an initial loading dose), as determined by the physician in charge. Blood samples and CSF samples from the proximal port (CSF_P) or distal port (CSF_D) of the EVD system were collected for measurements of vancomycin concentrations and clinical parameters (19). All samples were collected based on leftover materials from blood gas analyses, routine blood sampling, routine CSF sampling, and remaining CSF in the drainage reservoir.

The sample volumes and collecting times of CSF samples were documented, as well as basic demographic information, including age, sex, weight, and height. The actual time of the CSF_P samples is the respective recording time, while the actual time of the CSF_D samples was calculated with the following formula: (recording time) − (sampling duration)/2. The estimated drainage rate of CSF_D samples was then calculated with the formula (CSF_D sample volume)/(sample duration), and the estimated time delay (applied for the sensitivity analysis only) was then calculated with the formula (dead volume [7 mL])/(estimated drainage rate). The glomerular filtration rate (eGFR) was estimated using the Chronic Kidney Disease Epidemiology Collaboration (CKD-EPI) 2021 equation, creatinine clearance (CrCL) was estimated using the Cockcroft-Gault equation (39, 40), and body surface area (BSA) was calculated using the DuBois and DuBois equation (41).

Analytics. Vancomycin was quantified by high-performance liquid chromatography (HPLC)-UV spectroscopy using a Prominence LC20 modular HPLC system equipped with an SPD-M30A PDA detector (detection wavelength, 240 nm) and LabSolution software (Shimadzu, Duisburg, Germany). The autosampler was cooled to 6°C, and the column temperature was 40°C. Separation was performed using a

CORTECS T3 2.7-μm particle size, 100- by 3-mm column (Waters, Eschborn, Germany) preceded by a guard column (Nucleoshell RP 18, 2.7-μm particle size, 4 by 3 mm; Macherey-Nagel, Düren, Germany). The mobile phase consisted of 0.05 M sodium phosphate buffer with 7.86% (vol/vol) acetonitrile, pH adjusted to 3.6 or 2.9. At a flow rate of 0.4 mL/min, vancomycin eluted after 3.8 min at pH 3.6 or 5.1 min at pH 2.9. The total vancomycin concentrations in plasma were determined following a repeatedly described method for the analysis of beta-lactam antibiotics (42). The sample preparation included diluted phosphoric acid instead of phosphate buffer, to achieve quantitative recovery (43). In brief, plasma (100 μL) was acidified with 0.1 M *o*-phosphoric acid (200 μL) and mixed with acetonitrile (500 μL). After separation of the precipitated proteins and extraction of acetonitrile into dichloromethane (1.3 mL), an aliquot (2 μL) of the aqueous layer was injected into the HPLC system. Free vancomycin concentrations were determined after ultrafiltration as described previously (42). In brief, plasma (300 μL) was buffered with 10 μL of 3 M potassium phosphate (pH 7.4) in a Vivafree 500 30-kDa Hydrosart centrifugal ultrafiltration device (Vivaproducts, Inc., Littleton, MA, USA) and then incubated in a microcentrifuge (Eppendorf 5417R; Eppendorf, Hamburg, Germany) for 10 min at 100 $\times$ *g* and 37°C and centrifuged for 20 min at 1,000 $\times$ *g* and 37°C. An aliquot (0.5 μL) of the ultrafiltrate was injected into the HPLC system. CSF was centrifuged at 12,000 $\times$ *g* for 3 min, and an aliquot (0.5 μL) of the supernatant was injected into the HPLC system. Calibration was performed by external standardization, as no matrix effect is observed when using HPLC-UV, in contrast to liquid chromatography-tandem mass spectrometry (LC-MS/MS) (44). The linearity of the assay ($R > 0.998$) has been proven from 300 mg/L down to 0.3 mg/L in plasma and 0.1 mg/L in saline as a surrogate for CSF or ultrafiltrate, respectively. These lowest nonzero standards on the calibration curves were defined as the lower limit of quantification (LLOQ). Based on in-process quality controls (QCs; plasma of healthy subjects spiked with 80 mg/L, 25 mg/L, or 6.25 mg/L vancomycin) the coefficients of variation (CVs) of intra- and interassay determinations of total drug in plasma were <3% (imprecision), and the accuracy was 99.1%. The f_u of vancomycin in these QCs was 79.5% $\pm$ 1.6% (CV = 2.0%). The QCs were analyzed as single samples, as in preliminary experiments, the difference between duplicates was as low as 1%, i.e., in the range of the imprecision of the injection system. The accuracy regarding the determination of the free concentrations in plasma cannot be specified, as the extent of protein binding in a particular plasma sample is not known (45). The CVs of the intra- and interassay determinations of vancomycin in saline as a surrogate for CSF or ultrafiltrate (QCs of 5 mg/L and 0.5 mg/L) were <4% (imprecision), and the accuracy was 98.6%. The stability of the processed samples in the autosampler (16 to 18 h/6°C) was 98.3% $\pm$ 2.5% for total plasma concentrations, 99.4% $\pm$ 1.5% for free plasma concentrations, and 95.1% $\pm$ 7.2% for CSF concentrations.

Population pharmacokinetic modeling. The PopPK model was developed and diagnosed using the nonlinear mixed-effects model software NONMEM (version 7.4.0; ICON Development Solutions, USA) and Perl-speaks-NONMEM (PsN) (version 5.3.0; Uppsala University, Sweden) (46, 47). The model was developed using first-order conditional estimation with interaction, where a decrease of >3.84 in the objective function value (OFV) between 2 nested models ($P < 0.05$) upon the inclusion of a parameter was used as a statistical criterion. The nonnested models were compared using the Akaike information criterion (AIC), and the model with the lower AIC was selected (48). Covariates were assessed by stepwise forward inclusion ($P = 0.05$) using the stepwise covariate modeling tool in PsN. Statistics and graphic visuals were performed using R (version 4.2.0). The model was developed based on total vancomycin concentrations in plasma and CSF. Samples with concentrations below the limit of quantification (BLQ) were omitted during model development because the percentage of BLQ data was less than 2% (49).

The interindividual variables (IIVs) for PK parameters were described by the exponential equation $\theta_i = \theta \times e^{\eta_i}$, where θ_i is the value of the individual predicted parameter and θ is the population point estimate of the parameter. Different error models, including additive-only and proportional-only error models and the combination thereof, were evaluated separately. The plasma data were initially used to establish the basic model with one-, two-, and three-compartment model attempts. Subsequently, covariates related to plasma PK parameters were tested, including age, sex, weight, height, BSA, primary CNS infection, eGFR, and CrCL.

On the basis of the plasma model, a CSF compartment was directly linked to the central compartment with the intercompartment clearance between plasma and CSF (Q_{CSF}), as well as the CSF compartment volume (V_{CSF}). Two empirical methods to describe the elimination of the drug from the CSF compartment were tested separately. The first was to introduce a transit compartment between the CSF compartment and the central compartment with an independent parameter of transit compartment rate; in the meantime, the V_{CSF} was fixed to be weight $\times$ 0.002 L/kg based on the reported value of human CSF volume (Fig. 4, left) (50, 51). The other was to introduce an additional clearance, i.e., bulk flow (Q_{BULK} = 0.025 L/h), when the drug was eliminated from the CSF compartment to the central compartment (Fig. 4, right) (18, 52). The following covariates were assessed using the two models described above in parallel: age, sex, weight, height, BSA, primary CNS infection, drainage rate, CSF sample volume, unbound fraction (f_u), albumin, bilirubin, C-reactive protein, leukocytes, and interleukin 6 and neuron-specific enolase (CSF), S100 protein (CSF), ferritin (CSF), erythrocytes (CSF), cell count (CSF), protein (CSF), glucose (CSF), interleukin 6 (CSF), and lactate (CSF). After the development of a reasonable CSF base model using all CSF sample data, the role of the two types of CSF samples was investigated by comparison of parameter estimates when including and excluding the CSF_P samples and by separation of residual errors for CSF_P and CSF_D samples. Only forward inclusion was used for covariates based on significant improvement of the model, because of the small sample size and the exploratory type of evaluation. Exponential and proportional models were compared for continuous covariates, and conditional effects was used for categorical covariates.

Internal model evaluation of the final model was performed by individual plots of predicted concentrations and observed concentrations, goodness-of-fit (GOF) plots, and prediction-corrected visual predictive

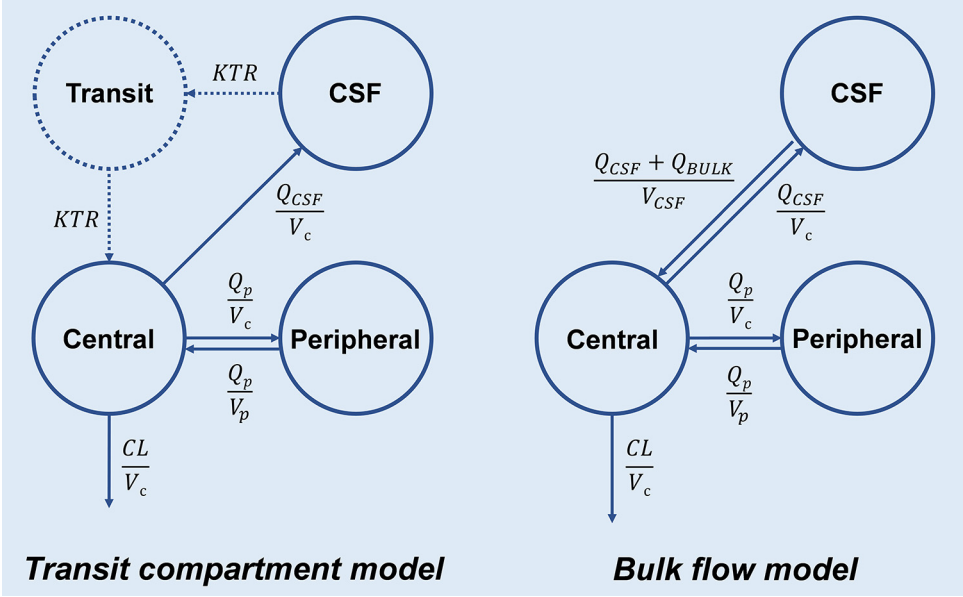

FIG 4 Scheme of the transit compartment model (left) and the bulk flow model (right; preferred and used for further evaluations) for the CSF compartment. In both models, vancomycin directly entered the central compartment with zero-order absorption. In the transit compartment model, vancomycin entered the CSF compartment from the central compartment (compartment volume, V_c) with an intercompartment clearance (Q_{CSF}), while the CSF compartment volume (V_{CSF}) was fixed at 0.002 L/kg × weight. Then, vancomycin returned to the central compartment through a separate transit compartment with an independent parameter transit rate (KTR). In the bulk flow model, vancomycin entered the CSF compartment from the central compartment with Q_{CSF}, but with an additional bulk flow (Q_{BULK}, 0.025 L/h) when vancomycin returned to the central compartment. Both models contain a peripheral compartment with the parameters intercompartment clearance (Q_p) and peripheral compartment volume (V_P). Vancomycin was ultimately eliminated by first order from the central compartment.

checks (pcVPC, n = 1,000) (53). Model stability and parameter precision were tested by a nonparametric bootstrap approach (n = 1,000 bootstraps).

To further assess a potential effect of the CSF sampling site on the results of the model, a sensitivity analysis was carried out. Although we were aware that the respective estimated time delay (calculated as described in "Study design and data organization," above) might not be reliable, to this end, CSF_D sampling times were adjusted by the individual estimated time delay with censoring of any adjusted times to the value of the previous shifted sampling time plus 0.01 h. Censoring was used to avoid disturbing the order of samples by this procedure. Parameter estimates and PTA calculation were compared between the final model and the model using data with adjusted times for CSF_D samples. We repeated this exercise with uniformly shifted CSF_D sampling times, assuming CSF flow rates of 12 and 36 mL/h, which reflects the reported range of CSF production rates (20).

Simulations. Different dosing regimens were tested separately in 3,000 simulated subjects with primary CNS infection on the basis of Monte Carlo simulations, where age, CrCL, and CSF protein concentrations were generated according to covariate distributions in our observational data. Three infusion modes, intermittent infusion, continuous infusion with a loading dose, and continuous infusion without a loading dose, were compared in terms of the daily area under the curve (AUC_{24}) in plasma and the trough concentration (C_{trough}; the concentration at 24 h or 120 h after the first dose for day 1 or steady state, respectively) in CSF, which are common PK/PD targets for vancomycin therapy (22, 33). For continuous infusion with a loading dose, the loading dose was chosen to be half of the daily dose on the first day of treatment, and the remaining daily dose was administered immediately after the loading dose was completed. From the second day, the daily dose was administered only by continuous infusion. Only total vancomycin concentrations in plasma and CSF were applied for PTA calculations, as a total vancomycin AUC/MIC of ≥400 has been advocated as a plasma target, while the protein binding of vancomycin in CSF is currently unknown and protein concentrations in CSF are negligible (3, 33).

SUPPLEMENTAL MATERIAL

Supplemental material is available online only.

SUPPLEMENTAL FILE 1, DOCX file, 0.7 MB.

ACKNOWLEDGMENTS

Zhendong Chen received a scholarship from the China Scholarship Council (CSC) for support of his Ph.D. studies. Chunli Chen was financed by the International Postdoctoral Exchange Fellowship Program from the Office of China Postdoctoral Council (grants

number 2020106 and PC2020013) and the National Natural Science Foundation of Heilongjiang Province (grant number YQ2022C017).

The funders had no role in design, collection, analysis and interpretation of data, and writing and publication of the manuscript.

REFERENCES

1. Beer R, Lackner P, Pfausler B, Schmutzhard E. 2008. Nosocomial ventriculitis and meningitis in neurocritical care patients. J Neurol 255:1617–1624. https://doi.org/10.1007/s00415-008-0059-8.
2. Blassmann U, Roehr AC, Frey OR, Vetter-Kerkhoff C, Thon N, Hope W, Briegel J, Huge V. 2016. Cerebrospinal fluid penetration of meropenem in neurocritical care patients with proven or suspected ventriculitis: a prospective observational study. Crit Care 20:343. https://doi.org/10.1186/s13054-016-1523-y.
3. Rybak M, Lomaestro B, Rotschafer JC, Moellering R, Jr, Craig W, Billeter M, Dalovisio JR, Levine DP. 2009. Therapeutic monitoring of vancomycin in adult patients: a consensus review of the American Society of Health-System Pharmacists, the Infectious Diseases Society of America, and the Society of Infectious Diseases Pharmacists. Am J Health Syst Pharm 66:82–98. https://doi.org/10.2146/ajhp080434.
4. Matzke GR, Zhanel GG, Guay DR. 1986. Clinical pharmacokinetics of vancomycin. Clin Pharmacokinet 11:257–282. https://doi.org/10.2165/00003088-198611040-00001.
5. Matzke GR, McGory RW, Halstenson CE, Keane WF. 1984. Pharmacokinetics of vancomycin in patients with various degrees of renal function. Antimicrob Agents Chemother 25:433–437. https://doi.org/10.1128/AAC.25.4.433.
6. Rodvold KA, Blum RA, Fischer JH, Zokufa HZ, Rotschafer JC, Crossley KB, Riff LJ. 1988. Vancomycin pharmacokinetics in patients with various degrees of renal function. Antimicrob Agents Chemother 32:848–852. https://doi.org/10.1128/AAC.32.6.848.
7. Ackerman BH, Taylor EH, Olsen KM, Abdel-Malak W, Pappas AA. 1988. Vancomycin serum protein binding determination by ultrafiltration. Drug Intell Clin Pharm 22:300–303. https://doi.org/10.1177/106002808802200404.
8. Golper TA, Noonan HM, Elzinga L, Gilbert D, Brummett R, Anderson JL, Bennett WM. 1988. Vancomycin pharmacokinetics, renal handling, and nonrenal clearances in normal human subjects. Clin Pharmacol Ther 43:565–570. https://doi.org/10.1038/clpt.1988.74.
9. Bailey EM, Rybak MJ, Kaatz GW. 1991. Comparative effect of protein binding on the killing activities of teicoplanin and vancomycin. Antimicrob Agents Chemother 35:1089–1092. https://doi.org/10.1128/AAC.35.6.1089.
10. Monteiro JF, Hahn SR, Gonçalves J, Fresco P. 2018. Vancomycin therapeutic drug monitoring and population pharmacokinetic models in special patient subpopulations. Pharmacol Res Perspect 6:e00420. https://doi.org/10.1002/prp2.420.
11. Broeker A, Nardecchia M, Klinker KP, Derendorf H, Day RO, Marriott DJ, Carland JE, Stocker SL, Wicha SG. 2019. Towards precision dosing of vancomycin: a systematic evaluation of pharmacometric models for Bayesian forecasting. Clin Microbiol Infect 25:1286.e1–1286.e7. https://doi.org/10.1016/j.cmi.2019.02.029.
12. Lutsar I, McCracken GH, Jr, Friedland IR. 1998. Antibiotic pharmacodynamics in cerebrospinal fluid. Clin Infect Dis 27:1117–1127. https://doi.org/10.1086/515003.
13. Rybak MJ. 2006. The pharmacokinetic and pharmacodynamic properties of vancomycin. Clin Infect Dis 42(Suppl 1):S35–S39. https://doi.org/10.1086/491712.
14. Popa D, Loewenstein L, Lam SW, Neuner EA, Ahrens CL, Bhimraj A. 2016. Therapeutic drug monitoring of cerebrospinal fluid vancomycin concentration during intraventricular administration. J Hosp Infect 92:199–202. https://doi.org/10.1016/j.jhin.2015.10.017.
15. Beach JE, Perrott J, Turgeon RD, Ensom MHH. 2017. Penetration of vancomycin into the cerebrospinal fluid: a systematic review. Clin Pharmacokinet 56:1479–1490. https://doi.org/10.1007/s40262-017-0548-y.
16. Li X, Wu Y, Sun S, Mei S, Wang J, Wang Q, Zhao Z. 2015. Population pharmacokinetics of vancomycin in postoperative neurosurgical patients. J Pharm Sci 104:3960–3967. https://doi.org/10.1002/jps.24604.
17. Li X, Wu Y, Sun S, Zhao Z, Wang Q. 2016. Population pharmacokinetics of vancomycin in postoperative neurosurgical patients and the application in dosing recommendation. J Pharm Sci 105:3425–3431. https://doi.org/10.1016/j.xphs.2016.08.012.
18. Jalusic KO, Hempel G, Arnemann PH, Spiekermann C, Kampmeier TG, Ertmer C, Gastine S, Hessler M. 2021. Population pharmacokinetics of vancomycin in patients with external ventricular drain-associated ventriculitis. Br J Clin Pharmacol 87:2502–2510. https://doi.org/10.1111/bcp.14657.
19. Kinast CB, Paal M, Liebchen U. 2022. Comparison of cerebrospinal fluid collection through the proximal and distal port below the overflow system from an external ventricular drain. Neurocrit Care 37:775–778. https://doi.org/10.1007/s12028-022-01615-y.
20. Beidler PG, Novokhodko A, Prolo LM, Browd S, Lutz BR. 2021. Fluidic considerations of measuring intracranial pressure using an open external ventricular drain. Cureus 13:e15324. https://doi.org/10.7759/cureus.15324.
21. Sinha Ray A, Haikal A, Hammoud KA, Yu AS. 2016. Vancomycin and the risk of AKI: a systematic review and meta-analysis. Clin J Am Soc Nephrol 11:2132–2140. https://doi.org/10.2215/CJN.05920616.
22. Rybak MJ, Le J, Lodise TP, Levine DP, Bradley JS, Liu C, Mueller BA, Pai MP, Wong-Beringer A, Rotschafer JC, Rodvold KA, Maples HD, Lomaestro BM. 2020. Therapeutic monitoring of vancomycin for serious methicillin-resistant Staphylococcus aureus infection: a revised consensus guideline and review by the American Society of Health-System Pharmacists, the Infectious Diseases Society of America, the Pediatric Infectious Diseases Society, and the Society of Infectious Diseases Pharmacists. Am J Health Syst Pharm 77:835–864. https://doi.org/10.1093/ajhp/zxaa036.
23. Yamamoto M, Kuzuya T, Baba H, Yamada K, Nabeshima T. 2009. Population pharmacokinetic analysis of vancomycin in patients with gram-positive infection and the influence of infectious disease type. J Clin Pharm Ther 34:473–483. https://doi.org/10.1111/j.1365-2710.2008.01016.x.
24. Deng C, Liu T, Zhou T, Lu H, Cheng D, Zhong X, Lu W. 2013. Initial dosage regimens of vancomycin for Chinese adult patients based on population pharmacokinetic analysis. Int J Clin Pharmacol Ther 51:407–415. https://doi.org/10.5414/CP201842.
25. Ishikawa M, Yamazaki S, Suzuki T, Uchida M, Iwadate Y, Ishii I. 2019. Correlation between vancomycin penetration into cerebrospinal fluid and protein concentration in cerebrospinal fluid/serum albumin ratio. J Infect Chemother 25:124–128. https://doi.org/10.1016/j.jiac.2018.10.013.
26. Chow E, Troy SB. 2014. The differential diagnosis of hypoglycorrhachia in adult patients. Am J Med Sci 348:186–190. https://doi.org/10.1097/MAJ.0000000000000217.
27. Pleines UE, Morganti-Kossmann MC, Rancan M, Joller H, Trentz O, Kossmann T. 2001. S-100 beta reflects the extent of injury and outcome, whereas neuronal specific enolase is a better indicator of neuroinflammation in patients with severe traumatic brain injury. J Neurotrauma 18:491–498. https://doi.org/10.1089/089771501300227297.
28. Wang J, Chen S, Wang X, Gu H, Liu J, Wang X, Liu L. 2019. Value of NSE and S100 protein of Kawasaki disease with aseptic meningitis in infant. Open Life Sci 14:358–362. https://doi.org/10.1515/biol-2019-0040.
29. Wong FW. 2011. Cerebrospinal fluid collection: a comparison of different collection sites on the external ventricular drain. Dynamics 22:19–24.
30. Alihodzic D, Broeker A, Baehr M, Kluge S, Langebrake C, Wicha SG. 2020. Impact of inaccurate documentation of sampling and infusion time in model-informed precision dosing. Front Pharmacol 11:172. https://doi.org/10.3389/fphar.2020.00172.
31. Giuliano C, Haase KK, Hall R. 2010. Use of vancomycin pharmacokinetic-pharmacodynamic properties in the treatment of MRSA infection. Expert Rev Anti Infect Ther 8:95–106. https://doi.org/10.1586/eri.09.123.
32. Aljefri DM, Avedissian SN, Rhodes NJ, Postelnick MJ, Nguyen K, Scheetz MH. 2019. Vancomycin area under the curve and acute kidney injury: a meta-analysis. Clin Infect Dis 69:1881–1887. https://doi.org/10.1093/cid/ciz051.
33. Blassmann U, Hope W, Roehr AC, Frey OR, Vetter-Kerkhoff C, Thon N, Briegel J, Huge V. 2019. CSF penetration of vancomycin in critical care patients with proven or suspected ventriculitis: a prospective observational study. J Antimicrob Chemother 74:991–996. https://doi.org/10.1093/jac/dky543.
34. Hanrahan TP, Harlow G, Hutchinson J, Dulhunty JM, Lipman J, Whitehouse T, Roberts JA. 2014. Vancomycin-associated nephrotoxicity in the critically

ill: a retrospective multivariate regression analysis. Crit Care Med 42:2527–2536. https://doi.org/10.1097/CCM.0000000000000514.
35. Jankovska E, Svitek M, Holada K, Petrak J. 2019. Affinity depletion versus relative protein enrichment: a side-by-side comparison of two major strategies for increasing human cerebrospinal fluid proteome coverage. Clin Proteom 16:9. https://doi.org/10.1186/s12014-019-9229-1.
36. Ng K, Mabasa VH, Chow I, Ensom MH. 2014. Systematic review of efficacy, pharmacokinetics, and administration of intraventricular vancomycin in adults. Neurocrit Care 20:158–171. https://doi.org/10.1007/s12028-012-9784-z.
37. Chen K, Wu Y, Wang Q, Wang J, Li X, Zhao Z, Zhou J. 2015. The methodology and pharmacokinetics study of intraventricular administration of vancomycin in patients with intracranial infection after craniotomy. J Crit Care 30:218.e1–218.e5. https://doi.org/10.1016/j.jcrc.2014.09.020.
38. Li X, Sun S, Ling X, Chen K, Wang Q, Zhao Z. 2017. Plasma and cerebrospinal fluid population pharmacokinetics of vancomycin in postoperative neurosurgical patients after combined intravenous and intraventricular administration. Eur J Clin Pharmacol 73:1599–1607. https://doi.org/10.1007/s00228-017-2313-4.
39. Meeusen JW, Kasozi RN, Larson TS, Lieske JC. 2022. Clinical impact of the refit CKD-EPI 2021 creatinine-based eGFR equation. Clin Chem 68:534–539. https://doi.org/10.1093/clinchem/hvab282.
40. Cockcroft DW, Gault MH. 1976. Prediction of creatinine clearance from serum creatinine. Nephron 16:31–41. https://doi.org/10.1159/000180580.
41. DuBois D, DuBois EF. 1916. A formula to estimate the approximate surface area if height and weight be known. Arch Intern Med 17:863.
42. Dorn C, Kratzer A, Schießer S, Kees F, Wrigge H, Simon P. 2019. Determination of total or free cefazolin and metronidazole in human plasma or interstitial fluid by HPLC-UV for pharmacokinetic studies in man. J Chromatogr B Analyt Technol Biomed Life Sci 1118–1119:51–54. https://doi.org/10.1016/j.jchromb.2019.04.025.
43. Beckmann J, Kees F, Schaumburger J, Kalteis T, Lehn N, Grifka J, Lerch K. 2007. Tissue concentrations of vancomycin and moxifloxacin in periprosthetic infection in rats. Acta Orthop 78:766–773. https://doi.org/10.1080/17453670710014536.
44. An G, Bach T, Abdallah I, Nalbant D. 2020. Aspects of matrix and analyte effects in clinical pharmacokinetic sample analyses using LC-ESI/MS/MS—two case examples. J Pharm Biomed Anal 183:113135. https://doi.org/10.1016/j.jpba.2020.113135.
45. Nilsson LB. 2013. The bioanalytical challenge of determining unbound concentration and protein binding for drugs. Bioanalysis 5:3033–3050. https://doi.org/10.4155/bio.13.274.
46. Boeckmann A, Sheiner L, Beal S. 2001. NONMEM users guide—part V. University of California, San Francisco, CA.
47. Lindbom L, Pihlgren P, Jonsson EN. 2005. PsN-Toolkit—a collection of computer intensive statistical methods for non-linear mixed effect modeling using NONMEM. Comput Methods Programs Biomed 79:241–257. https://doi.org/10.1016/j.cmpb.2005.04.005.
48. Mould DR, Upton RN. 2013. Basic concepts in population modeling, simulation, and model-based drug development—part 2: introduction to pharmacokinetic modeling methods. CPT Pharmacometrics Syst Pharmacol 2:e38. https://doi.org/10.1038/psp.2013.14.
49. Irby DJ, Ibrahim ME, Dauki AM, Badawi MA, Illamola SM, Chen M, Wang Y, Liu X, Phelps MA, Mould DR. 2021. Approaches to handling missing or "problematic" pharmacology data: pharmacokinetics. CPT Pharmacometrics Syst Pharmacol 10:291–308. https://doi.org/10.1002/psp4.12611.
50. Büsker S, Jäger W, Poschner S, Mayr L, Al Jalali V, Gojo J, Azizi AA, Ullah S, Bilal M, El Tabei L, Fuhr U, Peyrl A. 2022. Pharmacokinetics of metronomic temozolomide in cerebrospinal fluid of children with malignant central nervous system tumors. Cancer Chemother Pharmacol 89:617–627. https://doi.org/10.1007/s00280-022-04424-4.
51. Miller RD. 2020. Miller's anesthesia, 9th ed. Elsevier, Philadelphia, PA.
52. Segal MB. 1993. Extracellular and cerebrospinal fluids. J Inherit Metab Dis 16:617–638. https://doi.org/10.1007/BF00711896.
53. Bergstrand M, Hooker AC, Wallin JE, Karlsson MO. 2011. Prediction-corrected visual predictive checks for diagnosing nonlinear mixed-effects models. AAPS J 13:143–151. https://doi.org/10.1208/s12248-011-9255-z.